

Stonehaven Bay Coastal Flood Protection Study

Interim Modelling Report

Final Report

January 2019

www.jbaconsulting.com

JBA Project Manager

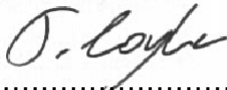
Nicci Buckley BSc MSc CSci MCIWEM C.WEM
 Unit 2.1 Quantum Court
 Research Avenue South
 Heriot Watt Research Park
 Riccarton
 Edinburgh
 EH14 4AP

Revision history

Revision Ref/Date	Amendments	Issued to
P01 / 02 November 2018	-	G McCallum L Watson S McFarland
P02 / 18 January 2019	Climate change modelling added and comments from SEPA and Aberdeenshire Council addressed.	G McCallum L Watson S McFarland

Contract

This report describes work commissioned by Gavin Penman on behalf of Aberdeenshire Council by a letter dated 27 February 2018 and Purchase Order number 1002287. Dougall Baillie’s representative for the contract was Scott Macphail and Aberdeenshire Council’s representative for the contract was Graeme McCallum. Johnny Coyle, Hannah Otton, Douglas Pender and Nicci Buckley of JBA Consulting carried out this work.

Prepared by 

Johnny Coyle BSc MSc
Analyst

Prepared by

Hannah Otton BSc
Assistant Analyst

Reviewed by 

Douglas Pender MEng PhD MCIWEM
Senior Engineer

Reviewed by 

Nicci Buckley BSc MSc CSci MCIWEM C.WEM
Principal Analyst

Approved by 

David Bassett BSc MSc CEnv MCIWEM C.WEM
Director

Purpose

This document has been prepared as a Draft Report for Aberdeenshire Council. JBA Consulting accepts no responsibility or liability for any use that is made of this document other than by the Client for the purposes for which it was originally commissioned and prepared.

JBA Consulting has no liability regarding the use of this report except to Aberdeenshire Council.

Acknowledgements

JBA would like to thank Aberdeenshire Council, SEPA and the Stonehaven Flood Action Group for the provision of data and information to support this work.

Copyright

© Jeremy Benn Associates Limited 2018.

Carbon footprint

JBA is aiming to reduce its per capita carbon emissions.

Executive summary

This Interim Modelling Report was undertaken by JBA Consulting for Aberdeenshire Council as part of a Flood Protection Study (FPS) to consider options to reduce coastal flood risk within Stonehaven and Cowie. The report consists of three sections: flood modelling; geomorphological assessment; and baseline economics.

The flood modelling process used SEPA's offshore multivariate dataset in conjunction with still water levels from the Coastal Flood Boundary dataset to estimate flood risk to Stonehaven from both wave overtopping and extreme sea levels. Testing of the methodology using hindcast data was undertaken to provide confidence in the modelling outputs, with the results giving good agreement with historic observed overtopping and flooding. Modelling of the extreme conditions shows that there are multiple properties at risk of flooding within the study area, even at low return periods.

The geomorphological assessment showed that there are high levels of variability in local beach levels and volumes. Cross-shore transport is the primary control mechanism, leading to berm building and the burying of the defences during extreme events. While this renders the sea wall obsolete as an overtopping defence, anecdotal evidence supports the theory that a higher, steeper beach provides more protection by dissipating energy further offshore. A longshore gradient also exists, as can be seen from the general increase in beach width from north to south. The control structures at the mouths of both the Cowie and Carron appear to be inefficient at retaining beach sediment, with the volume of sediment to the south of the Carron outfall less than that placed there manually by Aberdeenshire Council. The data used for the analysis was not available at the frequency required to fully understand the performance and changes in the beach during extreme conditions, however the morphology of the beach is clearly a key component in the protection against and exacerbation of flood risk within the bay.

Present value damages calculated from the baseline economical appraisal are approximately £12.6 million. The high frequency of flooding and number of properties at risk during low return periods has significantly capped these. Overall the damages without capping are over £50 million suggesting that without intervention, set back or change of use of the properties there is significant potential for ongoing losses within the community.

Recreational losses through erosion of the beach; risk to life from wave overtopping; critical infrastructure at risk from erosion and sea level rise and climate change will be incorporated into the damage assessment prior to full options appraisal and will cause overall present value damages to increase for the appraisal period.

Contents

1	Introduction	10
1.1	Overview	10
2	Flood modelling	11
2.1	Coastal flood risk drivers.....	11
2.2	Historical flood events	11
2.3	Modelling schematisation	11
2.4	Multivariate datasets	13
2.4.1	MDA generation	14
2.5	Water level transformations	16
2.6	Wave transformation	17
2.6.1	Model domain	18
2.6.2	Topography representation.....	19
2.6.3	Harbour representation	20
2.6.4	Calibration.....	21
2.7	Emulation	22
2.7.1	Emulator locations.....	22
2.7.2	Emulator training	23
2.7.3	Emulated datasets.....	29
2.7.4	Emulation validation and performance and wave buoy	29
2.7.5	Integration	30
2.8	Wave overtopping	31
2.8.1	Wave overtopping schematisations.....	31
2.8.2	Wave overtopping calibration.....	38
2.8.3	Extreme overtopping rates	43
2.9	Flood inundation modelling.....	45
2.9.1	Digital terrain model.....	46
2.9.2	Feature representation.....	46
2.9.3	Model files.....	47
2.9.4	TUFLOW model validation.....	48
2.10	Tidal reach of the Cowie Water	54
2.10.1	Historical configuration	54
2.10.2	Present day configuration	56
2.10.3	Coastal flood risk in the tidal reach.....	59
2.11	Tidal reach of the River Carron	62
2.11.1	Historical configuration	62
2.11.2	Present day configuration	65
2.11.3	Coastal flood risk in the tidal reach.....	66
2.12	Impacts of sea level rise on sewer network flood risk	69
3	Geomorphology Assessment.....	77
3.1	Overview	77
3.2	Geology	77

3.3	Sediment transport and morphology.....	77
3.4	Current sediment management practices	78
3.5	Long term trends	78
3.6	Topographic Analysis.....	81
3.6.1	Data	81
3.6.2	Sections.....	81
3.6.3	MHWS variations.....	85
3.6.4	Volumetric Analysis	85
3.6.5	Cross sectional analysis.....	90
3.6.6	Volumetric trends.....	91
3.6.7	Coastal structure performance	92
3.7	Erosion modelling	97
3.7.1	XBeach requirements.....	97
3.7.2	Modelling of the 2017 event.....	100
3.8	Undefended erosion modelling	104
3.8.1	Coastal defence conditions and residual life	105
3.8.2	2017 event.....	105
3.8.3	Design Events.....	107
3.9	Erosion assessment summary.....	112
3.10	Erosion assessment recommendations.....	113
4	Baseline economic assessment.....	114
4.1	Estimation of flood damages.....	114
4.1.1	Damage calculations	114
4.1.2	Depth damage curve	116
4.1.3	Threshold levels	117
4.1.4	Residential property capping.....	117
4.1.5	Non-residential property capping.....	117
4.1.6	Intangible damages (Health)	118
4.2	Indirect damages	121
4.2.1	Local authority and emergency services losses.....	121
4.2.2	Evacuation losses	121
4.3	Modelling Results	121
4.3.1	Flood damages.....	125
5	Conclusions and recommendations	126
5.1	Flood modelling	126
5.2	Erosion Modelling	126
5.3	Baseline economic appraisal	127

List of Figures

Figure 1-1: Location plan	10
Figure 2-1: Components of coastal flood risk	11
Figure 2-2: Scottish offshore multivariate datasets	13
Figure 2-3: Multivariate data (turquoise) vs MDA data (red)	15
Figure 2-4: Extreme still water level equation for the model domain, based on Northing change relative to Aberdeen	16
Figure 2-5: SWAN wave model mesh (left) and bathymetry (right)	18
Figure 2-6: SWAN wave model mesh within Stonehaven Bay ² , depths in meters below ODN	19
Figure 2-7: SWAN representation of Stonehaven Harbour ²	20
Figure 2-8: Modelled vs observed Hs for final SWAN model set up	21
Figure 2-9: SWAN model output locations	23
Figure 2-10: Emulator performance at wave buoy - mid Oct 2016 event	29
Figure 2-11: Emulator performance at wave buoy - early Feb 2017 event	29
Figure 2-12: Emulator performance at wave buoy - mid Feb 2017 event	30
Figure 2-13: Overtopping profile locations	32
Figure 2-14: Overtopping output of forcing conditions with overtopping training data. Output from Overtopping.ing.unibo.it.	42
Figure 2-15: TUFLOW model domain and inflows	45
Figure 2-16: Observed overtopping during the December 2012 event	48
Figure 2-17: Offshore Hs (light blue) and SWL (dark blue) at Stonehaven for December 2012	49
Figure 2-18: Modelled flood extent for 15th December 2012 event, along with photo evidence from Aberdeenshire Council	50
Figure 2-19: Modelled flood extent for 15th December 2012 event, along with overtopping rates and estimated water depths at key locations	51
Figure 2-20: Overtopping rate for four selected cross sections for a 1 in 200 year event	52
Figure 2-21: Example tidal graphs for 2018 and 2118 200-year events	53
Figure 2-22: Historical configuration of the Cowie Water and River Carron at the coast ⁵⁵	55
Figure 2-23: Image showing historical path of the Cowie Water, River Carron and the shingle bar	56
Figure 2-24: Image showing the river mouths in 1948 following the Cowie breaking through the shingle bank	56
Figure 2-25: Aerial image showing the present day mouth of the Cowie Water	57
Figure 2-26: Looking upstream from the mouth of the Cowie Water to the weir and B979 road bridge	58
Figure 2-27: Right bank and footbridge at the mouth of the Cowie Water	58
Figure 2-28: Left bank training wall at the mouth of the Cowie Water	59
Figure 2-29: SWL compared to top of bank levels; left bank	59
Figure 2-30: SWL compared to top of bank levels; right bank	60
Figure 2-31: Elevations at mouth of Cowie Water from scan data	61
Figure 2-32: SWL plus waves compared to top of bank levels; left bank	62
Figure 2-33: SWL plus waves compared to top of bank levels; right bank	62
Figure 2-34: Historical natural outfall of the River Carron	63
Figure 2-35: Recommended training wall option from HR Wallingford report	64
Figure 2-36: Proposed extension to the training structures, 2007	65
Figure 2-37: Current configuration at the mouth of the River Carron	66
Figure 2-38: Long section of the River Carron – downstream boundary sensitivity analysis	66
Figure 2-39: Long section of River Carron – SWLs in rock armour section of channel	67

Figure 2-40: Tidal and fluvial boundaries for Q200cc design run from Mott MacDonald model	68
Figure 2-41: Wave propagation up the River Carron on 15 December 2012	69
Figure 2-42: Local drainage network from ICM	71
Figure 2-43: 30 year tidal flood event (2018)	72
Figure 2-44: 30 year tidal flood event (2118)	73
Figure 2-45: 200 year tidal flood event (2018)	74
Figure 2-46: 200 year tidal flood event (2118)	75
Figure 3-1: MHWS fluctuations from NCCA data	79
Figure 3-2: Historical fluvial flow routes	80
Figure 3-3: MHWS fluctuations at the mouth of the River Carron	80
Figure 3-4: Division of Stonehaven Bay into sections	81
Figure 3-5: Section A/XS08: Vertical sea wall and sandy beach	82
Figure 3-6: Section B/XS12: Stepped revetment and shingle beach	82
Figure 3-7: Cowie Water estuary from the south with sediment accumulation	83
Figure 3-8: Section C/XS17: Seawall with sediment build up and shingle beach	83
Figure 3-9: Section D/XS20: Seawall with sediment build up. Shingle and coarse sand beach.	84
Figure 3-10: Section E/XS26: Boardwalk at the top of the beach; River Carron discharging into the sea across the beach	84
Figure 3-11: MHWS fluctuations from 2008, 2013 and 2018	85
Figure 3-12: Elevation change from 2008 to 2013 across Stonehaven Bay	88
Figure 3-13: Elevation change from 2013 to 2018 across Stonehaven Bay	89
Figure 3-14: Elevation change from 2008 to 2018 across Stonehaven Bay	89
Figure 3-15: Cross sections at Stonehaven Bay	90
Figure 3-16: Sediment volume below MHWN from 2008 to 2018	91
Figure 3-17: Cowie Water: elevation change from 2013 to 2018	92
Figure 3-18: Profile 14	93
Figure 3-19: Profile 15	94
Figure 3-20: River Carron: Elevation change from 2013 to 2018 (NB: the area of no data is the current course of the River Carron which was not included in the topographic survey from 2018.)	95
Figure 3-21: Profile 25	95
Figure 3-22: Profile 26	96
Figure 3-23: Topographic profiles extended to nearest wave buoy	97
Figure 3-24: XS08 topographic profile	98
Figure 3-25: XS12 topographic profile	98
Figure 3-26: XS17 topographic profile	99
Figure 3-27: XS20 topographic profile	99
Figure 3-28: XS26 topographic profile	100
Figure 3-29: February 2017 event Wave Height and SWL	101
Figure 3-30: XS08 modelled profile and beach level at the defence toe	102
Figure 3-31: XS12 modelled profile and beach level at the defence toe	102
Figure 3-32: XS17 modelled profile and beach level at defence toe	103
Figure 3-33: XS20 modelled profile and beach level at toe	103
Figure 3-34: XS26 modelled profile and beach level at defence toe	104
Figure 3-35: undefended modelled profiles	106
Figure 3-36: Relationship between Hs and Tp	107
Figure 3-37: 0.5% AP (200 year) profiles	108
Figure 3-38: Projected HAT retreat by 2050, 2080 and 2118.	110
Figure 3-39: Crest changes from the 200-year event (XS08 on left, XS12 on right)	111
Figure 4-1: Aspects of flood damage	114

Figure 4-2: Property vulnerability index for properties in Stonehaven	120
Figure 4-3: Two year flood extent with impacted properties	123
Figure 4-4: 200 year flood extent with impacted properties	124
Figure 4-5: Proportion of components contributing to 2018 flood damages	125

List of Tables

Table 2-1: Calibration RMSE scores of different model setups, given as a percentage of observed spectra	21
Table 2-2: SWAN output locations	22
Table 2-3: Best performing emulator scores and functions	24
Table 2-4: Diagnostic plots for locations with poor emulation performance	26
Table 2-5: Comparison between SWAN and EurOtop toe elevations	30
Table 2-6: Wave overtopping cross sections	33
Table 2-7: Hindcast maximum boundary conditions for events	39
Table 2-8: Historical overtopping events in Stonehaven	40
Table 2-9: Modelled overtopping rates for historical events (l/s/m)	41
Table 2-10: 2018 overtopping rates for a range of return periods (l/s/m)	44
Table 2-11: 2118 overtopping rates for a range of return periods (l/s/m)	44
Table 2-12: Feature Manning's <i>n</i> classification	47
Table 2-13: Details of TUFLOW model files	47
Table 2-14: Present day and climate change still water levels for a range of return periods	54
Table 2-15: Maximum depth limited wave heights for a range of SWL	61
Table 2-16: Still water levels for key return periods at Stonehaven	70
Table 2-17: At risk assets - 30 year, 2018	72
Table 2-18: At risk assets - 30 year, 2118	73
Table 2-19: At risk assets - 200 year, 2018	74
Table 2-20: At risk assets - 200 year, 2118	76
Table 3-1: Summary of historical beach recycling operations	78
Table 3-2: Stonehaven Bay sections summary	82
Table 3-3: Volumetric changes within each section (2008 to 2013)	86
Table 3-4: Volumetric changes within each section (2013 to 2018)	86
Table 3-5: Volumetric changes within each section (2008 to 2018)	86
Table 3-6: Volumetric changes above the toe of the Cowie training wall	92
Table 3-7: Volumetric changes within Carron recharge area	96
Table 3-8: Preferred model setups for each section	100
Table 3-9: Annual Average Retreat (m/year) for each profile	109
Table 3-10: Extreme Sea Levels from UKCP18	111
Table 3-11: Crest elevation variation	111
Table 4-1: Direct flood damage assumptions	116
Table 4-2: Average property for Stonehaven (prices taken from Zoopla, Sept. 2018)	117
Table 4-3: Rateable values applied to non-residential receptors	118
Table 4-4: Count of inundated properties for Present day scenarios	122
Table 4-5: Breakdown of 2018 flood damages	125

Abbreviations

1D	One Dimensional (modelling)
2D	Two Dimensional (modelling)
AAD	Annualised Average Damages

CFBD	Coastal Flood Boundary Dataset
DEFRA	Department of the Environment, Food and Rural Affairs (formerly MAFF)
DTM	Digital Terrain Model
FCERM	Flood and Coastal Erosion Risk Management (R&D programme)
FPS	Flood Protection Scheme
HR	Hydraulic Research, Wallingford
Hs	Significant Wave Height
LiDAR	Light Detection And Ranging
mAOD	metres Above Ordnance Datum
MDA	Maximum Difference Algorithm
MHWN	Mean High Water Neaps
MHWS	Mean High Water Springs
MSL	Mean sea level
NCCA	National Coastal Change Assessment
OS	Ordnance Survey
PvD	Present Value Damages
RMSE	Root Mean Square Error (objective function)
SEPA	Scottish Environment Protection Agency
Tp	Wave Period
TUFLOW	Two-dimensional Unsteady FLOW (a hydraulic model)

1 Introduction

1.1 Overview

Stonehaven is a coastal town located approximately 20 km to the south of Aberdeen, with the village of Cowie located immediately to the north. The two communities sit within Stonehaven Bay on the shore of the North Sea, with the Rivers Carron and Cowie discharging into the bay (Figure 1-1).

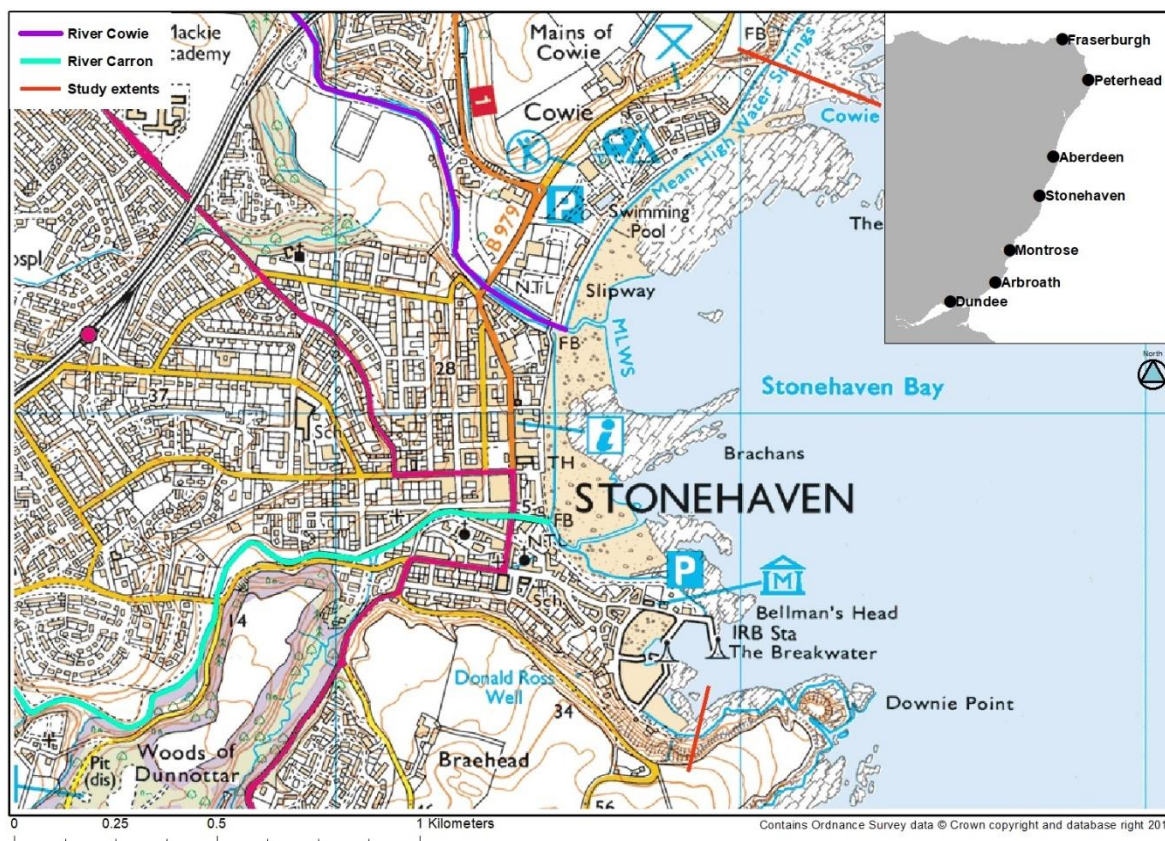


Figure 1-1: Location plan

JBA were commissioned by Aberdeenshire Council to undertake a coastal Flood Protection Study (FPS) to consider options to reduce coastal flood risk within Stonehaven and Cowie. The key project stages, and where this Interim Modelling Report fits into the context of the wider project are summarised below:

Information Review Report	Complete
Supplementary studies	Complete
Modelling and baseline economics	Interim Modelling Report
Engineering and options appraisal	Underway

This report has been prepared to present the modelling methodology for review purposes. It is split into three main chapters covering (i) flood modelling, (ii) geomorphological assessment, and (iii) baseline economics.

2 Flood modelling

2.1 Coastal flood risk drivers

The first stage in coastal flood modelling involves consideration of the local coastal processes and key mechanisms of flooding, as it is essential that the modelling accounts for these processes in as realistic manner as possible.

Figure 2-1 illustrates the main components that contribute to coastal flooding during a storm event. Historical events have shown that flood risk due to still water levels (SWL) alone is limited within Stonehaven and Cowie, with wave overtopping being the primary mechanism that results in coastal inundation.

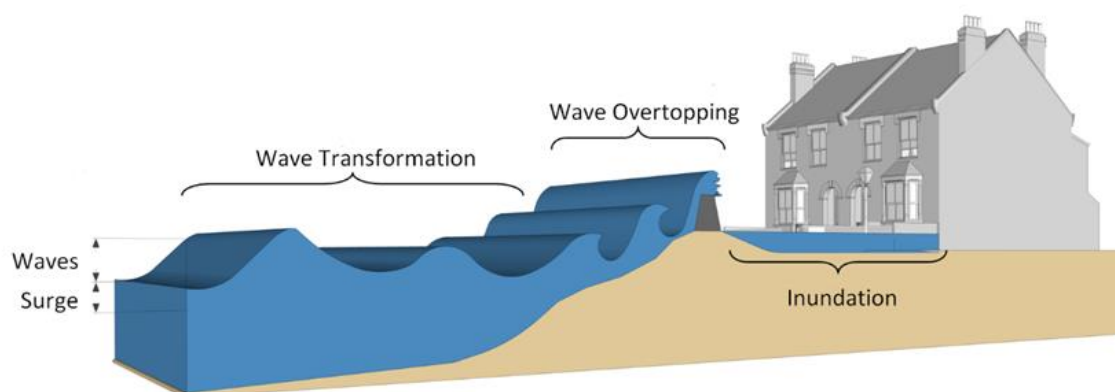


Figure 2-1: Components of coastal flood risk

2.2 Historical flood events

A review of historical flood events is crucial to provide context and develop an understanding of local flood mechanisms, as well as providing an evidence base for model development and calibration. A review of historical events in Stonehaven and Cowie was undertaken within the Information Review Report¹, with the events documented ranging from waves overtopping the outer harbour walls with no effect on roads or properties, to large scale events that resulted in flooding to multiple properties and evacuations.

The most significant event in recent years occurred in December 2012. This resulted in significant flooding, structural damage and risk to life. The December 2012 event has formed the main focus of model calibration herein.

2.3 Modelling schematisation

There is no one modelling package available that can simulate all of the elements of coastal flood risk simultaneously. As such, the modelling undertaken herein required the development and coupling of a suite of numerical models. The steps are outlined below:

Multivariate statistics – SEPA’s offshore multivariate (MV) dataset was used to produce dependence models that describe the relationships between offshore waves, wind and still water levels. The size of the extreme multivariate condition datasets (ca. 2 million iterations of offshore conditions) meant it was unfeasible to run the wave transformation model for each condition. A sub-set of the full MV dataset was therefore derived using a maximum difference algorithm (MDA); this was taken

¹ Stonehaven Bay Coastal Flood Protection Study, Information Review Report, Final Report, September 2018
AKI-JBAU-00-00-RP-HM-0002-S3-P02-Interim_Modelling_Report

forward to the wave model, with the results used to train emulator functions and provide results for the full multivariate dataset in the nearshore.

Still water level transformations – Still water level elevations for a range of return periods were readily available from the updated (2018) Coastal Flood Boundary Dataset (CFBD).

Wave transformation - SEPA's existing SWAN model developed for the AnAc coastal flood forecasting system and used within SEPA's coastal flood map updates was used as the basis of a cut-down SWAN model, used to transform the offshore waves to the nearshore. The model was calibrated using the Stonehaven wave buoy.

Emulation – The MDA was run through the calibrated SWAN model, with the results used to train emulators at the toe of each defence. The emulators were subsequently used to provide nearshore conditions for the full multivariate dataset.

Wave overtopping – The defences within Stonehaven and Cowie were schematised using the Neural Network within EurOtop II. The schematisations were calibrated using historical events and the full multivariate dataset run through the models to provide overtopping rates for a range of return periods.

Flood inundation – SEPA's existing TUFLOW model developed for SEPA's coastal flood map updates was used as the basis of a detailed flood inundation model. This was forced by an offshore tidal graph in conjunction with overtopping inflows so as to produce a single flood extent that represents the risk from both mechanisms.

Each of these steps is discussed in detail below.

2.4 Multivariate datasets

In 2017, SEPA developed offshore multivariate datasets for offshore wave, wind and water level conditions across Scotland. Here, point JP2 has been used. This combines wind from point 2625 and waves from point 2664 of CEFAS' WavewatchIII offshore wave model. The location of this can be seen in Figure 2-2.

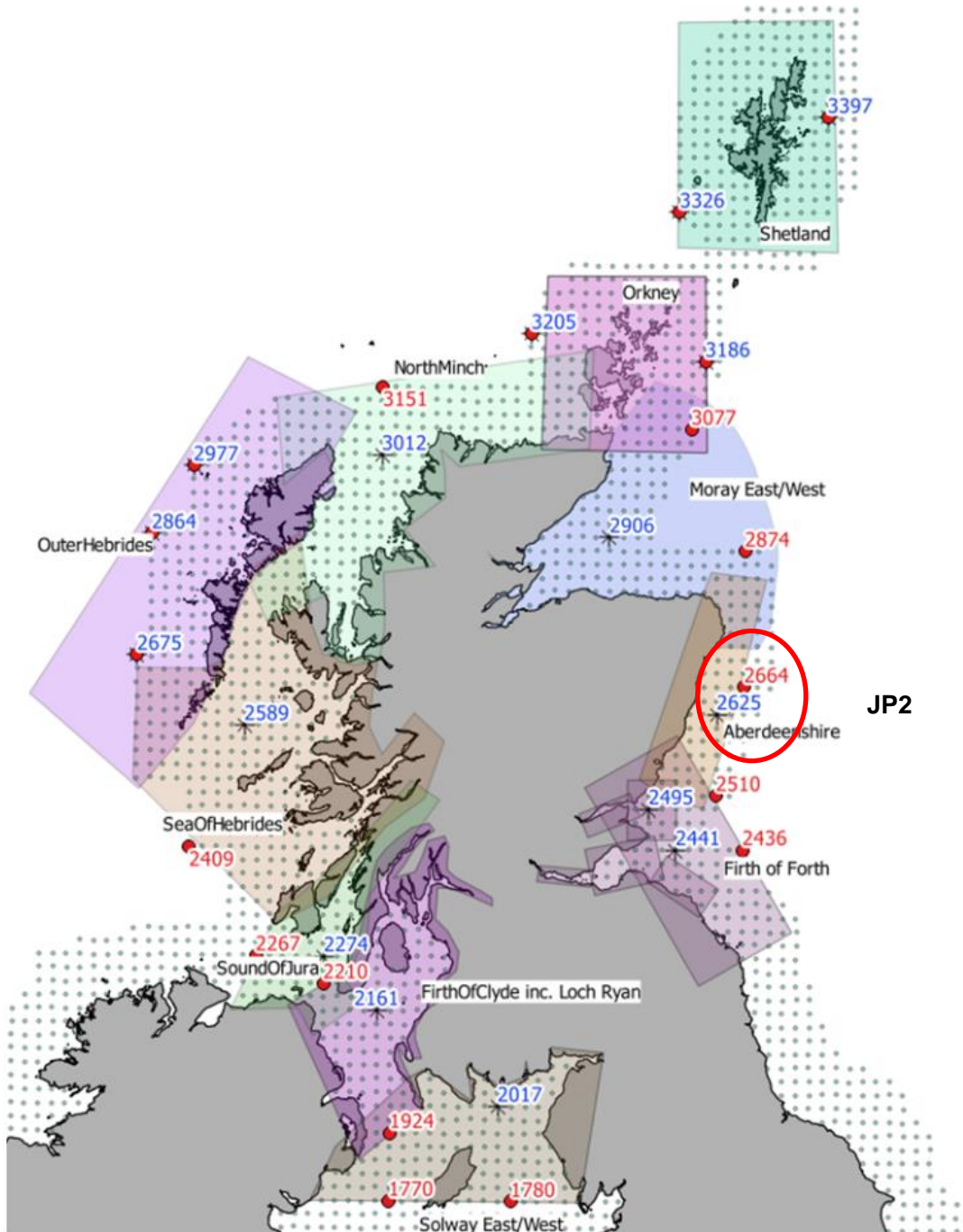


Figure 2-2: Scottish offshore multivariate datasets

The JP2 offshore multivariate dataset provided by SEPA consists of 2,038,804 discrete events expressed as a combination of wind speed, wind direction, wave height, wave direction, wave steepness, directional spreading and water level. This dataset is representative of 10,000 years of events at the offshore location, with water levels based off Aberdeen.

Prior to use of the dataset, wave steepness and H_s were used to estimate peak period (T_p). This was done by first estimating T_e (peak energy period) from H_s and Steepness (s) using the equation below, with T_p then estimated using a standard JONSWAP spectrum.

$$T_e = \sqrt{\frac{2\pi H_s}{sg}}$$

The dataset was subsequently assessed to remove events that do not result in overtopping of the defences. Events were removed if they satisfied the following criteria:

- The water level was below a level that would not produce extreme (1yr) overtopping. Testing of depth limited waves showed the onset of overtopping to be aligned with water levels above 1mAOD.
- If both wind and waves were originating from the west sector (200° - 360°).
- If the water level was below Mean High Water Springs (MHWS) (2.07mAOD), offshore H_s was below 2.25m and wind speed was below 15m/s; these values were selected through SWAN modelling and overtopping calculations.

This reduced dataset constituted the starting point for present day extreme conditions. The same filtering was then applied to the 2118 event set, with uplifted water levels for future scenarios.

2.4.1 MDA generation

The datasets (2018 and 2118) defined above were taken as the basis from which to create the MDA dataset of ca. 1,000 events for use in the SWAN model and emulator training and validation. The MDA and the combined multivariate datasets are provided in Figure 2-3. The figure clearly shows the filtering applied for water level and direction.

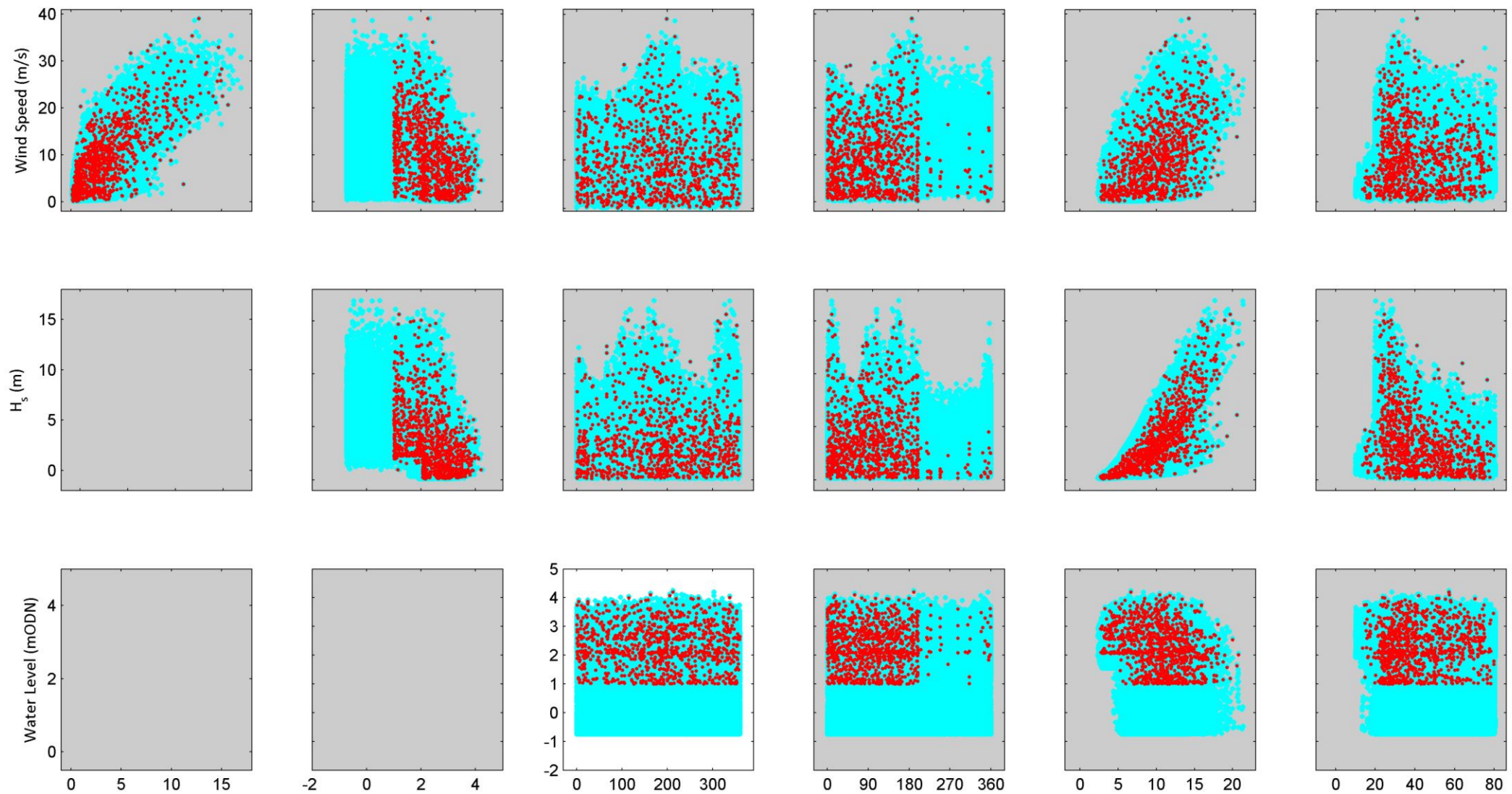


Figure 2-3: Multivariate data (turquoise) vs MDA data (red)

2.5 Water level transformations

The multivariate water levels are based on the BODC A class gauge at Aberdeen. For use in this study these values required transformation to Stonehaven. To achieve this a water level equation was generated by fitting a function to the 1 in 50 year return period water levels from the Coastal Flood Boundary Dataset (CFBD) using the northing coordinate and based on the distance from Aberdeen. This fitting and equation can be seen in Figure 2-4.

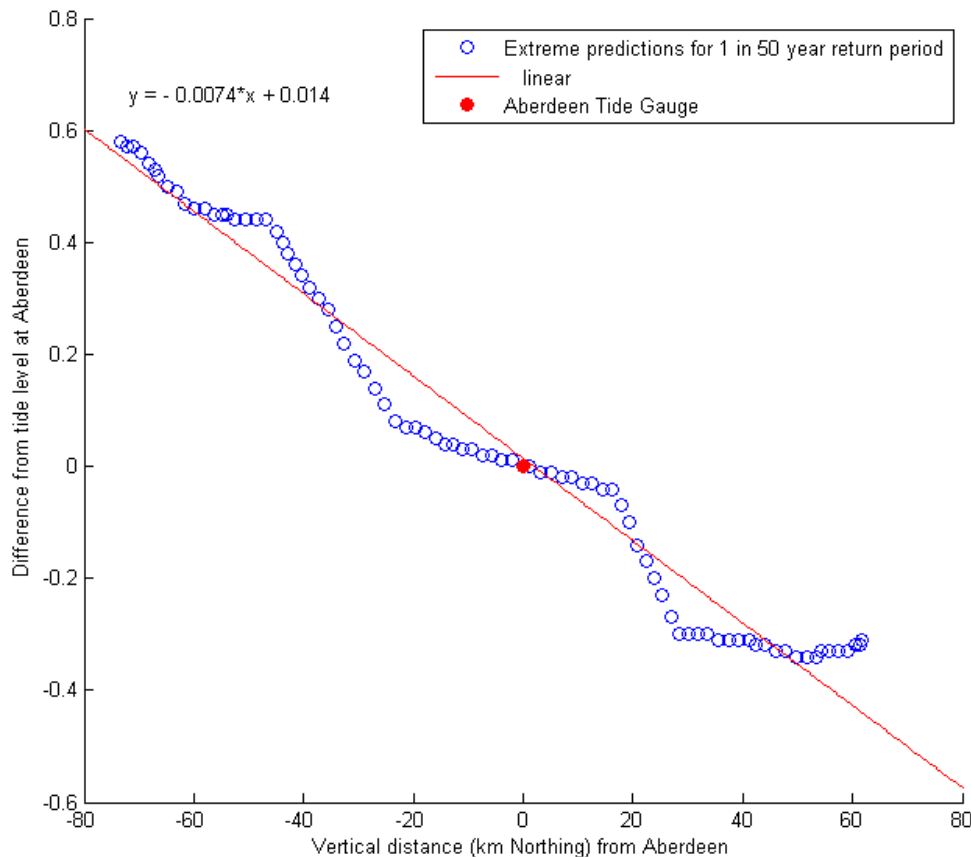


Figure 2-4: Extreme still water level equation for the model domain, based on Northing change relative to Aberdeen

This method of water level transformation was used within the SWAN modelling, creating a varying water-level grid within the model domain. This method was also used in the AnAc FFS system and the coastal flood mapping update, and has been found to be appropriate for locations along the coastline.

2.6 Wave transformation

Wave action is a complex process controlled by a number of factors. Waves are generated in deep water and then propagate towards land. As they do so, they enter shallower bathymetry where wave transformation processes occur, including shoaling, diffraction, refraction, depth limitation and breaking. The waves are also subject to the additional influence of wind. The consequence of these processes is that the properties of the waves when they reach the base of coastal defences are quite different to those in deep water. In terms of coastal flood risk, it is the nearshore waves that are of the greatest importance, as it is these that interact with beaches and defences and ultimately lead to wave overtopping and inundation.

To simulate the nearshore wave characteristics at the defences along the study frontage, a wave transformation model was developed using the industry standard SWAN (Simulating Waves Nearshore) modelling software. SWAN is a third-generation wave model capable of simulating the following nearshore wave transformation processes:

- Wind-wave interactions - the transfer of wind energy into wave energy, leading to the growth of waves.
- Shoaling - the build-up of energy as a wave enters shallow water, causing an increase in wave height.
- Refraction - the change in wave speed as waves propagate through areas of changing depth, causing a change in wave direction.
- Wave breaking - the destabilisation of a wave as it enters shallow water, causing broken waves with the characteristic whitewash or foam on the crest.
- Wave dissipation - limits the size of waves through white-capping, bottom friction and depth-induced breaking.

SWAN calculates stationary wave statistics for specific inputs of wave height, period and direction at an offshore boundary, and wind speed and direction applied across the model domain.

2.6.1 Model domain

The SWAN model domain covers the coastline from Montrose in the south to Aberdeen in the north and extends offshore to SEPA’s JP2 multivariate point (Figure 2-5).

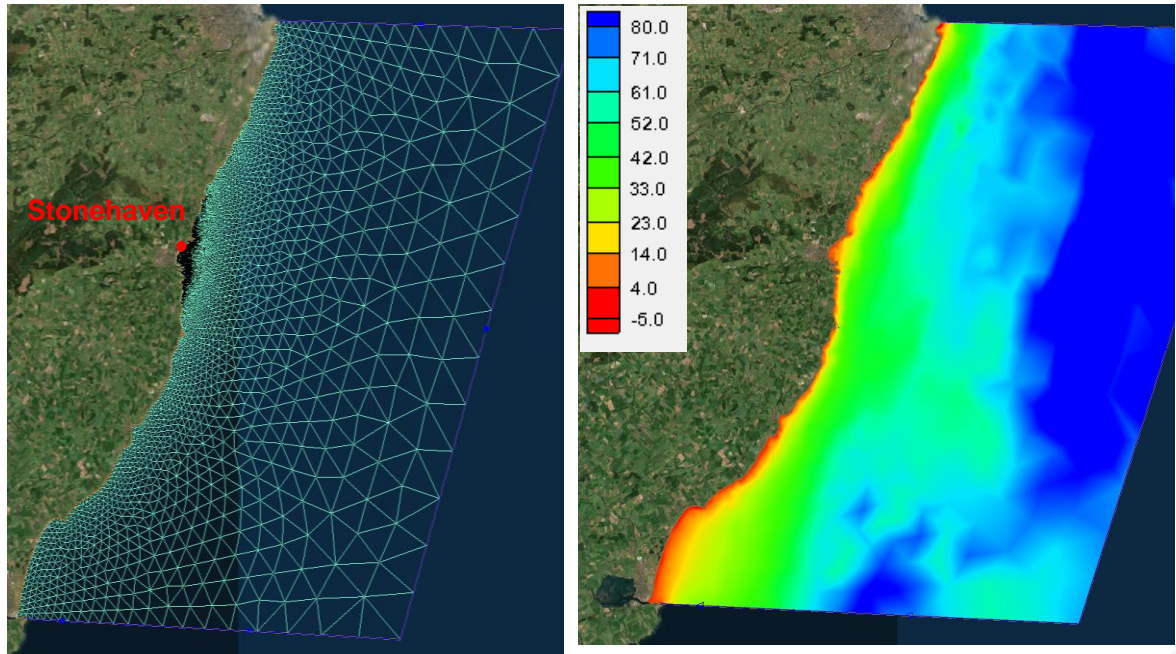


Figure 2-5: SWAN wave model mesh (left) and bathymetry (right)²

² Background imagery from SMS World Imagery (2018). All depths in SWAN model given in meters Below Ordnance Datum. AKI-JBAU-00-00-RP-HM-0002-S3-P02-Interim_Modelling_Report

2.6.2 Topography representation

The coastline and bathymetry within Stonehaven Bay is complex, with 40m high cliffs to the north and to the south and extensive shore platforms and other rocky features controlling the underlying geometry of the sea bed within the bay. To effectively model wave transformation here, these features were included within the mesh through appropriate refinement (Figure 2-6). Of particular interest is the feature in the centre of the bay (The Brachans) and the extensive shore platforms fronting Cowie and Bellman’s head due to their influence on the shoaling and diffraction/refraction of incoming waves. These features are well represented within the model mesh.

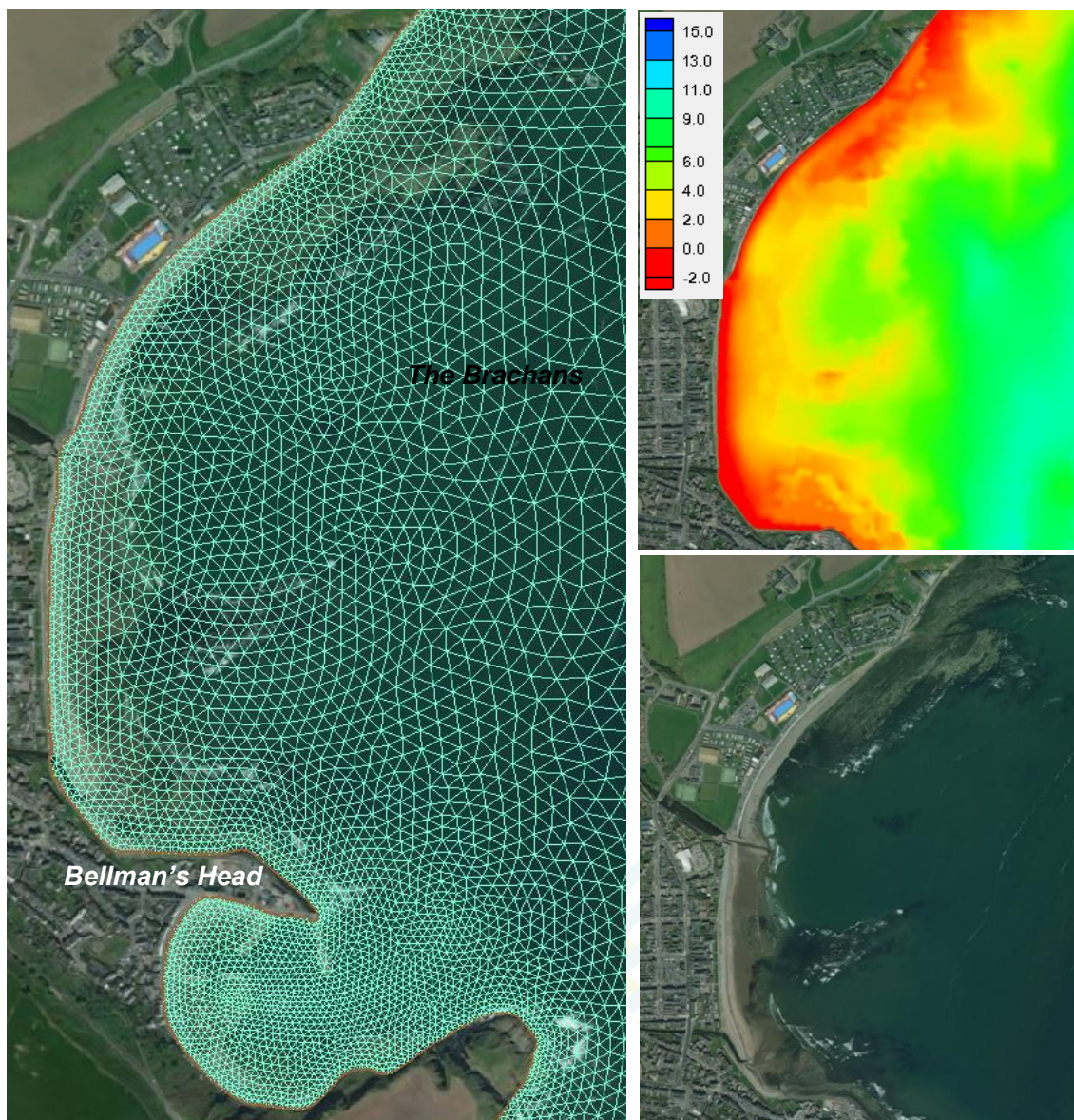


Figure 2-6: SWAN wave model mesh within Stonehaven Bay², depths in meters below ODN

2.6.3 Harbour representation

SWAN is a phase averaging wave transformation model and does not resolve the sea surface, rather the overall statistics. As such, in areas where significant wave transformation occurs over a small distance (such as around a breakwater or within a harbour) SWAN cannot accurately represent wave conditions. These environments are better represented by phase resolving models. However, the computational requirements of these calculations make them unfeasible for the approach adopted here. Whilst the representation of processes is somewhat poor within SWAN, two wave overtopping output locations are required within the harbour (Figure 2-7) to effectively represent observed inundation. To assist model convergence within the harbour, only the outer harbour wall was represented within SWAN; the remaining three breakwaters were not represented within the mesh.

Initially, results for along Shorehead (SH_H_01) were extracted at point a below. However, results at this location did not represent the level of risk that has been observed historically, likely due to the limitations of the SWAN model within the harbour environment. As such, results for along Shorehead were subsequently extracted at the centre of the harbour (point b), resulting in greater correlation between the model results and historical events. Results at the southern extent of the harbour are extracted at point SH_H_02.

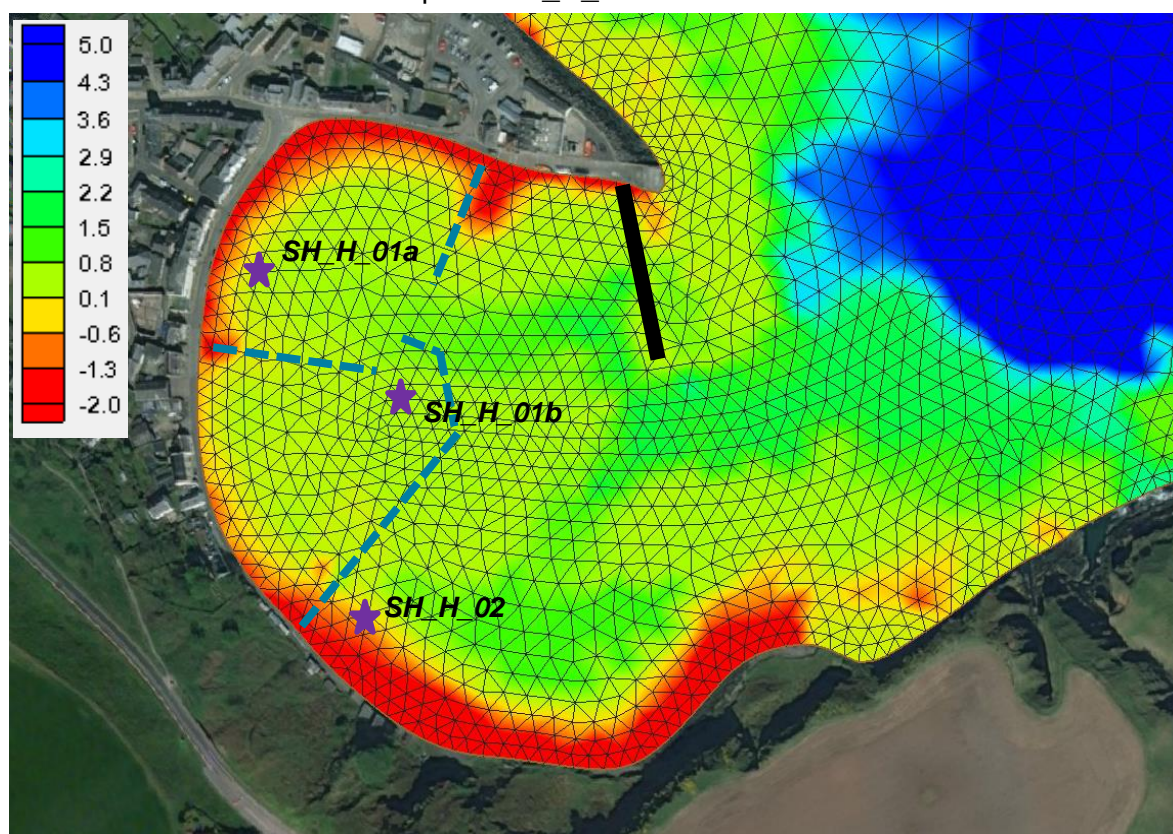


Figure 2-7: SWAN representation of Stonehaven Harbour²

2.6.4 Calibration

To improve the accuracy of the model and provide confidence in outputs a calibration process was undertaken using observed data at the Aberdeenshire Council wave buoy within Stonehaven Bay. Eight events were considered, comparing the percentage RMSE (Route Mean Squared Error) of Hs, Tp and Dir for each potential model setup. These results are presented in Table 2-1.

Table 2-1: Calibration RMSE scores of different model setups, given as a percentage of observed spectra

Model setup parameters		RMSE Hs (%)	RMSE Tp (%)	RMSE Dir score
Wind growth	Friction			
JANS	JSWP	12.62%	9.90%	9.83
JANS	Coll	12.38%	9.90%	9.81
JANS	Mads	13.04%	9.81%	9.76
Kom	JSWP	13.08%	9.82%	9.31
Kom	Coll	12.78%	9.82%	9.30
Kom	Mads	13.18%	9.73%	9.22
Westh	JSWP	13.57%	9.53%	9.26
Westh	Coll	13.40%	9.53%	9.25
JANS	JSWP	12.62%	9.90%	9.83
JANS	Coll	12.38%	9.90%	9.81

The final model set up uses the Komen wind growth model and Collins friction model with a bias correction for hindcast conditions identified by HR-Wallingford and Royal Haskoning DHV as part of the development of the multivariate data. The performance of this setup can be seen in Figure 2-8. This was found to be the best performing model setup based on the results of the calibration.

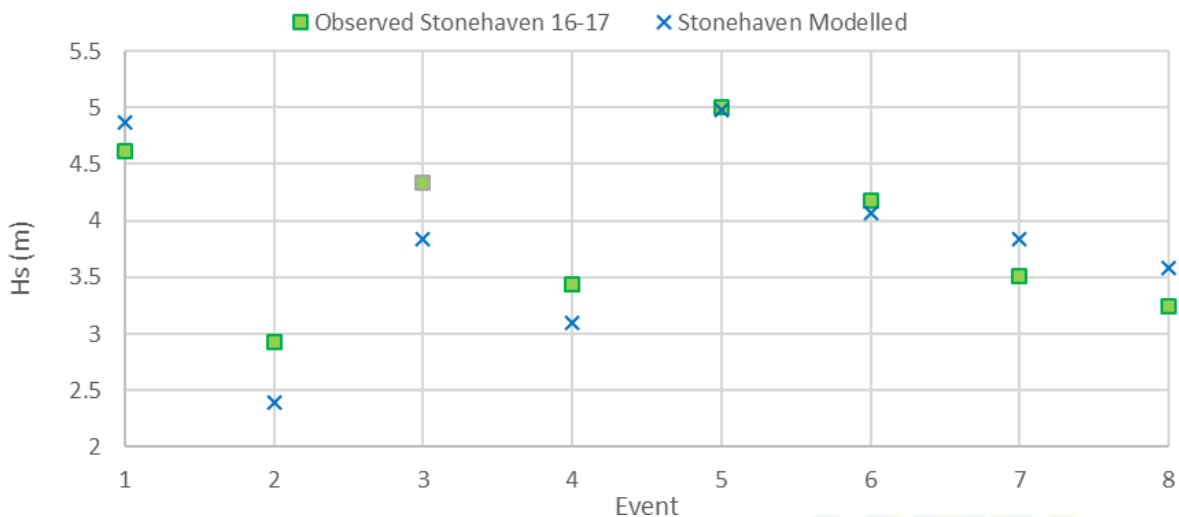


Figure 2-8: Modelled vs observed Hs for final SWAN model set up

2.7 Emulation

2.7.1 Emulator locations

The offshore wave conditions for the MDA sample were transformed to the nearshore using the SWAN wave model. Results were output at ten nearshore toe locations as well as at the wave buoy. The output locations are provided in Table 2-2 and can be seen graphically in Figure 2-9.

Table 2-2: SWAN output locations

Cross section ref.	SWAN model node	Easting	Northing
SH02	4264	387995.9	786750.3
SH06	4421	387912.3	786646
SH12	4446	387618.7	786327.9
SH17	5579	387573.6	786089.7
SH20	6055	387568.0	785941.2
SH25	6564	387624.3	785668.7
SH28	7402	387557.0	785662.0
SH29	7778	387883.5	785575.1
SH_H_01a	8796	387709.5	785437.8
SH_H_01b	8958	387777.5	785397.4
SH_H_02	9088	387786.6	785253.8
Cal_Buoy	6316	388669.9	786159.2



Figure 2-9: SWAN model output locations

2.7.2 Emulator training

The MDA events were used to derive functions that describe the relationship between the input variables (water level, offshore wave spectra, wind speed and wind

direction) and modelled nearshore wave conditions. In order to produce a dataset for training the emulators and a separate, independent dataset for validation, the modelled SWAN results were divided, with 90% of the results used to create the emulators (training data) and the remaining 10% used for validation of these emulation functions (validation data).

The training data was used to select the empirical function that best describes the relationships between offshore and nearshore wave conditions, specifically the wave height, period and direction. A range of functions and coefficients are fitted to SWAN outputs with the validation dataset then being used to establish a Nash-Sutcliffe (NS) score (using the equation below) for the function.

$$E = 1 - \frac{\sum_{t=1}^T (Q_m^t - Q_o^t)^2}{\sum_{t=1}^T (Q_o^t - \bar{Q}_o)^2}$$

The error stat measures the accuracy of the model predictions, with a value of 1 indicating a perfect match, 0 indicating that the function is as accurate as the mean of the modelled data, and < 0 indicating that the mean of the modelled data is a better estimate than the function. The results are presented in Table 2-3.

Table 2-3: Best performing emulator scores and functions

Toe Ref.	Hs Func	Hs NS	Tp Func	Tp NS	Dir Func	Dir NS
SH02	Cubic	0.628	Cubic	0.960	Thin Plate	0.840
SH06	Cubic	0.707	Cubic	0.969	Thin Plate	0.852
SH12	Cubic	0.799	Thin Plate	0.941	Thin Plate	0.836
SH17	Cubic	0.787	Cubic	0.962	Thin Plate	0.860
SH20	Cubic	0.760	Default	0.967	Thin Plate	0.817
SH25	Cubic	0.759	Thin Plate	0.937	Thin Plate	0.708
SH28	Cubic	0.603	Thin Plate	0.972	Thin Plate	0.875
SH29	Cubic	0.739	Thin Plate	0.970	Thin Plate	0.919
SH_H_01a	Linear	0.831	Thin Plate	0.872	Linear	0.743
SH_H_01b	Cubic	0.925	Thin Plate	0.809	Linear	0.283
SH_H_02	Cubic	0.791	Thin Plate	0.808	Thin Plate	0.129
Cal_Buoy	Cubic	0.985	Cubic	0.964	Thin Plate	0.906

Generally, the emulation performs better for the deeper toe locations. This is due to these having a greater number of events available with which to train the emulation functions. For toes that are located at a higher elevation, the number of events available is reduced as the toe is essentially 'dry' for events with a lower water level.

The NS scores for Hs mostly rest between 0.70 and 0.93 with the exception of select higher level toes (SH02 and SH28). These similarly score lower for direction. As does the higher toe (SH_H_02) within the harbour. This can be attributed to the lower number of training runs and the complex shore bathymetry present at the toe of these structures. Overall, the emulators perform well for wave period, only dropping below 0.90 within the harbour.

Emulator diagnostics plots for all toes are provided in Appendix A. Potential sources of errors for the poorest performing emulation locations are outlined below, with diagnostic plots provided in Table 2-4.

Toe SH02

The NS score for Hs emulation at SH02 is 0.63, with an R^2 value of 0.70. The emulation function here improves as the modelled wave heights increase; lower wave heights (below 0.6m) show the greatest scatter in modelled vs emulated wave heights. The larger errors in this dataset come from runs with dissonance between wave and wind directional forcing. Period and direction emulate well, scoring above 0.80.

It is considered that the emulation of large waves is appropriate for use in overtopping modelling of extreme events and the low NS score can be predominantly attributed to a poor performance of small waves or non-standard events (opposing wind /wave directions). Such events are unlikely to significantly impact extreme overtopping.

Toe SH28

The NS score for Hs emulation at SH28 is 0.60, with an R^2 value of 0.67. The wave and wind roses displayed in Table 2-4 show that for events with large waves (greater than 0.6m) there is a high degree of divergence between input wave and wind directions (waves from the SE and wind from the NNE). The remainder of the dataset appears to perform well with relatively low errors between emulated and modelled. Emulated wave period and direction performed well with both scoring above 0.87.

It is considered that the emulation of large waves is appropriate for use in overtopping modelling of extreme events and the low NS score can be predominantly attributed to a poor performance of small waves, or offshore wind conditions. Such events are unlikely to significantly impact extreme overtopping

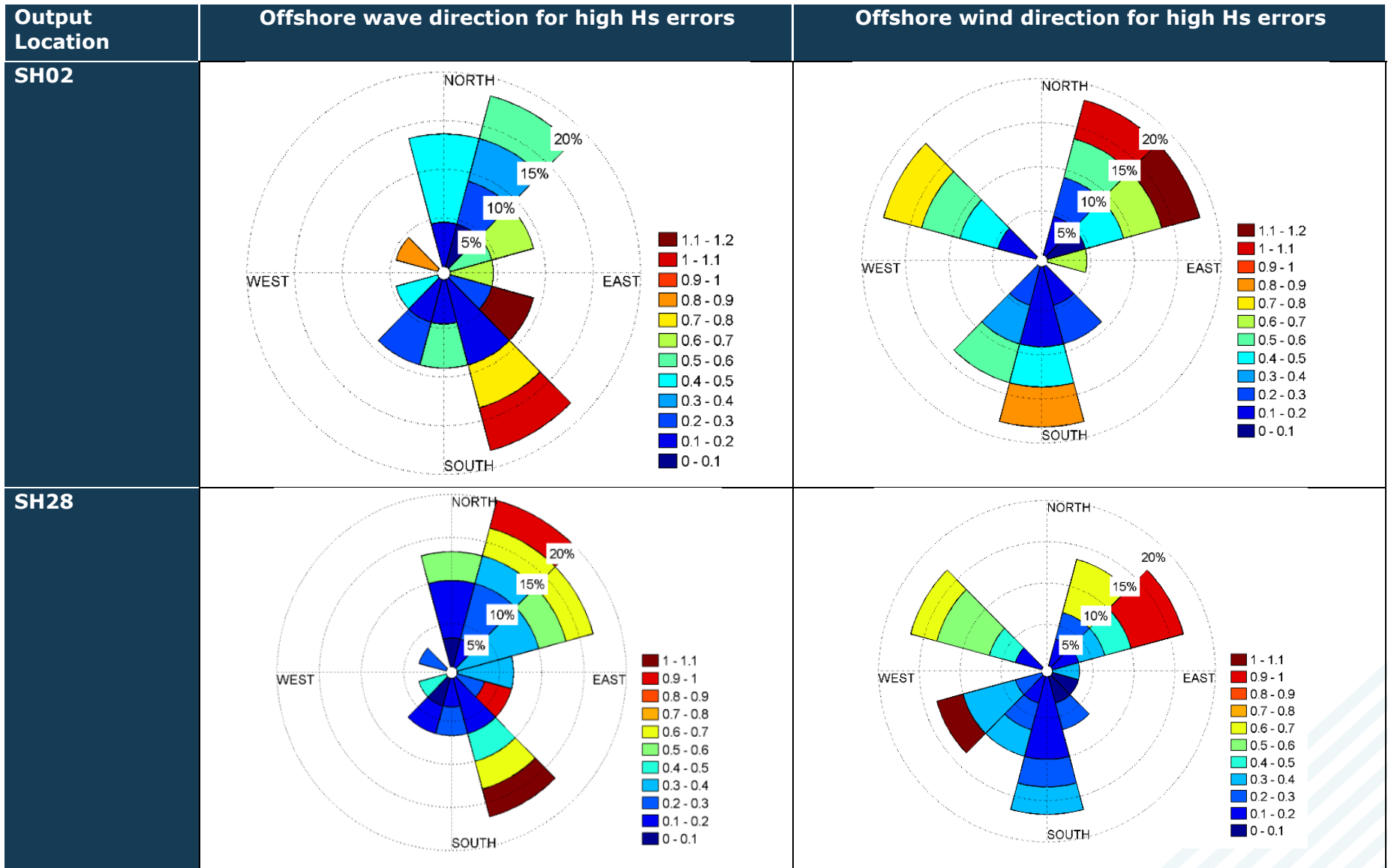
Toes SH_H_01a, SH_H_01b and SH_H_02

Both nearshore toes within the harbour have poor directional emulation scores, particularly SH_H_02. Both SH_H_01 and SH_H_02 output toes are at high elevations and, despite only the harbour curtain wall being included within modelling, within areas of complex bathymetry. This poor emulation is attributed to variance in the phase averaging method of wave modelling of SWAN within harbours and the small variation in the direction of incoming waves. This is a limitation of the method and highlights that there is a greater uncertainty associated with modelling waves within the harbour.

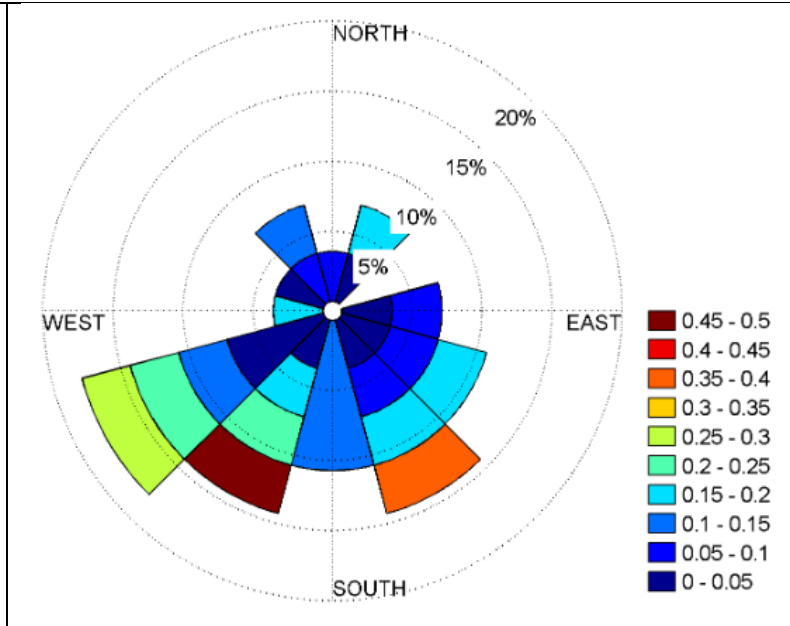
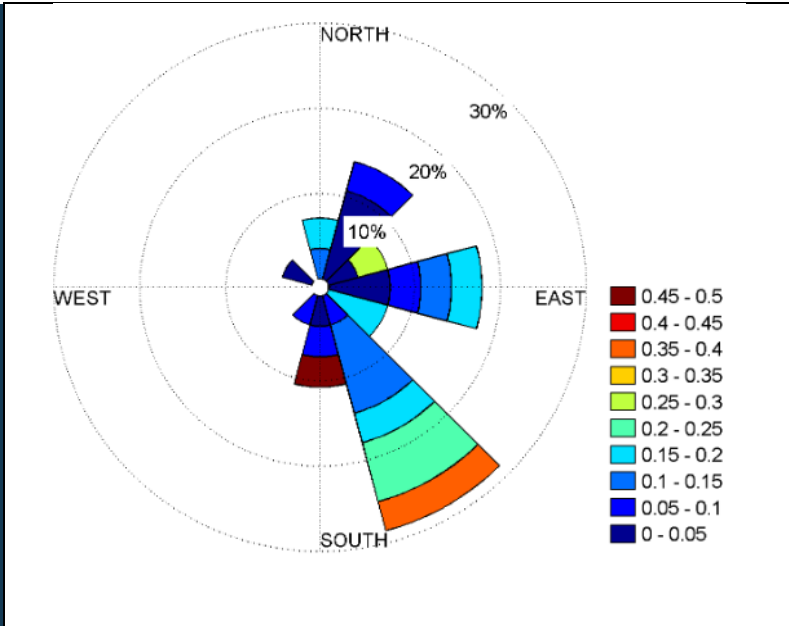
Toe SH_H_1b is an additional wave output point for cross-section SH_H_01 with greater exposure and in deeper water. This output location was included to mitigate short fallings in the phase averaging approach to wave transformation in SWAN and poor representation of non-linear interactions within the harbour. This is confirmed with greater wave heights simulated within both hindcast and multivariate datasets.

This uncertainty is inherent in the modelling of this section and is a limitation of the wave transformation methodology. This uncertainty has been mitigated by the calibration of overtopping rates in the hindcast (discussed in section 2.8). This, however does not eliminate the potential for computational inaccuracies within the modelling and it is accepted that the rates for these sections are more uncertain than the other output locations.

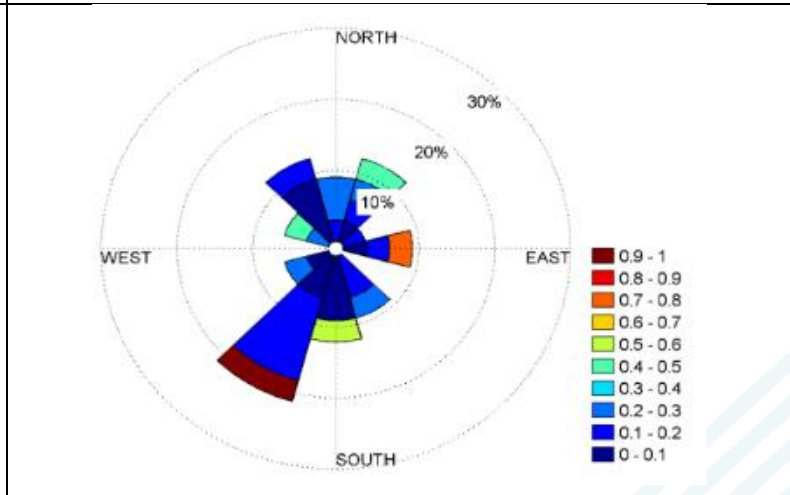
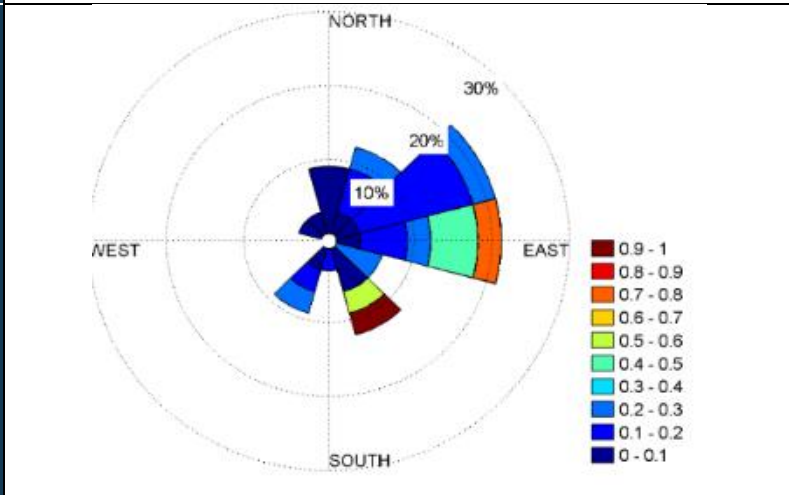
Table 2-4: Diagnostic plots for locations with poor emulation performance



SH_H_01a



SH_H_02



2.7.3 Emulated datasets

The preferred emulator functions were used to transform the offshore wave and wind conditions to the nearshore for both the present day and future datasets. The full, unfiltered, dataset was transformed to the wave buoy location to inform the complete climate here.

In addition, hindcast data from CEFAS WaveWatch III was estimated at all locations. This dataset was then used to provide validation against recorded wave heights at the buoy and historic overtopping events at the defences.

2.7.4 Emulation validation and performance and wave buoy

The emulated data at the buoy was validated against three observed events at the wave buoy in Stonehaven Bay. These events can be seen below in Figure 2-10 to Figure 2-12. They show good performance of wave transformation at the wave buoy with regard to wave heights, timings and the duration of the events.

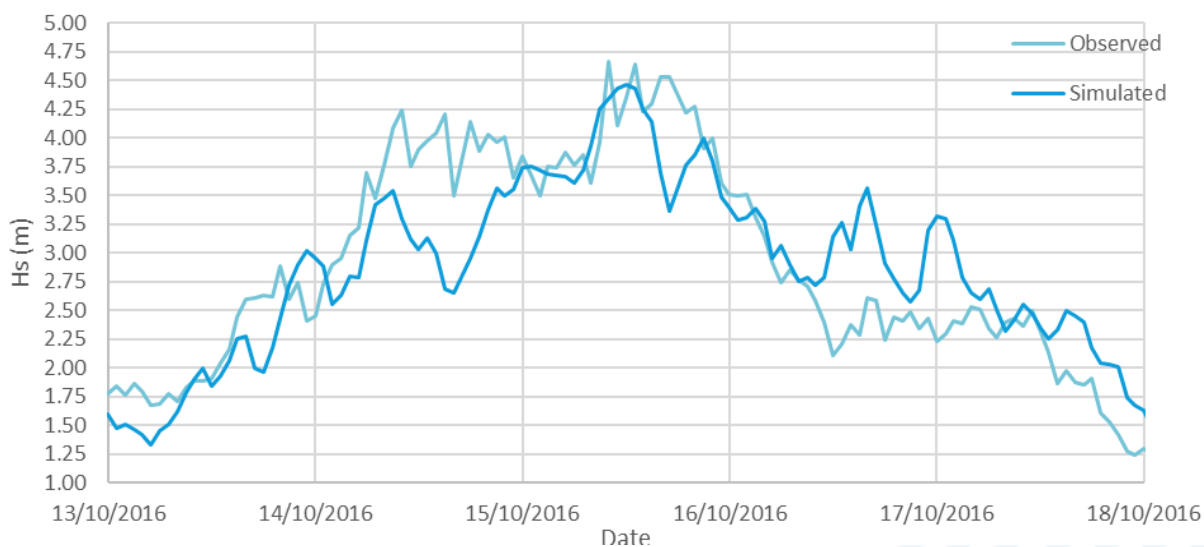


Figure 2-10: Emulator performance at wave buoy - mid Oct 2016 event

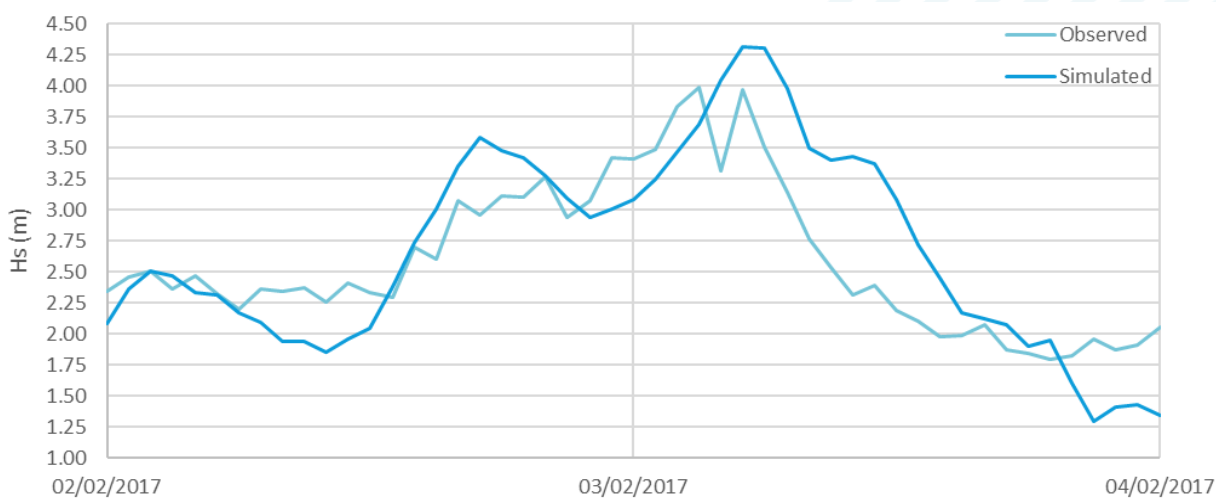


Figure 2-11: Emulator performance at wave buoy - early Feb 2017 event

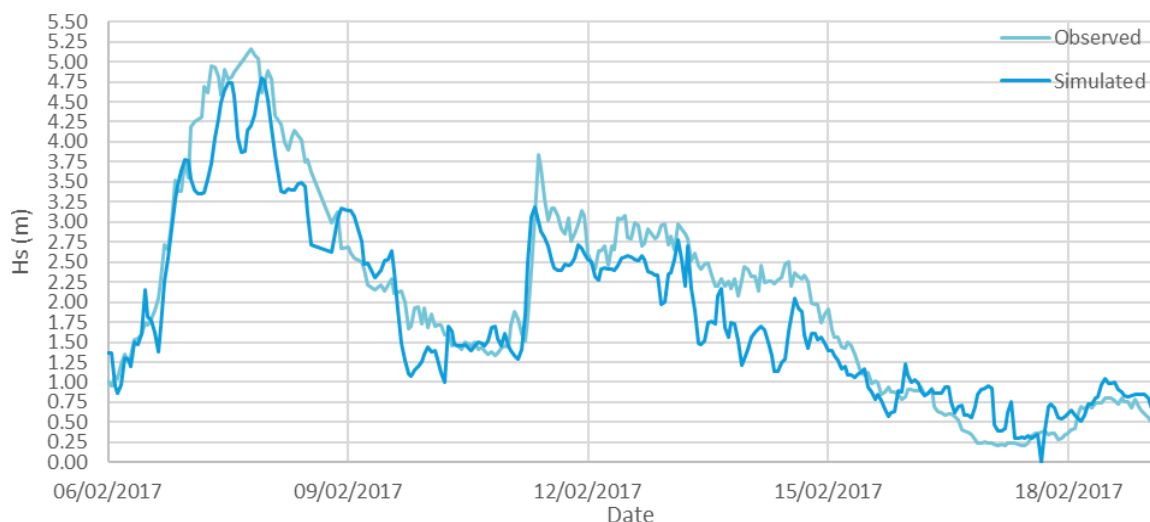


Figure 2-12: Emulator performance at wave buoy - mid Feb 2017 event

2.7.5 Integration

To provide consistency between the SWAN wave model and the overtopping models, the level of the SWAN output node and the schematised toe depths within the overtopping models must be at a similar depth. Table 2-5 shows the depths of each of these, while Figure 2-13 shows their location. The majority of the toe depths match the SWAN toes, with the exception of toes that have been elevated to calibrate with observed overtopping rates (SH02, SH28 and SH29). Wave conditions forcing SH_H_01 are taken at deeper water depths to maximise wave heights. The difference seen at these toes is discussed further within section 2.8.

Table 2-5: Comparison between SWAN and EurOtop toe elevations

Profile Ref.	EurOtop toe depth (mAOD)	SWAN toe depth (mAOD)	Difference (m)
SH02	1.0	1.44	-0.44
SH06	1.0	0.98	-0.02
SH12	-0.30	-0.26	-0.04
SH17	-0.30	-0.31	0.01
SH20	0.20	0.26	-0.06
SH25	1.0	1.18	0.18
SH28	-0.07	-0.71	0.64
SH29	0.50	0.01	0.49
SH_H_01a	1.50	0.91	-0.59
SH_H_01b	1.50	-0.27	1.16
SH_H_02	1.50	1.51	-0.01

2.8 Wave overtopping

The wave overtopping modelling considers how the waves at the toe of the defences interact with the beach and structures to provide estimates of overtopping volume.

This was undertaken using the industry standard EurOtop II³ Neural Network tool. This is considered the most suitable method to assess complex multi-component defence structures, such as those present within the study area.

The Neural Network model uses nearshore wave characteristics at the toe of a defence structure, defence geometry and sea level data to quantify a mean overtopping discharge rate. This rate is expressed in terms of litres per second, per metre length of defence (l/s/m).

Estimates of wave overtopping have large levels of uncertainty associated with them. As such, the focus of the work undertaken herein is on the calibration of results using the historical flood information available. The following sections present the schematisation of the defences as well as the results from the overtopping modelling undertaken.

2.8.1 Wave overtopping schematisations

The Neural Network tool requires several inputs, including the nearshore wave conditions and a defence 'schematisation', based on the geometry, orientation, height and structure material. Schematising the wave overtopping profiles with respect to defence geometry has the following steps:

1. Identification of suitable locations for the profiles
2. Schematisation of the defences at these locations

The locations themselves are provided in Figure 2-13; these are deemed sufficient to quantify the variation in risk, exposure and structure type within the bay. Table 2-6 presents these more specifically along with the Neural Network schematisations developed from the JBA survey.

³ EurOtop – Manual on wave overtopping of sea defences and related structures, Second Edition, 2016
AKI-JBAU-00-00-RP-HM-0002-S3-P02-Interim_Modelling_Report



250 125 0 250 Meters

Contains OS data © Crown copyright and database right 2018

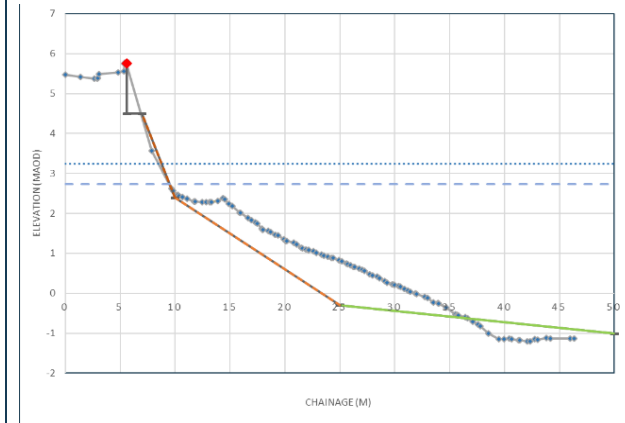
Figure 2-13: Overtopping profile locations



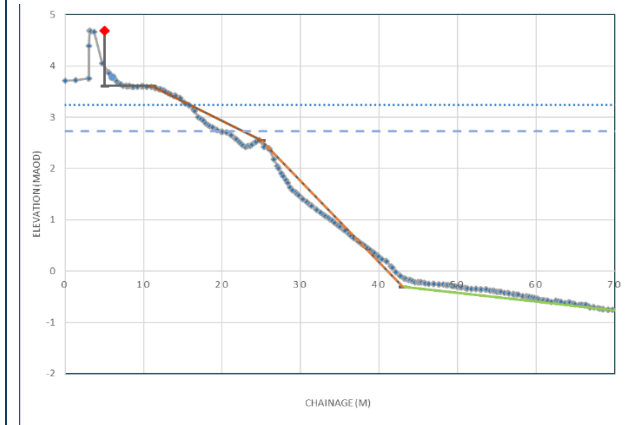
Table 2-6: Wave overtopping cross sections

XS Ref.	Location on aerial imagery	Photograph	Schematised and measured cross section
SH02			
SH06			

SH12

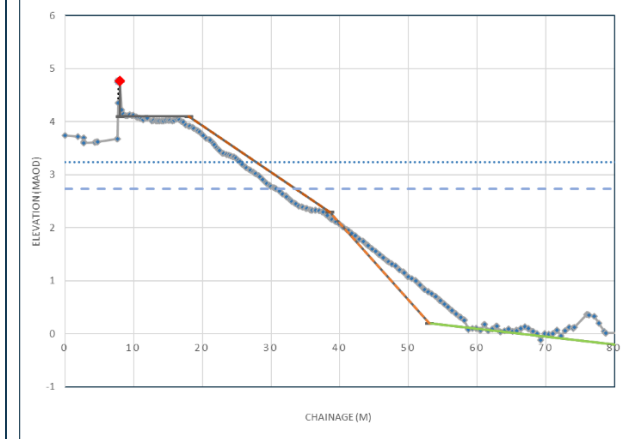


SH17

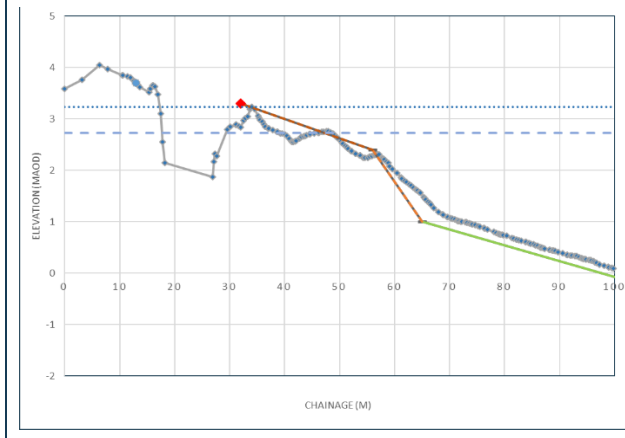
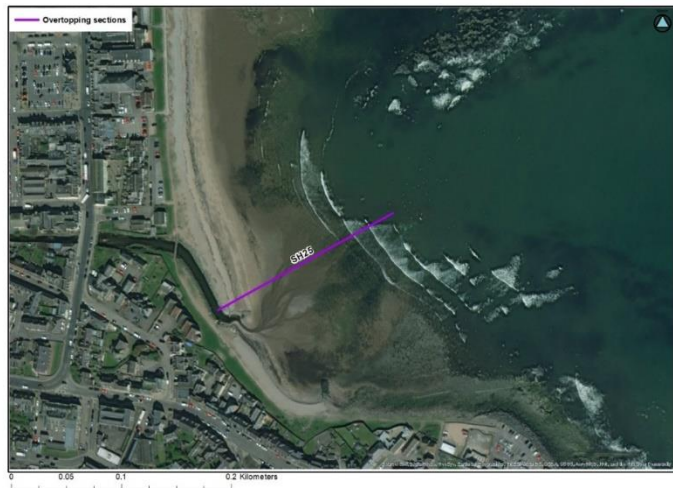


- ◆— Measured Profile
- Schematised Profile
- foreshore slope
- - - Structure lower slope
- - - Structure upper slope
- ◆— Crest Level
- - - T1
- T200

SH20

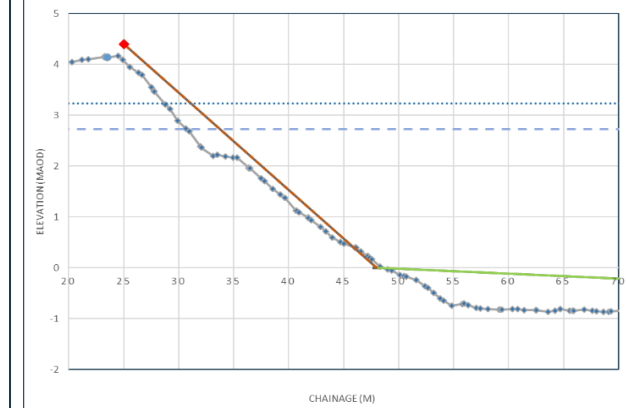


SH25

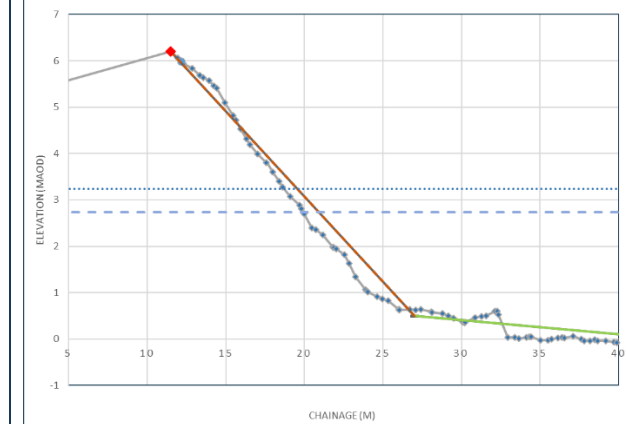


- ◆— Measured Profile
- Schematised Profile
- foreshore slope
- - - Structure lower slope
- - - Structure upper slope
- ◆— Crest Level
- - - T1
- T200

SH28

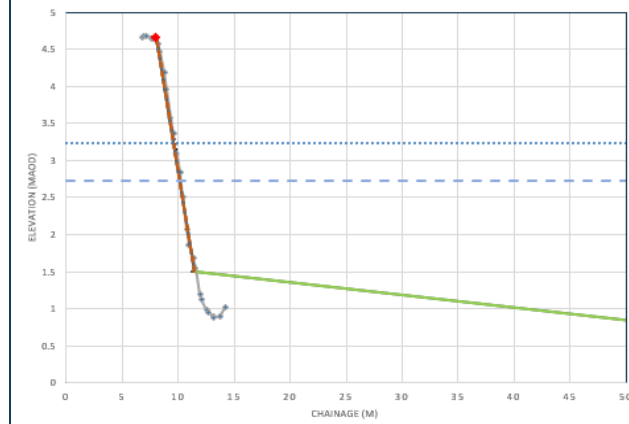


SH29

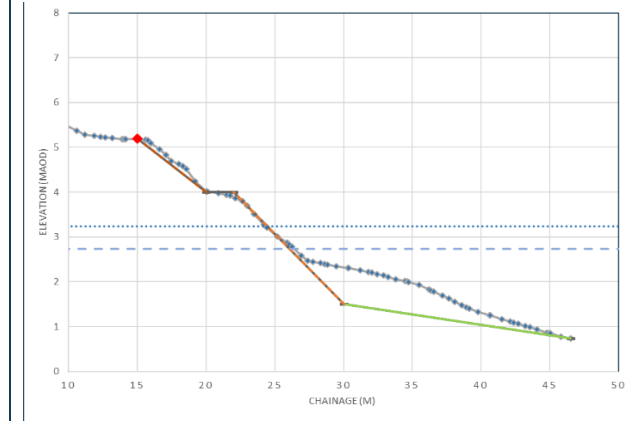
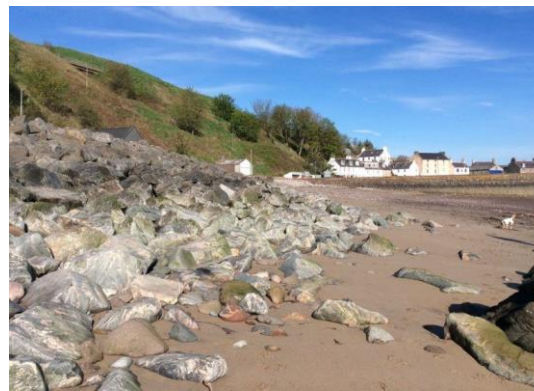


- Measured Profile
- Schematised Profile
- foreshore slope
- Structure lower slope
- Structure upper slope
- Crest Level
- T1
- T200

SH_H_01



SH_H_02



- Measured Profile
- Schematised Profile
- foreshore slope
- Structure lower slope
- Structure upper slope
- Crest Level
- T1
- T200

2.8.2 Wave overtopping calibration

The emulated hindcast data (discussed in Section 2.6) was applied to the Neural Network and used to calibrate the schematisations so that appropriate overtopping rates were obtained. To do this, overtopping rates for thirteen known events were assessed at the 10 defences, with calibration being conducted to fulfil the following objectives:

1. The peak overtopping rates are within the order of magnitude expected given the observed overtopping and damage.
2. The variation in rates within the bay is representative of the differences in observed risk (e.g. SH12 > SH17 > SH20).
3. The annual average overtopping rates are plausible given the observed risk.

Calibration of these overtopping cross sections was undertaken by the modification of the schematised profile whilst keeping the schematisation relevant to the observed defences at each frontage. This constituted the inclusion/omission of berm features (SH28), the modification of crest widths (SH20, to simulate different widths of beach) and the manipulation of toe levels (SH06, SH_H_01 and SH_H_02). It should also be noted that cross sections were taken along a typical defensive profile for each defence whereas wave output locations are situated at an appropriate depth within the model. This is anticipated to have minimal impact on incoming wave spectra.

The events and a brief description of the impacts are presented in Table 2-8. The hindcast boundary conditions used to drive emulation can be seen in Table 2-7. All events, with the exception of 29/10/2014 had a water level in excess of 2mAOD and incoming wave directions from 044 to 176, impacting the shoreline. Events can all be considered extreme considering the MHS level 2.05m AOD, the average modelled Hs (1.5m) and Tp (7.2 sec) over the hindcast period.

It should be noted that the 1 in 20 year SWL event observed in Aberdeen on 5/12/2013 has been omitted from the analysis. This is due to erroneous WaveWatch III hindcast data for this event showing high offshore waves coming onshore; photographic evidence and buoy records do not corroborate this in the nearshore and so this event was removed from the analysis. Similarly, the event on the 12/01/2009 predicted long period waves and large water levels from the south, these combined with the opposing hindcast wind and wave directions confounded emulation, predicting larger waves than observed within the nearshore. This is a source of uncertainty that is inherent in the approach to the modelling, in that the hindcast data can be inconsistent with observed conditions and so overtopping may not match observed values for all events. For reference, the input values used for each event (observed water levels and wind and wave data from the hindcast model) are provided within Table 2-7, with a summary of the impacts of each event within Table 2-8.

For the December 2012 event, both the early morning and the afternoon tide were run through the modelling, with the early morning tide providing the highest rates, as occurred during the event.

Crest elevations from each cross sections were taken from surveyed data obtained by JBA in 2018.

Table 2-7: Hindcast maximum boundary conditions for events

Date	WL, AOD (max)	Hs (max)	Tp (max)	Dir (mean)
01/04/2006	2.40	1.95	10.20	44
20/02/2007	2.60	2.13	7.04	152
06/03/2007	2.50	5.18	9.62	161
10/03/2008	2.66	5.11	10.20	153
12/01/2009	2.81	3.63	9.90	176
08/09/2010	2.26	3.96	9.62	103
08/11/2010	2.38	5.32	10.10	144
15/12/2012	2.58	8.36	13.51	93
29/01/2014	1.65	5.90	10.87	108
03/02/2014	2.28	4.13	8.62	160
07/10/2014	2.29	5.53	12.50	80
24/12/2015	2.50	4.88	10.10	169
10/01/2016	2.05	3.77	10.99	92

Table 2-8: Historical overtopping events in Stonehaven

Event date	Description of impact
01/04/2006	Coastal erosion and collapse of sea wall foundations.
21/02/2007	Overtopping of Stonehaven and Cowie promenade.
06/03/2007	Overtopping and significant overland flow at Beach Road/The Links.
10/03/2008	Shingle and rock armour thrown over sea wall, damage to Cowie sea wall copings. Seafront properties and amenity land flooded, particularly towards Cowie.
12/01/2009	Overtopping of promenade, Boatie Row and Cowie shorefront.
08/09/2010	Overtopping at Boatie Row and along The Links. Flooding behind.
08/11/2010	Outer and inner harbour walls overtopping with overtopping along Stonehaven shorefront.
15/12/2012	Significant overtopping and damage to shorefront properties as well as evacuations.
29/01/2014	Outer and inner harbour walls overtopping. Mostly foam.
04/02/2014	Overtopping at swimming pool and Boatie Row.
07/10/2014	Significant overtopping at Stonehaven harbour wall and along the promenade.
24/12/2015	Overtopping of frontage and shingle strewn across road.
10/01/2016	Overtopping of defences along The Links.

The hindcast modelling shows overtopping for at most cross sections for each event considered. Following an initial review, some schematisations were adjusted to modify overtopping rates to better match the anecdotal impacts.

The modelled overtopping rates at each cross section are presented in Table 2-9. It should be noted that the values presented are average overtopping rates; in some locations the damage observed could have resulted from large infrequent waves, versus some areas where small volumes overtop frequently.

The rates are considered appropriate for the events selected given the records available and evidence of flooding, with each section along the frontage discussed below.

Table 2-9: Modelled overtopping rates for historical events (l/s/m)⁴

Event date	SH02	SH06	SH12	SH17	SH20	SH25	SH28	SH29	SH_H_0 1a	SH_H_0 1b	SH_H_0 2
01/04/2006	0.27	0.15	0.29	0.09	0.05	6.50	0.01	0.03	-	-	-
20/02/2007	0.42	0.95	0.13	0.03	0.02	0.14	-	0.07	-	-	-
06/03/2007	0.49	0.46	0.75	0.32	0.05	6.90	<0.01	0.03	-	-	-
10/03/2008	1.43	0.89	2.94	1.94	0.47	18.70	0.02	0.05	-	0.13*	0.75
12/01/2009	3.14	2.15	3.67	2.27	0.44	30.30	<0.01	0.12	-	-	-
08/09/2010	0.16	0.13	0.37	0.16	0.06	6.79	<0.01	0.05	-	-	-
08/11/2010	0.27	0.22	0.92	0.51	0.12	14.50	0.01	0.05	-	0.16*	-
15/12/2012	1.10	0.59	4.92	3.86	0.77	56.70	0.19	0.10	-	0.171	0.77
29/01/2014	-	-	0.09	0.01	0.01	<0.01	0.01	-	-	-	-
04/02/2014	0.18	0.16	0.53	0.21	0.06	6.02	<0.01	0.04	-	-	-
07/10/2014	0.25	0.33	1.18	0.52	0.10	13.40	0.07	0.04	-	-	-
24/12/2015	0.54	0.44	1.77	0.96	0.19	2.58	<0.01	0.03	-	-	-
10/01/2016	0.22	0.15	0.51	0.13	0.03	1.84	0.01	-	-	-	-

⁴ * indicates poor representation within neural network training data – rates not reliable.

Harbour cross sections

Initially, with the toe location at SH_H_01a, the cross section within the inner harbour showed no overtopping for the events assessed. As SWAN is known to be poor within confined harbours this is not unexpected. Overtopping from events in the multivariate data exist but it is likely that the risk was underestimated at this location. As a result of this under-performance at the toe, the larger waves simulated at output location SH_H_01b were used to generate overtopping. This produced more appropriate overtopping for observed events and so was taken forward within the modelling.

Emulators found wave heights at this location to be largely independent of depth and predicted generally small waves (<0.8m) with longer periods which were used to produce overtopping. Figure 2-14 shows the small number of simulated hindcast events that satisfy filtering applied for toe SH_H_01b (Crest freeboard : $H_s < \text{five}$, RC/H_s), plotted against the CLASH training data. Approximately five records in the training database have a RC/H_s ratio greater than four, with none of these being in the range of our hindcast data. Subsequently, much of the simulated events undergo high degree of interpolation/ extrapolation to produce overtopping rates. To mitigate this, a lower RC/H_s ratio of four was selected for this location as, although waves with a ratio of between four and five produced overtopping, these were not considered accurate.

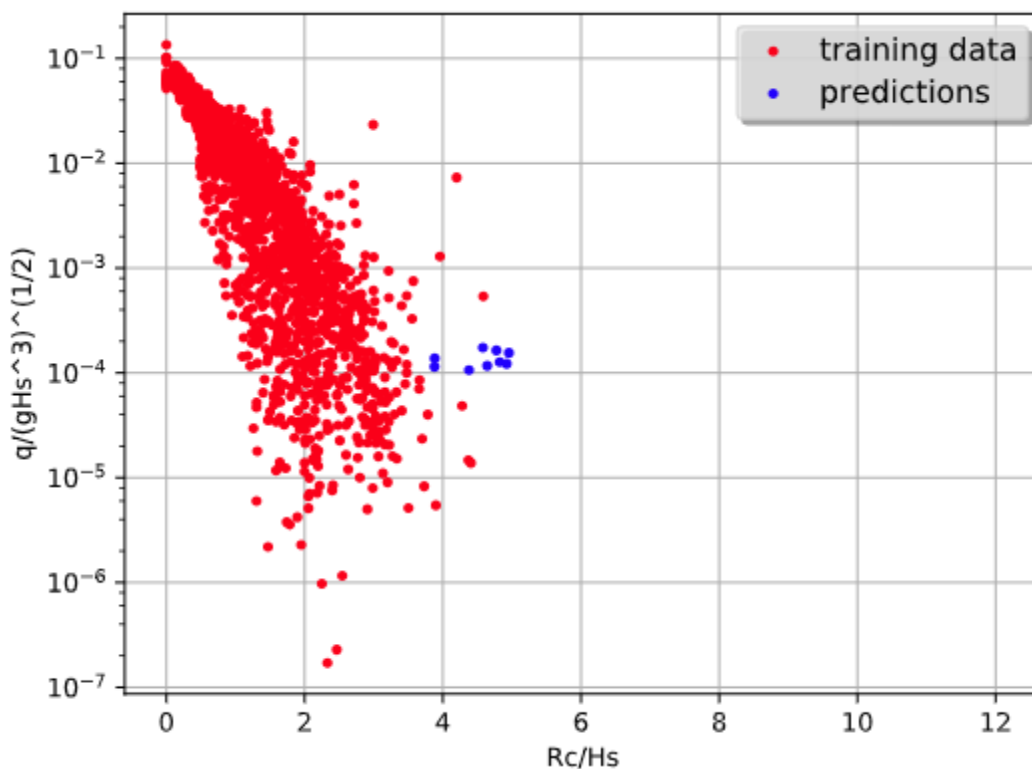


Figure 2-14: Overtopping output of forcing conditions with overtopping training data. Output from Overtopping.ing.unibo.it.

The cross-section to the south of the harbour overtops to a greater magnitude than the more sheltered cross section located within the harbour, and notably is modelled to overtop on 15/12/12, when anecdotal evidence exists of damage to the sheds situated here.

Bellman's Head cross sections

For cross-section SH28 it was necessary to elevate the schematised toe level from -0.71 to -0.07 to reduce the incoming wave heights, similar limitations were applied to SH29 (0.0m to 0.5m). This is not inconsistent with levels along the frontage however it does deviate from the SWAN node depth. An additional depth-limitation check shows this to have minimal impact on integration with SWAN/emulated outputs.

The cross-sections at Bellman's Head show consistently moderate levels of overtopping for all events. The rates are considered appropriate as large waves rarely propagate from a northerly direction, directly impacting SH28, and SH29 is largely protected by bathymetric features fronting the section.

River Carron mouth

Cross-section SH_25 is situated at the mouth of the River Carron. The overtopping rates are included here to address concerns over wave impacts within the river channel and are considered largely appropriate for the lower crest level of the defence.

Central wall cross sections

Two cross-sections are present along the central frontage of Stonehaven. Both consist of similar beach morphology and defence but are impacted by differing wave conditions. SH20 is more sheltered (from the Brachans) with SH17 being more exposed. This is reflected in the outputs for these cross-sections, with SH20 consistently having lower overtopping rates than SH17.

Cowie cross sections

Three overtopping cross-sections exist within Cowie, with SH12 estimating overtopping at Cowie Pool and shops, and SH6 and SH2 calculating overtopping at Boatie Row and to the north of Stonehaven Bay. These cross-sections have consistently high rates for events where there are reports of significant overtopping at Cowie (e.g. 24/12/2015, 04/02/2012 and 08/09/2010).

2.8.3 Extreme overtopping rates

The overtopping rates for a range of return periods for the present day (2018) and future (2118) are outlined in Table 2-10 and Table 2-11. These rates were estimated by ranking the overtopping rate for all of the multivariate dataset events and assigning probabilities of occurrence based on it being representative of 10,000 years. Again, the variation in risk typically observed along the frontage is evident (e.g. SH12 > SH17 > SH 20).

It should be noted that the overtopping rates for SH25 are not used in the inundation modelling and rather provide an indication of the potential volume of water entering the Carron mouth under extreme conditions.

Table 2-10: 2018 overtopping rates for a range of return periods (l/s/m)

Return Period (years)	SH02	SH06	SH12	SH17	SH20	SH25	SH28	SH29	SH_H_01a	SH_H_01b	SH_H_02
2	0.52	0.58	1.36	0.76	0.22	43.90	0.03	0.08	-	-	0.47
5	1.00	1.09	1.99	1.26	0.37	67.90	0.07	0.11	-	0.04	0.58
10	1.63	1.74	2.57	1.81	0.56	91.70	0.14	0.15	-	0.07	0.70
30	3.56	3.57	3.89	3.11	1.00	140.00	0.36	0.25	<0.01	0.10	1.02
50	4.85	4.78	4.68	4.01	1.33	171.00	0.54	0.33	<0.01	0.11	1.21
100	7.60	7.48	5.91	5.77	1.95	217.00	0.97	0.50	0.01	0.12	1.77
200	11.60	11.60	8.19	8.12	2.99	271.00	1.64	0.76	0.02	0.13	2.72
1000	25.10	26.40	14.30	13.10	6.00	419.00	5.86	1.77	0.05	0.22	9.11

Table 2-11: 2118 overtopping rates for a range of return periods (l/s/m)

Return Period (years)	SH02	SH06	SH12	SH17	SH20	SH25	SH28	SH29	SH_H_01a	SH_H_01b	SH_H_02
2	18.50	17.20	10.70	10.20	3.46	511.00	3.71	1.01	0.01	0.06	4.14
5	29.50	27.10	14.80	14.60	5.32	632.00	7.32	1.59	0.03	0.10	7.48
10	41.50	37.60	18.50	18.60	7.13	733.00	11.90	2.35	0.04	0.12	11.40
30	65.30	58.70	25.70	27.00	11.30	911.00	25.00	4.33	0.06	0.15	24.10
50	77.90	69.30	29.70	32.20	14.30	1000.00	32.20	5.60	0.07	0.16	32.80
100	100.00	89.90	37.10	41.20	19.60	1150.00	45.10	8.47	0.08	0.19	53.20
200	127.00	116.00	46.60	52.70	25.50	1310.00	66.30	12.50	0.10	0.21	89.80
1000	201.00	176.00	69.70	81.10	46.90	1850.00	156.00	26.70	0.17	0.34	268.00

2.9 Flood inundation modelling

A 2D flood inundation model was constructed in the TUFLOW modelling package for Stonehaven and Cowie. The model extends from the mouth of the bay to high ground as well as along the rivers Carron and Cowie (Figure 2-15). It has been used to estimate flood extents and depths for extreme events from a combination of still water levels and wave overtopping.

The following sections provide a breakdown of the key model components, calibration and model outputs.



Figure 2-15: TUFLOW model domain and inflows

2.9.1 Digital terrain model

The base digital terrain model (DTM) was generated from four datasets. These were overlain in an appropriate order to make best use of the data available.

- Cross sectional survey of the River Carron. This data was available along the length of the River Carron from the previous fluvial assessments.
- Terrestrial Laser Scanned (TLS) topography of the beach, coastal frontage and areas within the harbour.
- Phase 2 1m LiDAR data provided by SEPA. This was filtered to remove the representation of the water surface within the model domain.
- Oceanwise bathymetry data within the bay. This was used for the area within the bay beyond the extents of the LiDAR and TLS data.

2.9.2 Feature representation

Not all features within the domain were accurately represented within the combined model DTM. As such, modifications to the DTM were applied; these are detailed below:

Coastal defences

The crest elevations and extents of the defences were not accurately represented within the DTM. These features have been added to the model by enforcing crest elevations from topographic survey. Defences were also added along the banks of the River Carron, thus assuming that the fluvial scheme is in place; these are only required to prevent SWL flooding under the climate change scenarios. Further details of the fluvial-coastal interactions are provided within section 0.

Buildings

Buildings within the model domain were defined from MasterMap data. Elevations for the buildings were taken from threshold survey data, collected either as part of the fluvial scheme or as part of this project. Where threshold data was unavailable a level was identified by the average LiDAR level plus two standard deviations. The levels were used to represent the buildings as 'stubby buildings'; this means that shallow flooding can flow around the buildings, whereas deeper flood depths are able to enter the building and flow through. This will have an impact on the accuracy of the inclusion of these buildings within the economic assessment (discussed in section 4). However, buildings without threshold data were predominately setback from the coastline.

River channels

The channel of the River Carron was included by interpolating bed levels from the fluvial survey data, with the channel of the Cowie Water represented as accurately as possible from available data.

Nearshore rock platforms

The extensive shore platforms along the frontage are uneven and impacted model stability. As the representation of these features was not important to the assessment of flood outlines, these features were smoothed out within the inundation model.

Roughness

The roughness (Mannings's n value) representation of features within the domain was varied according to land use classifications within the OS MasterMap, with the values used presented in Table 2-12.

Table 2-12: Feature Manning’s *n* classification

Manning’s <i>n</i>	Land use classification
0.030	Default floodplain value
0.300	Buildings
0.100	Structures
0.030	Inland and coastal water
0.070	Natural surface and gardens
0.025	Manmade surface, roads and paths
0.100	Trees
0.046	Marsh

2.9.3 Model files

Table 2-13 details the TUFLOW files used within the calibration and extreme event model runs.

Table 2-13: Details of TUFLOW model files

File type	File name	Comments
TUFLOW control file	<i>Stonehaven_~e1~_~s~.tcf</i>	<ul style="list-style-type: none"> - Specifies model start and end times (35h simulation for extreme events) - Specifies timestep of 1.5 sec - Calls all other model control files
TUFLOW general file	<i>Stonehaven_General_Comm ands_001.trd</i>	<ul style="list-style-type: none"> - Specifies model output parameters and locations - Includes standard wetting and drying depths, velocity cut offs, etc.
TUFLOW geometry file	<i>Stonehaven_001.tgc</i>	Specifies grid construction and modifications including: <ul style="list-style-type: none"> - Cell size (4m) and domain extent - DTM mosaic - Defense reinforcement (ZSH files) - Topography roughness - Stability smoothing patches
TUFLOW event file	<i>Stonehaven_Events_001.tef</i>	<ul style="list-style-type: none"> - Defines all events considered - Sets the initial water level for all events - Sets the file path for model checks
TUFLOW boundary file	<i>Stonehaven_Boundary_Control_001.tbc</i>	Specifies the boundary condition locations (OT and SWL) used in all simulations

2.9.4 TUFLOW model validation

The event on the 15th of December 2012 is documented as the most severe coastal flood event in Stonehaven’s recent history. This was used as the validation event for the overtopping and inundation modelling as the most information exists for observed inundation.

The performance of the emulation and calibration of the overtopping models is presented in the preceding sections and was found to tie in well with historical events. Whilst the focus of the validation of the inundation model is to compare the modelled flood extents and depths to records from the Dec 2012 event, by extension this will also provide additional validation of the overtopping rates and nearshore wave heights.

For reference, examples of the observed overtopping during Dec 2012 are presented in Figure 2-16. The photographs were provided by Aberdeenshire Council.



Figure 2-16: Observed overtopping during the December 2012 event

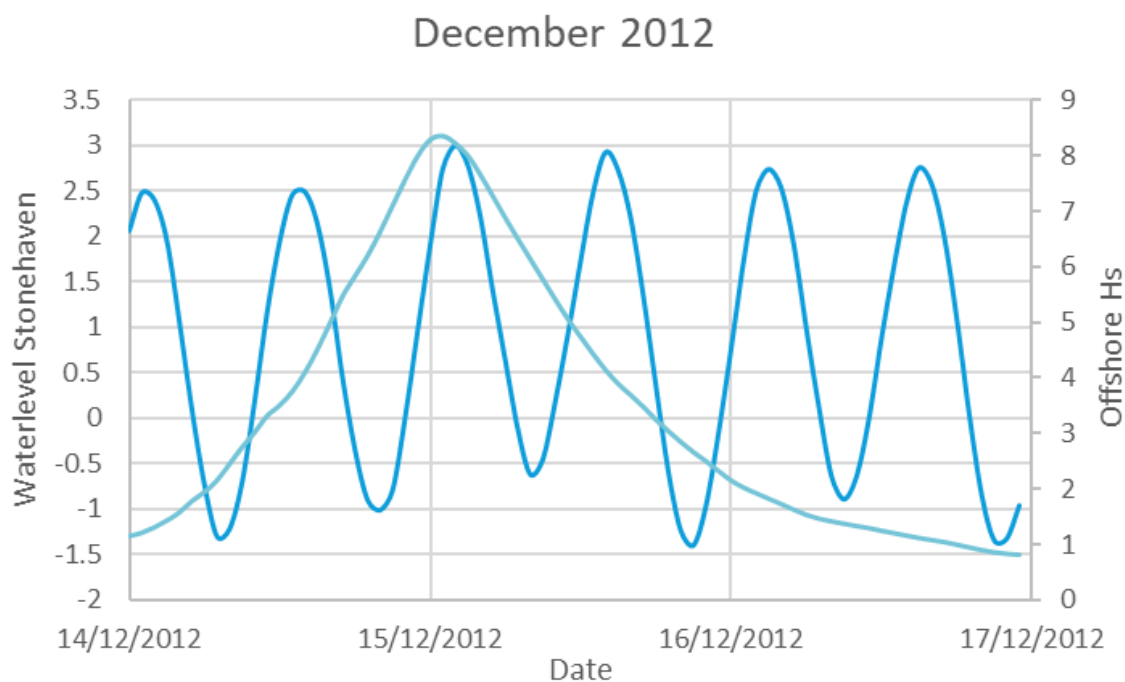


Figure 2-17: Offshore Hs (light blue) and SWL (dark blue) at Stonehaven for December 2012

This event caused evacuations of the sheltered housing along the frontage following to the onset of overtopping. Observations for this event report significant overtopping occurred over two high tides with the tide early in the morning of the 15th having the largest overtopping rate due to the highest offshore waves (Figure 2-17). The next high tide also produced overtopping albeit, at lower rates.

Along the Stonehaven frontage reports indicate that more overtopping occurred at the northern section (around SH_17) than at the middle and lower sections of the frontage. This is supported by the modelled results with higher rates and greater flood extents observed just south of the Cowie. This is considered appropriate and consistent with event observations.

The flood extent for this event can be seen in Figure 2-18 are shown to match well to observed inundation. This is particularly true in the sheltered housing (south of the Cowie) and the area surrounding the leisure centre. At Boatie Row, no photos of inundation are available although overtopping was reported along the Cowie frontage. Given the extent of previous flooding in the area, the modelled extent is appropriate for an event of this magnitude.

The output flood extent for this event can be seen in Figure 2-18 with modelled water levels output in Figure 2-19. Modelled levels at these points match well the onset of inundation and the approximate flood levels.

Observations also indicate a flow of inundated defences from south to north. This is corroborated by modelling which shows a watershed between Ironfield Lane and Cowie Lane from where water flows north toward Turners Court and ponds in the area to the south, surrounding Beachgate Lane.



Figure 2-18: Modelled flood extent for 15th December 2012 event, along with photo evidence from Aberdeenshire Council

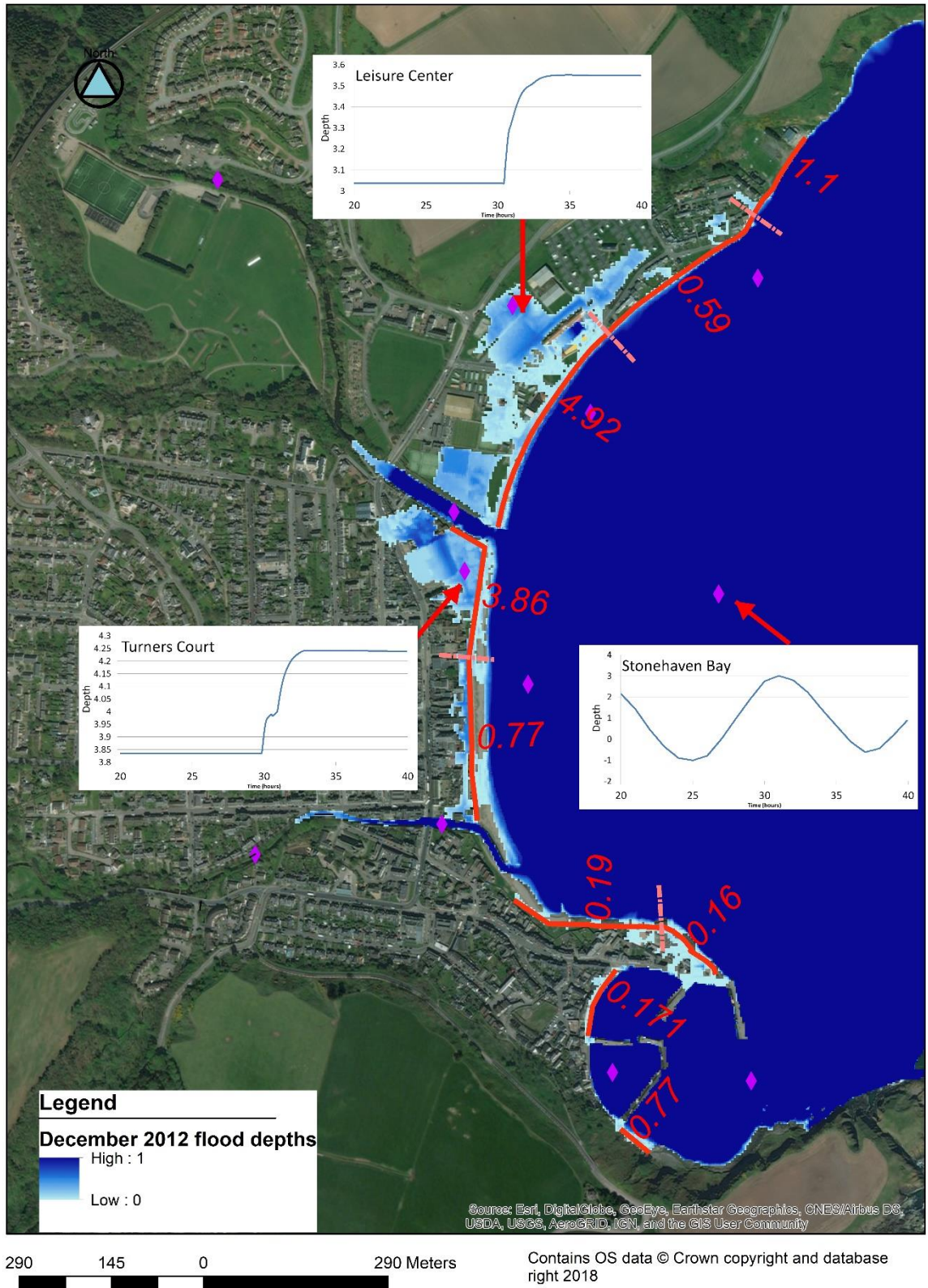


Figure 2-19: Modelled flood extent for 15th December 2012 event, along with overtopping rates and estimated water depths at key locations

Extreme events

Inundation extents and depths for the extreme events are required to inform the baseline economic assessment and the options appraisal. For coastal flood risk, inundation is typically represented as a composite risk from both SWL and wave overtopping. This means that each return period simulation is forced with the corresponding SWL and overtopping rate.

For communities where there is variation in the risk mechanism (e.g. SWL flooding within an estuary and overtopping at the sea) this allows for both to be accounted for. However, when SWL overtopping exists at the coastal defences, this can lead to double counting of flood volume as this will be included in the overtopping rates and simulated in TUFLOW from the tidal graphs. To account for this an additional check is made, where an approximate overtopping volume from the extreme tidal graph (using a broad crested weir equation) is removed from the overtopping rates.

It should be noted that, for all the defences where overtopping is applied in TUFLOW, none are predicted to overtop from SWL alone for present day conditions. Still water levels are anticipated to be close to the defensive crests (particularly within Cowie) for higher return periods in 2118.

Overtopping rates

The peak extreme overtopping rates estimated previously (section 2.8.3) were used to generate a variable rate based on a tidal curve using the underlying peak water level. The same wave conditions are applied throughout, with the wave heights used for overtopping being depth limited based on the water at the toe of the defences throughout the cycle.

The duration of the extreme event conditions is something that is not considered in the multivariate model. As such, it has been assumed that these persist over a single tidal cycle (12 hours). Figure 2-20 provides an example of the extreme overtopping rates at various locations.

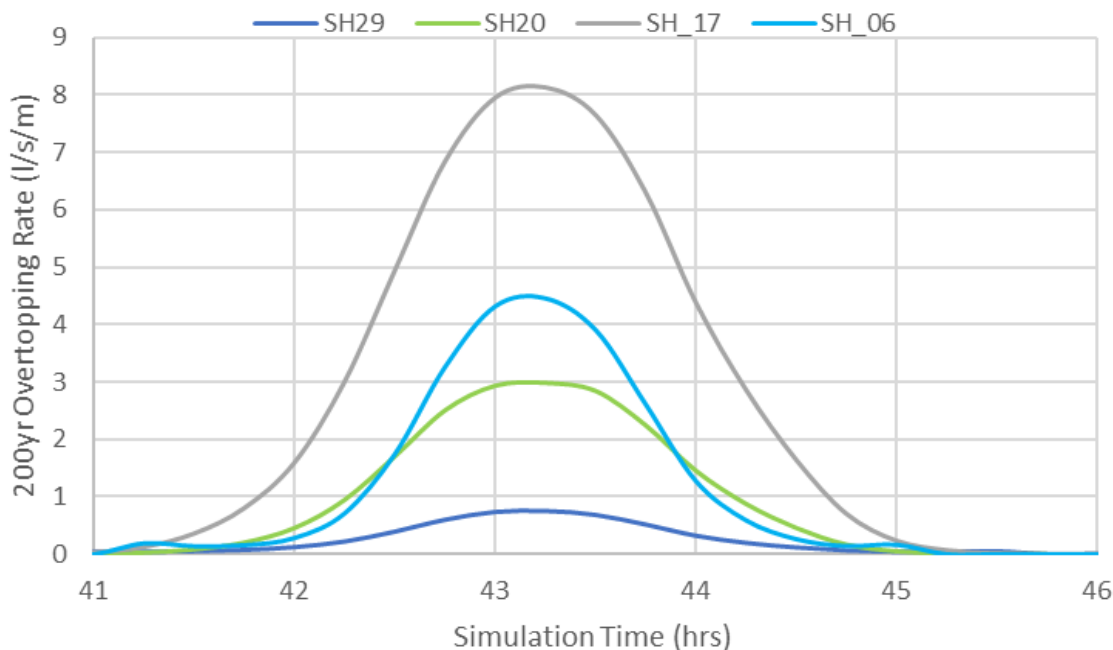


Figure 2-20: Overtopping rate for four selected cross sections for a 1 in 200 year event

SWL tidal graphs

The generation of the extreme SWL tidal graphs follows the CFB methodology⁵. It combines a base astronomical series at Stonehaven from Admiralty Total Tide, a surge shape from Aberdeen and extreme sea levels from the 2018 update to the CFB.

As specified in the guidance, the base astronomical tide has a peak level between MHWS and HAT (2.35mAOD). The surge peak is applied to the preceding trough of the astronomical tide to maximise the flood volume. Given that limited SWL flooding occurs and there are no large estuaries in Stonehaven, it is likely that the positioning of the surge has very little influence on extreme flood depths.

Sea level rise has been considered using the UKCP18 medium emissions, 95th percentile scenario. For climate change scenarios, the extreme sea level and base astronomical tide will be uplifted to 2118 levels. This gives an increase of 0.73m from present day (2018) conditions. Figure 2-21 provides examples of the 200-year tidal graphs for 2018 and 2118.

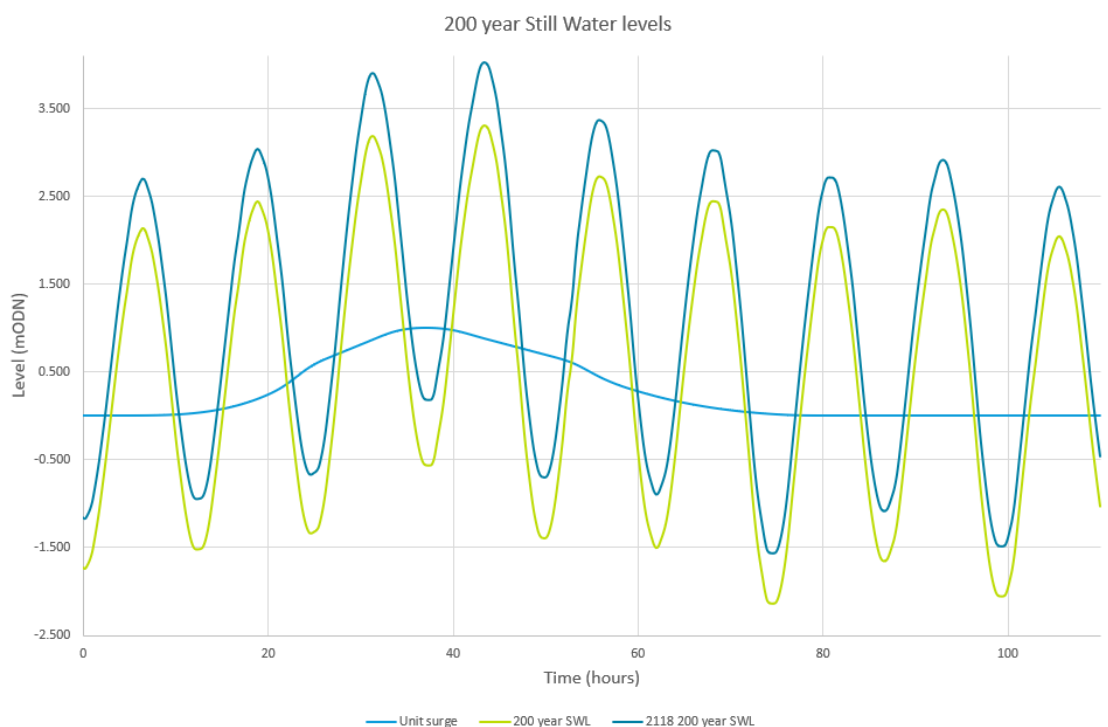


Figure 2-21: Example tidal graphs for 2018 and 2118 200-year events

Table 2-14 shows the still water levels for a range of return periods at Stonehaven. These levels are based on the nearest Coastal Flood Boundary (CFB) dataset node (3250) and represent the peak water level input into the TUFLOW model for each run.

⁵ DEPARTMENT FOR ENVIRONMENT FOOD AND RURAL AFFAIRS. 2011. Technical Report Design sea levels. R&D Report SC060064. Defra/Environment Agency.
AKI-JBAU-00-00-RP-HM-0002-S3-P02-Interim_Modelling_Report

Table 2-14: Present day and climate change still water levels for a range of return periods

Return Period (years)	Present day (2018) SWL (mAOD)	2118 SWL (mAOD)
2	2.824	3.548
5	2.924	3.648
10	2.994	3.718
30	3.108	3.832
50	3.164	3.888
100	3.234	3.958
200	3.304	4.028
1000	3.664	4.178

Extents

As part of this baseline assessment, extreme events for a range of return periods have been modelled. Flood depths and extents for the present day 2-year, 30-year, 100-year and 200-year events are provided in Appendix E along with 2118 flood extents for the 30-year and 200-year events. Section 4 provides a breakdown of the number of properties flooded at each return period.

2.10 Tidal reach of the Cowie Water

The Cowie Water discharges into the North Sea the south of Cowie promenade and to the north of Turners Court. The Cowie Water is tidally influenced up to the weir beneath the B979 road bridge.

2.10.1 Historical configuration

The configuration of the two watercourses at the coast was historically very different, with the Cowie Water running south along the front behind a large shingle bar, and the two merging prior to discharging out into the bay (Figure 2-22). It is understood that the Cowie Water broke through the shingle bank during a storm event in 1948. Anecdotal evidence suggests that large volumes of shingle were removed from the frontage during the 1940s, resulting in a reduced width of shingle⁶.

The photograph presented in Figure 2-23 was taken in 1932 and shows the historical flow path of the Cowie Water behind the shingle bar⁷, whereas Figure 2-24, which was taken in 1948, shows that the two rivers have separate outfalls onto the beach⁸.

⁶ Stonehaven beach shingle loss document supplied by Ian McDonald, Stonehaven resident

⁷ Extract from aerial view, 1932 (SPW040485) © Historic Environment Scotland

⁸ Photo extracted from YouTube video by Ian McDonald, Stonehaven resident
AKI-JBAU-00-00-RP-HM-0002-S3-P02-Interim_Modelling_Report

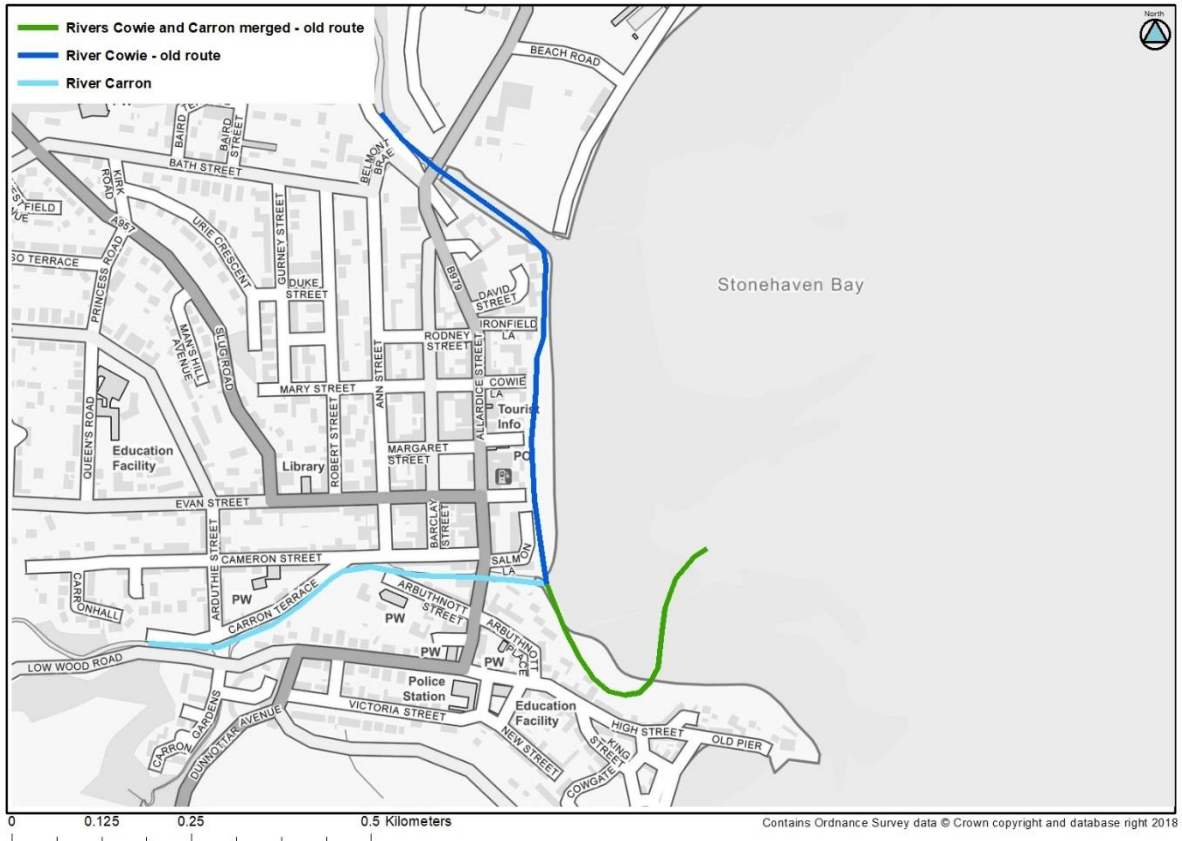


Figure 2-22: Historical configuration of the Cowie Water and River Carron at the coast



Figure 2-23: Image showing historical path of the Cowie Water, River Carron and the shingle bar



Figure 2-24: Image showing the river mouths in 1948 following the Cowie breaking through the shingle bank

2.10.2 Present day configuration

The mouth of the Cowie Water consists of concrete lined banks, with a training wall extending out from the left (northern) bank, a small amount of rock armour present at the end of the right bank, and a footbridge crossing the channel. Flow beneath the footbridge and out onto the beach is constricted by the deposition of shingle, which also extends further upstream along the right bank. Upstream of the

footbridge the channel sides are formed by sheet piles topped with a sloped concrete revetment (Figure 2-26). The current configuration can be seen within the aerial image presented in Figure 2-25; however, it should be noted that the path of the river at the mouth and across the beach does vary.

During storm conditions, it is understood that waves propagate into the mouth of the river. Video footage, provided by Aberdeenshire Council and dated 16 March 2018, shows waves breaking on the shingle bank, resulting in splash over the right hand bank of the river, with smaller waves then running along the right bank revetment and breaking on the weir beneath the B979 road bridge.



Figure 2-25: Aerial image showing the present day mouth of the Cowie Water



Figure 2-26: Looking upstream from the mouth of the Cowie Water to the weir and B979 road bridge



Figure 2-27: Right bank and footbridge at the mouth of the Cowie Water

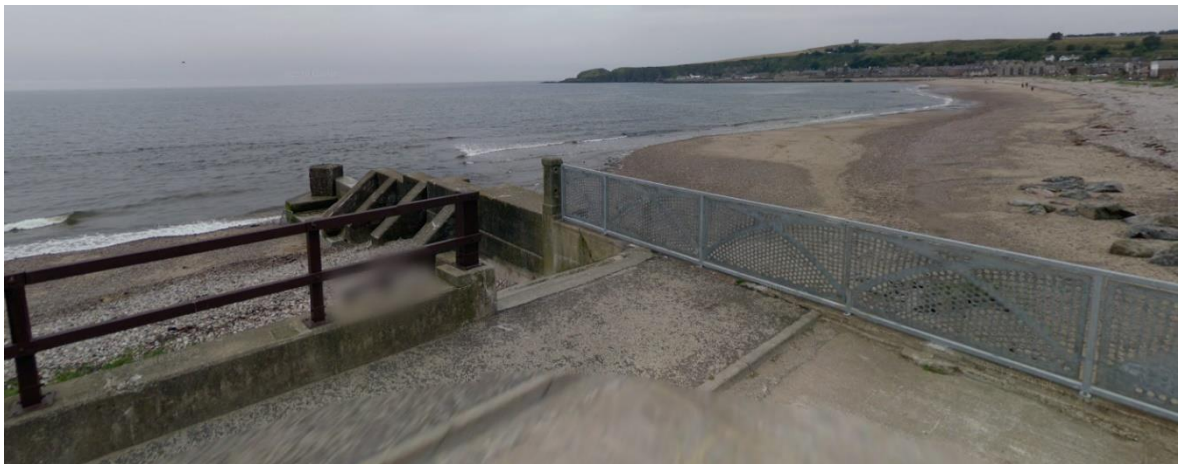


Figure 2-28: Left bank training wall at the mouth of the Cowie Water

2.10.3 Coastal flood risk in the tidal reach

Potential coastal flood risk within the tidal reach of the Cowie Water exists from both still water levels (SWL) and wave action; each of these are considered in turn below.

Still water levels

Due to the lack of a hydraulic model along the Cowie Water, the bank levels have been compared directly with tidal levels. Figure 2-29 and Figure 2-30 show the top of bank levels along the left and right hand banks of the Cowie downstream of the B979 road bridge respectively, and compare this to the extreme sea levels from the updated Coastal Flood Boundary Dataset (CFBD).

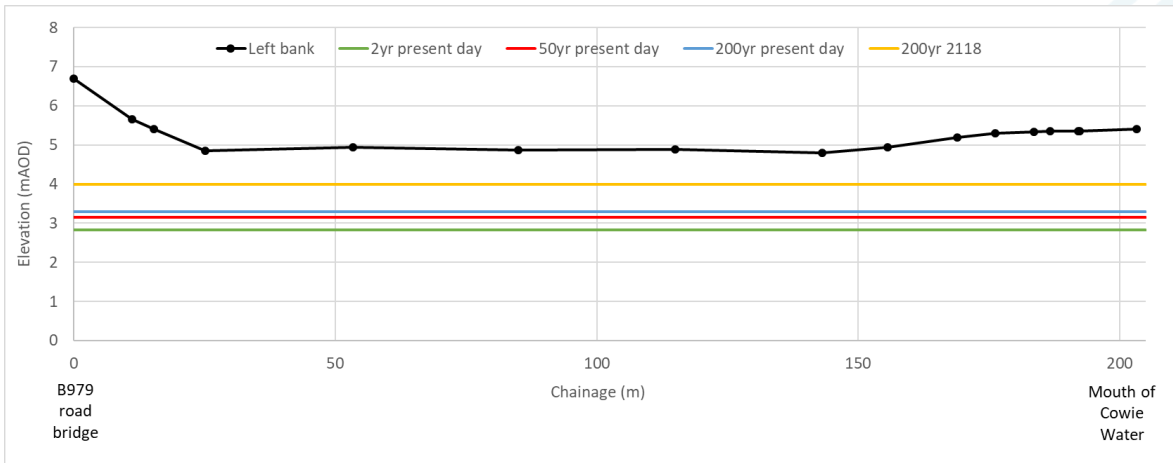


Figure 2-29: SWL compared to top of bank levels; left bank

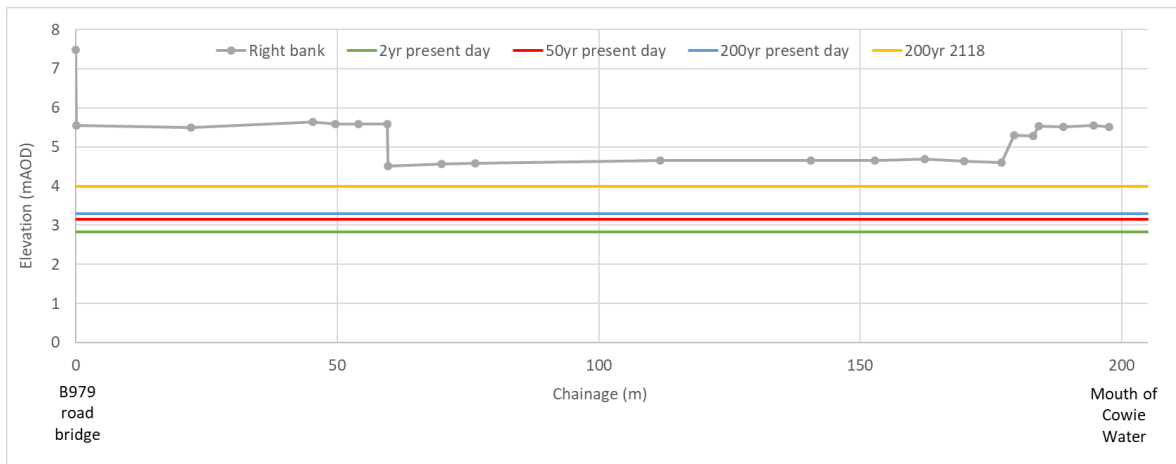


Figure 2-30: SWL compared to top of bank levels; right bank

It can be seen that for both banks, there is no risk from coastal flooding due to still water levels alone for up to and including the 200 year plus climate change event (to 2118 using the medium emissions 95th percentile data from UKCP18). For the left bank there is a freeboard of 0.81m and for the right bank there is a freeboard of 0.53m compared to the lowest point along each.

Waves

Additional coastal risk exists in the form of waves, and there is anecdotal evidence that waves can overtop the right hand bank of the Cowie within the tidal reach and then roll along the revetment, finally breaking on the weir beneath the B979 road bridge.

A video of waves at the mouth of the Cowie that was filmed on 16 March 2018 was provided by Aberdeenshire Council. The video shows waves breaking on the shingle bank, resulting in splash over the right hand bank of the river, with smaller waves then running along the right bank revetment and breaking on the weir beneath the B979 road bridge.

In order to model waves propagating up the channel of the Cowie Water, a phase resolving wave model would need to be developed; however, this is outwith the scope of the current project. As such, a methodology has been derived in order to undertake a simplified assessment of wave risk within the tidal reach of the Cowie.

Due to the presence of large volumes of shingle at the mouth of the river as well as upstream of the footbridge, waves entering the channel would become depth limited. Topographic levels around the river mouth, taken from the laser scan data, are presented in Figure 2-31.

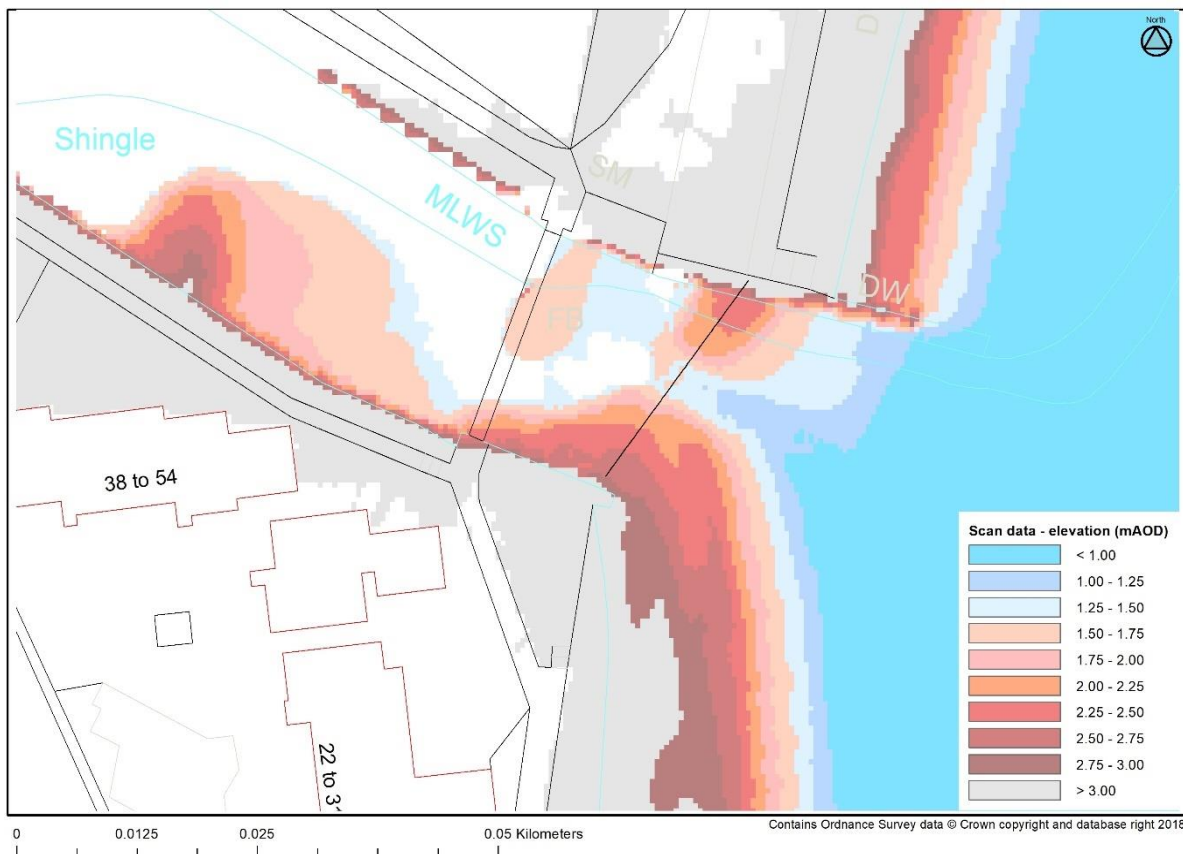


Figure 2-31: Elevations at mouth of Cowie Water from scan data

Based on the concept that waves entering the Cowie Water will become depth limited, the maximum height that a wave in the channel could be can be considered. Depending on the options that are considered, the level to depth limit waves to could vary (e.g. if an option includes removing the shingle); for the purpose of this assessment a conservative value of 1.5mAOD has been taken. Based on the extreme sea levels from the updated CFBD, the maximum depth limited wave heights that could occur within the channel are as presented within Table 2-15. The depth limited wave heights are based on a conservative factor of 0.8 of the water depth. Half of the wave height has subsequently been added onto the SWL to give a total height, and these are presented in comparison to the top of bank levels within Figure 2-32 and Figure 2-33.

Table 2-15: Maximum depth limited wave heights for a range of SWL

SWL return period	SWL (mAOD)	Depth limited wave height (m)	Total height (mAOD)
2 year	2.82	1.06	3.35
50 year	3.16	1.33	3.82
100 year	3.23	1.38	3.92
200 year	3.30	1.44	4.02
200 year 2118	3.99	1.99	4.99

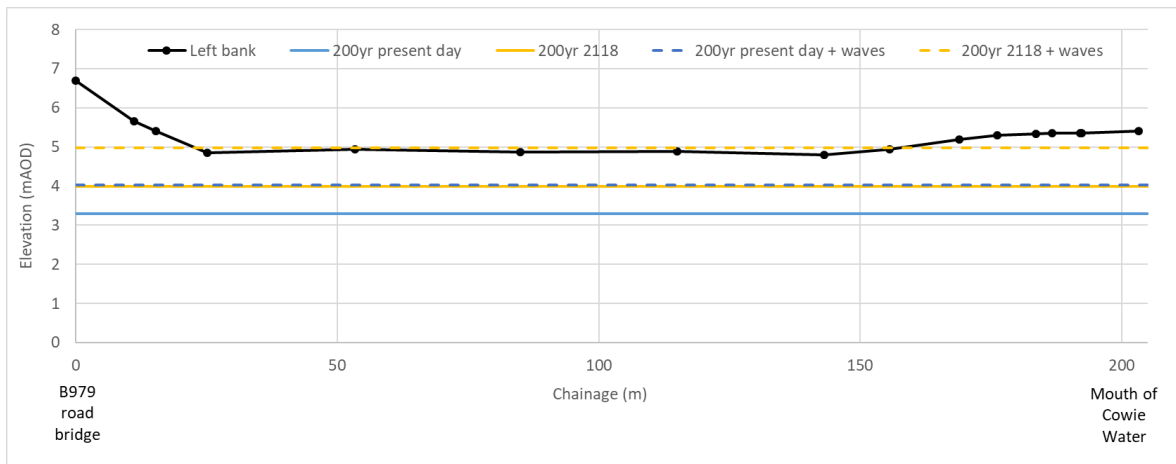


Figure 2-32: SWL plus waves compared to top of bank levels; left bank

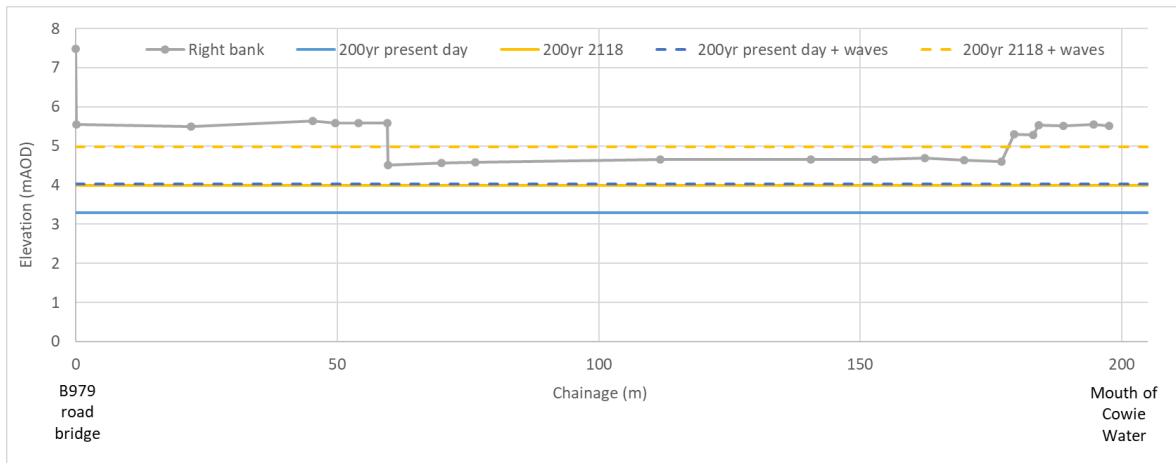


Figure 2-33: SWL plus waves compared to top of bank levels; right bank

It can be seen that, waves within the channel are only likely to become an issue for future extreme events. This is based on a conservative estimate of potential wave heights within the channel and this would vary according to the options that are progressed. Present day risk is deemed to be limited to the most seaward section, where oblique waves run up the shingle and result in some element of overtopping of the right bank. This has been accounted for within the modelling by extending the inflow in the TUFLOW model around the corner of the Cowie, and will be accounted for within the conceptual design by considering the depth limitation in conjunction with runoff calculations.

2.11 Tidal reach of the River Carron

The River Carron discharges into the North Sea to the north of the harbour and south of the main central beach. The tidal reach of the river is influenced by both still water levels (SWL) and waves. Construction of the fluvial flood protection scheme for the River Carron and its tributary the Glaslaw Burn is due to commence in 2019.

2.11.1 Historical configuration

The mouth of the River Carron prior to any training works being constructed can be seen in Figure 2-34.

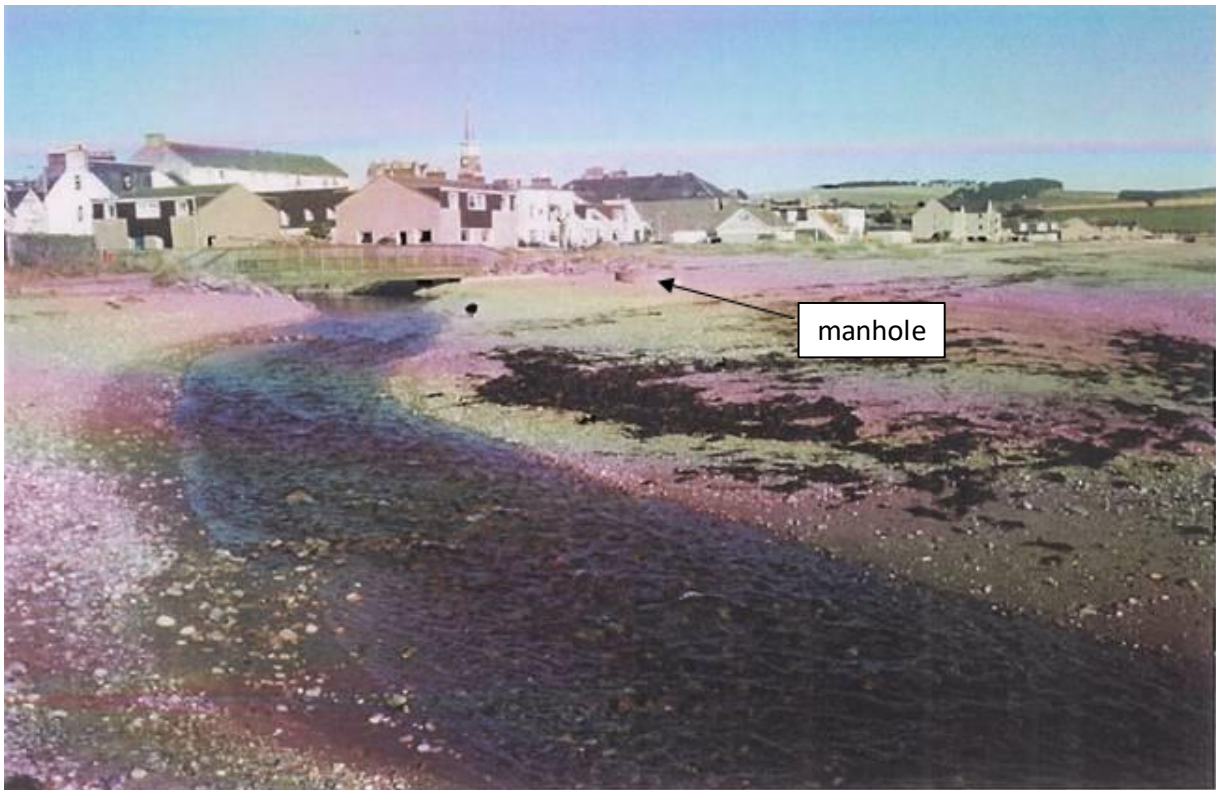


Figure 2-34: Historical natural outfall of the River Carron

In 1998 HR Wallingford were commissioned by Aberdeenshire Council to consider options for maintaining a channel for the River Carron across the beach; concerns were that the discharge of floodwater was being hampered by the low clearance of the footbridge crossing the channel as well as the deflection and partial siltation of the channel across the beach. The report⁹ considered a number of training wall configurations, with the recommended option presented within Figure 2-35.

⁹ Stonehaven Seawall, Aberdeenshire – Feasibility Study of Improvements, Report EX3731, November 1998
AKI-JBAU-00-00-RP-HM-0002-S3-P02-Interim_Modelling_Report

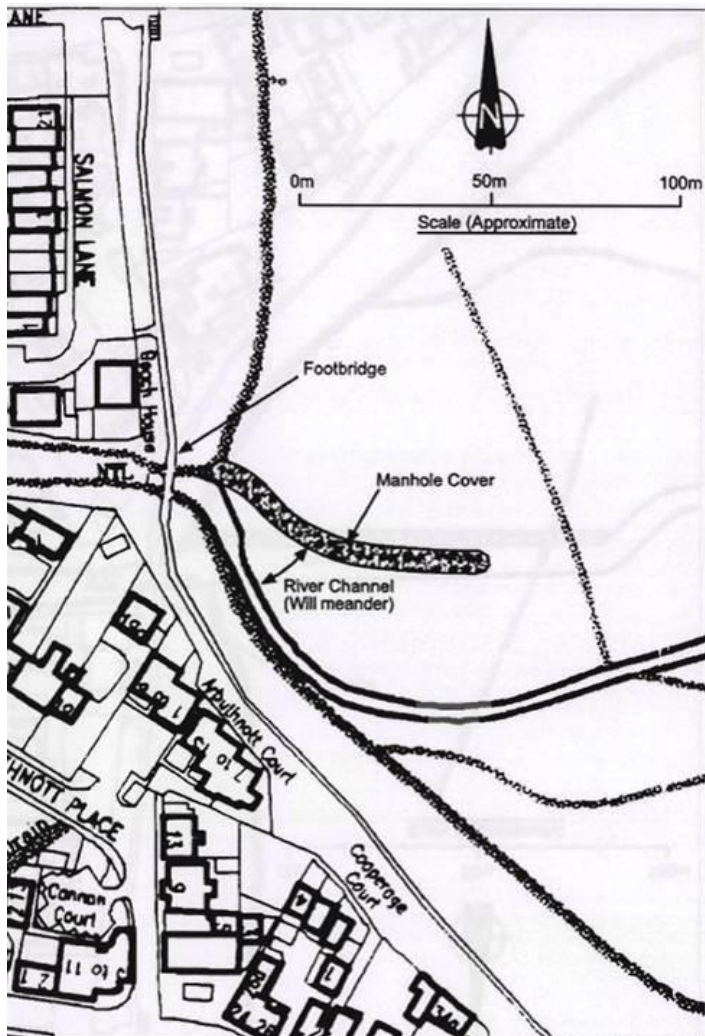


Figure 2-35: Recommended training wall option from HR Wallingford report

The configuration of the rock armour training structure that was built at the mouth of the Carron differs from that shown above. Details of the final design and the date of construction have been requested from Aberdeenshire Council, however the information available is limited. It is understood that initial training structures were built between 1998 and 2006, with these were then extended in 2008 (Figure 2-36).



Figure 2-36: Proposed extension to the training structures, 2007

2.11.2 Present day configuration

The present day configuration at the mouth of the Carron can be seen in Figure 2-37.



Figure 2-37: Current configuration at the mouth of the River Carron

2.11.3 Coastal flood risk in the tidal reach

Potential coastal flood risk within the tidal reach of the River Carron exists from both still water levels (SWL) and wave action; each of these are considered in turn below.
Still water levels

A number of hydraulic models are available for the River Carron. In 2011 JBA were commissioned by Aberdeenshire Council to undertake a Flood Alleviation Study, and as part of this constructed a 1D-2D linked model of the River Carron and Glaslaw Burn in InfoWorks-RS. The model was calibrated to the flood event that occurred on 1 November 2009 and was subsequently used by JBA to develop the outline design of the fluvial scheme. The downstream boundary of the model was in the form of a tidal graph, and this was timed so that the peak tidal level coincided with peak flows at the downstream limit of the model.

Sensitivity analysis undertaken as part of the original study with regard to the downstream boundary showed that for a 2 year fluvial event, the tidal downstream boundary effects flood levels up as far as White Bridge, and for a 200 year fluvial event this is limited to as far as Bridgefield Bridge (Figure 2-38).

Whilst the analysis shows that the combination of a high fluvial flow (Q200) with a lower return period tidal level (T2) results in the highest overall water levels, the dependency between the two was not assessed. As such, the report recommends that joint probability analysis between fluvial flows and tidal levels be undertaken at the detailed design phase. However, it should be noted that the combination of Q200 and T200 shows only a small difference in stage between Bridgefield and Beach bridges; becoming minimal at Bridgefield bridge.

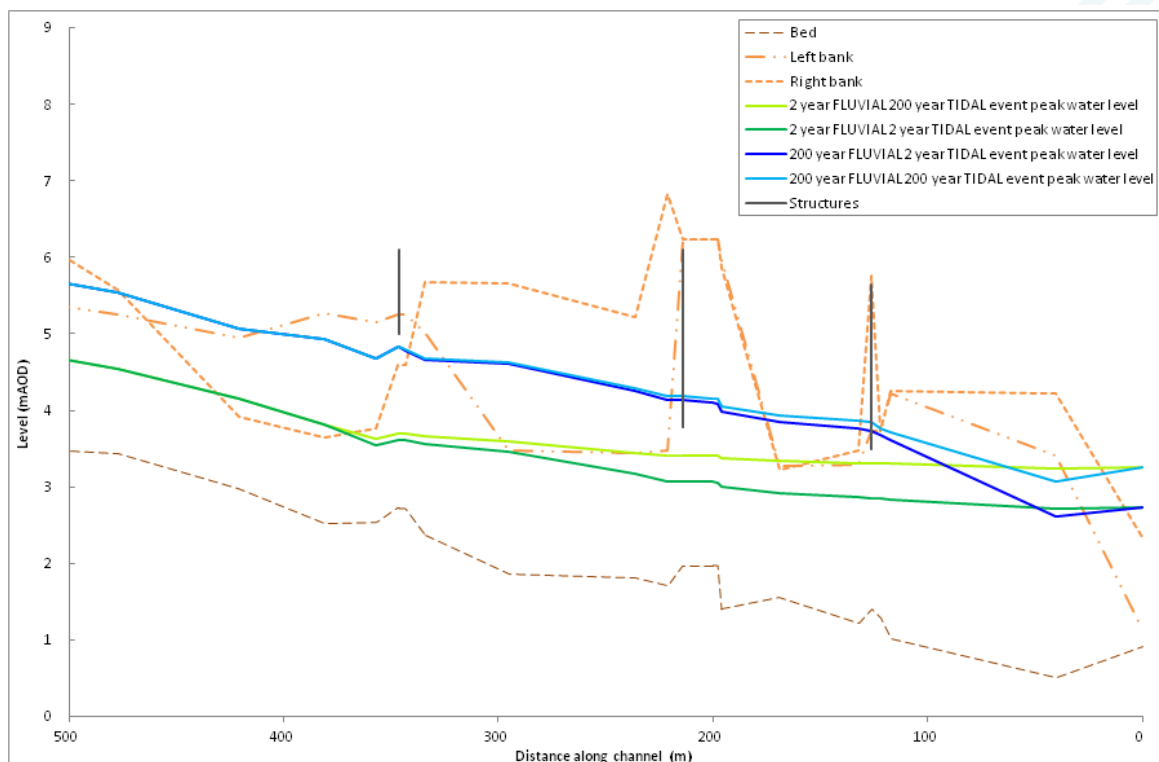


Figure 2-38: Long section of the River Carron – downstream boundary sensitivity analysis

The 2011 JBA report also considered the effect of the rock armour at the mouth of the River Carron on tidal levels within the channel. Specifically, this looked at the change in the tidal level within the rock armour section of the channel downstream of Beach Bridge (Figure 2-39). The report concluded that due to the water level downstream of Beach Bridge being relatively constant, should the reach length downstream of the bridge be reduced, there will be little change in water levels further upstream.

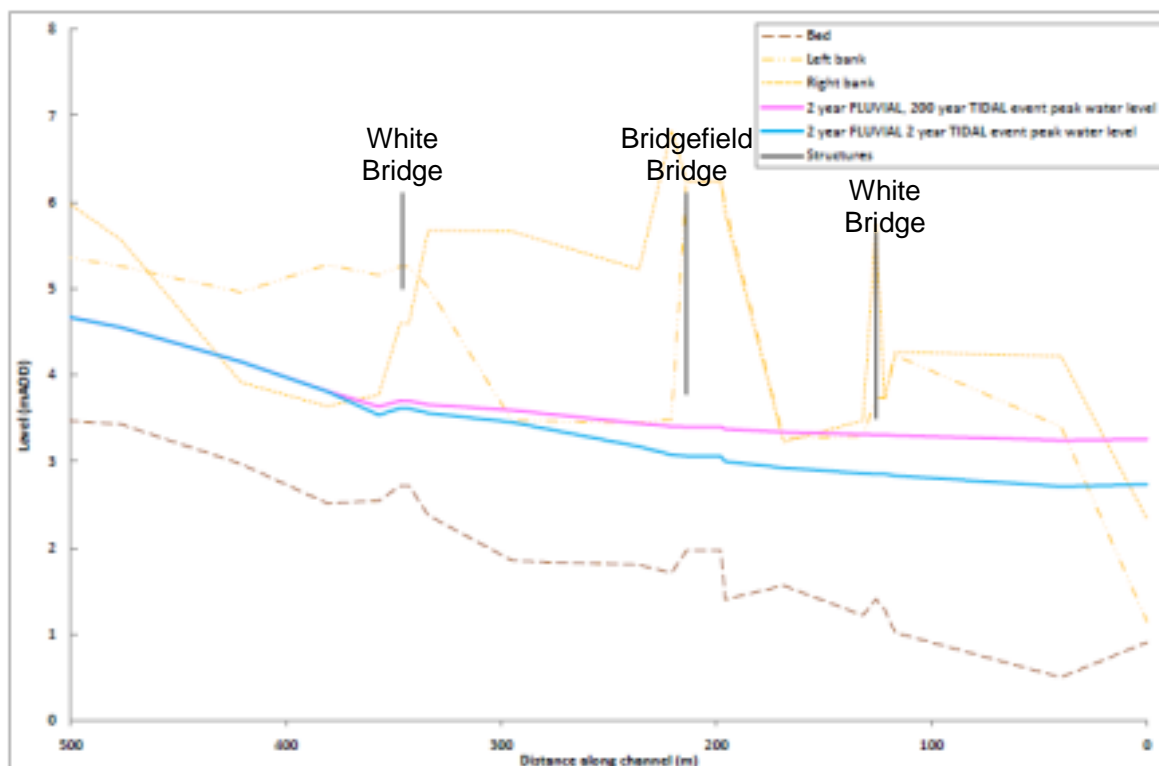


Figure 2-39: Long section of River Carron – SWLs in rock armour section of channel

The detailed design of the fluvial scheme was awarded to Mott MacDonald Limited, with their Hydrology and Hydraulic modelling report being released in June 2015¹⁰, supplemented by two addendums dated December 2015^{11,12}.

As part of the detailed design Mott MacDonald developed a 2D in-channel TUFLOW model of the River Carron and the Glaslaw Burn. The downstream boundary of this model is in the form of a HT boundary, with the peak level corresponding to a 1-year tide. However, the peak flow in the Carron is not aligned with the peak tidal level (Figure 2-40). It is aligned with the minimum cut off value of 1.5mAOD, which is between MHWS (2.07mAOD) and MHWN (1.17mAOD). As part of the modelling, sensitivity analysis was undertaken by increasing the downstream boundary by 0.5m, with the report concluding that the effects were negligible. It is assumed that the timing in the peaks was unaltered for the sensitivity testing, and as such a tidal level of 2.0mAOD was applied at the timing of the peak flow.

¹⁰ Stonehaven Flood Protection Scheme, Hydrology and Hydraulic Modelling, June 2015

¹¹ Stonehaven Flood Protection Scheme, Hydrology and Hydraulic Modelling - Addendum A to Revision A, December 2015

¹² Stonehaven Flood Protection Scheme, Hydrology and Hydraulic Modelling - Addendum B to Revision A, December 2015

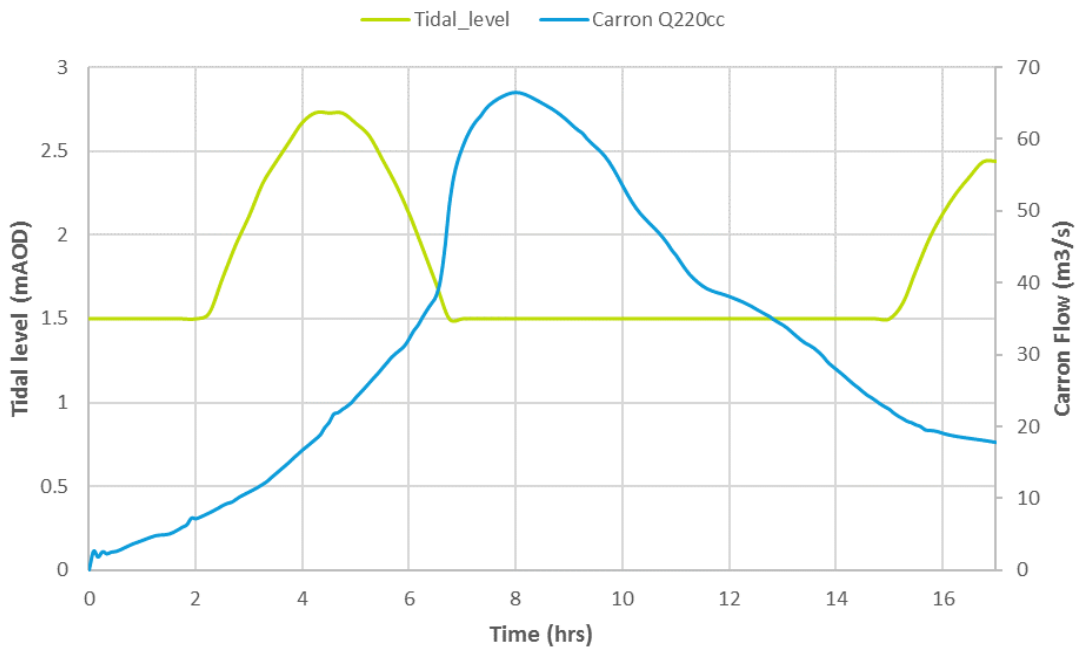


Figure 2-40: Tidal and fluvial boundaries for Q200cc design run from Mott MacDonald model

Whilst it is clear that the fluvial flows dominate flood levels within the Carron, the tide can affect levels within the downstream reach. It is understood that Aberdeenshire Council are happy with the freeboard allowance provided within the downstream reach in order to account for tidal levels. Should the coastal options being considered potentially effect levels within the Carron, the implications for the fluvial scheme will need to be investigated. Otherwise, no further work to consider still water levels in the tidal reach of the River Carron is required as part of this study.

Waves

In 2014 JBA were commissioned by Aberdeenshire Council to undertake a study to investigate wave propagation up the River Carron, as has been observed historically, e.g. as shown in Figure 2-41. The study combined information gathered from historical events with numerical modelling to assess potential wave heights within the downstream reach of the Carron and discuss the potential implications of this on the design of the fluvial scheme.



Figure 2-41: Wave propagation up the River Carron on 15 December 2012¹³

The report looks at a number of options to reduce wave heights within the channel and outlines high-level cost estimates of both a breakwater and the raising of the walls proposed as part of the fluvial scheme to account for wave action. The report details that in order to maintain a suitable freeboard, the walls would need to be raised by 0.9m.

It is understood that Aberdeenshire Council are satisfied with the freeboard provided by the proposed fluvial scheme and accept any residual risk from occasional wave overtopping. Should the coastal options being considered potentially increase waves within the Carron, the implications for the fluvial scheme will need to be investigated. Otherwise, no further work to consider waves in the tidal reach of the River Carron is required as part of this study.

2.12 Impacts of sea level rise on sewer network flood risk

As well as considering potential flood risk directly from the coast, it is important to consider the interaction between coastal flooding and other flood sources, especially with regard to climate change. To this end, an assessment of the impact of extreme sea levels on the drainage network within Stonehaven and Cowie has been undertaken. Multiple outfalls connect to the sea directly as well as into the lower reaches of the watercourses. During a coastal flood event, high sea levels can exacerbate flood risk in the drainage network through backup of the system and inability to discharge effectively; with the impact of climate change this risk is likely to increase.

To assess the implications of climate change on the local sewer system from tidal sources, Scottish Water's Integrated Catchment Model (ICM) has been utilised for surrounding drainage and sewer system of Stonehaven.

¹³ Photograph taken by Ian McDonald, Stonehaven resident
AKI-JBAU-00-00-RP-HM-0002-S3-P02-Interim_Modelling_Report

The network geometry used for this assessment is:

"STW001527_STW001543:NEEDS_MODEL:22_3_2017".

The ICM model contains the drainage and sewer network system of Stonehaven. Data was provided by Scottish Water and is part of the Aberdeen ICS catchment, which incorporates Stonehaven.

For this assessment the 1 in 30 year and 1 in 200 year flood events were considered. To gain an understanding of the impact of sea level rise these were assessed for the present day and the 2118 epoch, using the UKCP18 medium emission 95th percentile scenario. Table 2-16 shows the associated flood levels.

Table 2-16: Still water levels for key return periods at Stonehaven

Return Period	Level (mAOD)
30 (2018)	3.11
200 (2018)	3.30
30 (2118)	3.83
200 (2118)	4.03

ICM model STW001527_STW001543:NEEDS_MODEL:22_3_2017 was exported into shapefile format and assessed within ArcGIS. An assessment of the network indicated that some isolated manholes and conduits are located within the model (i.e. pipes discharging to soakaways). These features were excluded from consideration as this study is to assess the implications of climate change on the local sewer system from tidal sources. A schematic of the network is shown in Figure 2-42.

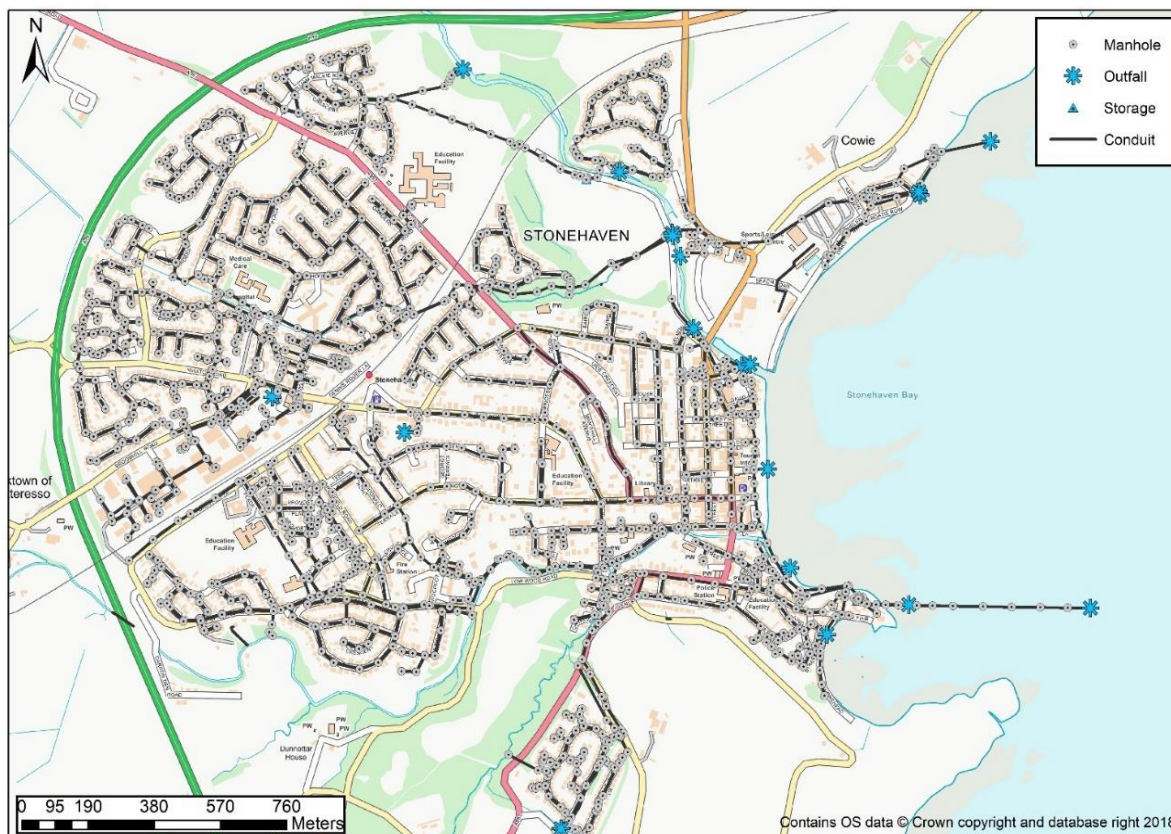


Figure 2-42: Local drainage network from ICM

In total, the following number of drainage features were identified within the drainage network of Stonehaven:

Outfalls: 19

Manholes: 2280

Storage features: 4

Within the ICM model, each node has a designated 'flood level'. This is the level at which flooding could occur from a node via the manhole opening or connected gullies; whichever is lower.

The outfalls that would be impacted during each flood event were identified. Using the 'at risk' outfalls as a starting point, 'at risk' manholes and storage features were identified by assessing those that have a flood level less than the associated tidal peak for each scenario. A sense check was subsequently undertaken on the identified attributes by tracing their location, via the plotted conduit lines, to an 'at risk' outfall.

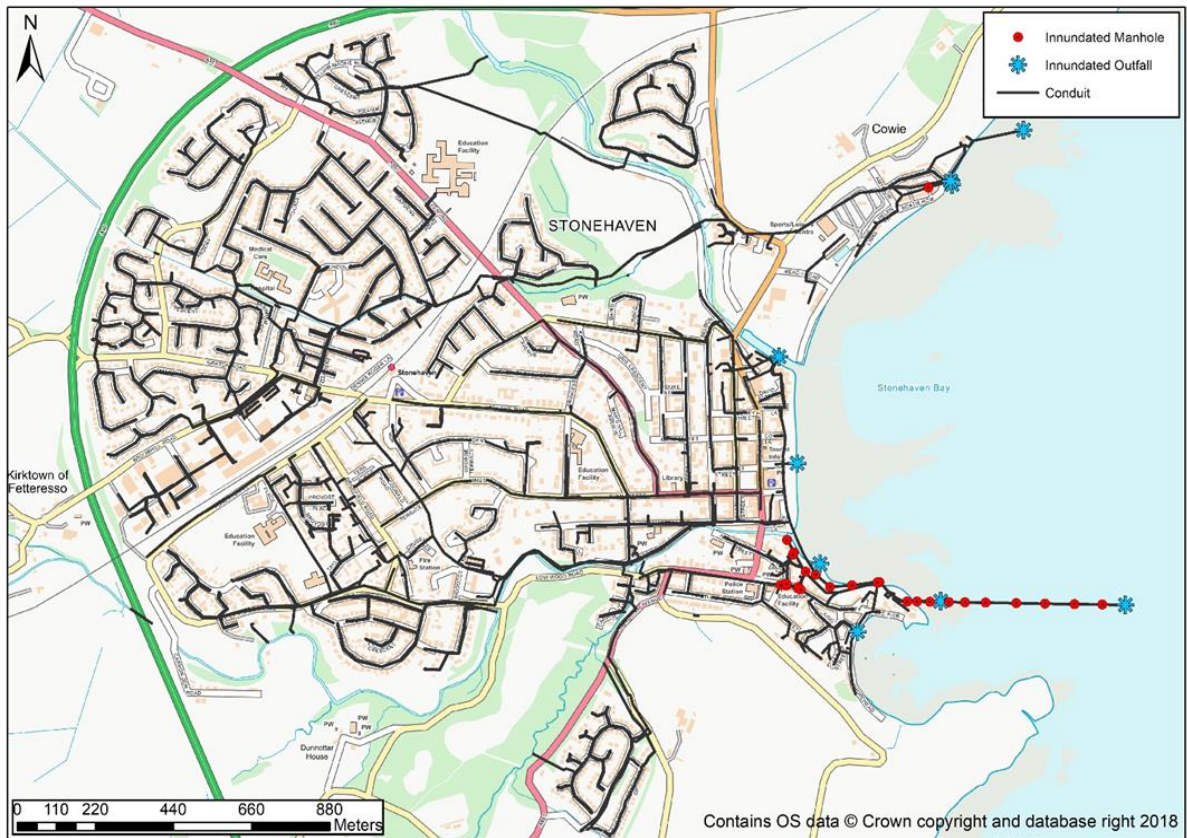


Figure 2-43: 30 year tidal flood event (2018)

During a present day 30-year tidal flood event, inundated outfalls and manholes are largely located where the Carron Water flows into Stonehaven Bay. Six manholes located along High Street are potentially at risk of flooding along with manholes located to the rear of the development, which backs onto the coastline. Isolated 'at risk' manholes are also located in Cowie, along a side street of Boatie Row.

A summary of 'at risk' drainage features identified during a present day 30-year tidal flood event is provided in Table 2-17.

Table 2-17: At risk assets - 30 year, 2018

Drainage Features.	Number identified as 'at risk'.	Percentage of drainage network considered 'at risk'.
Outfall	9	47.4%
Manholes	26	1.1%
Storage features	0	0%

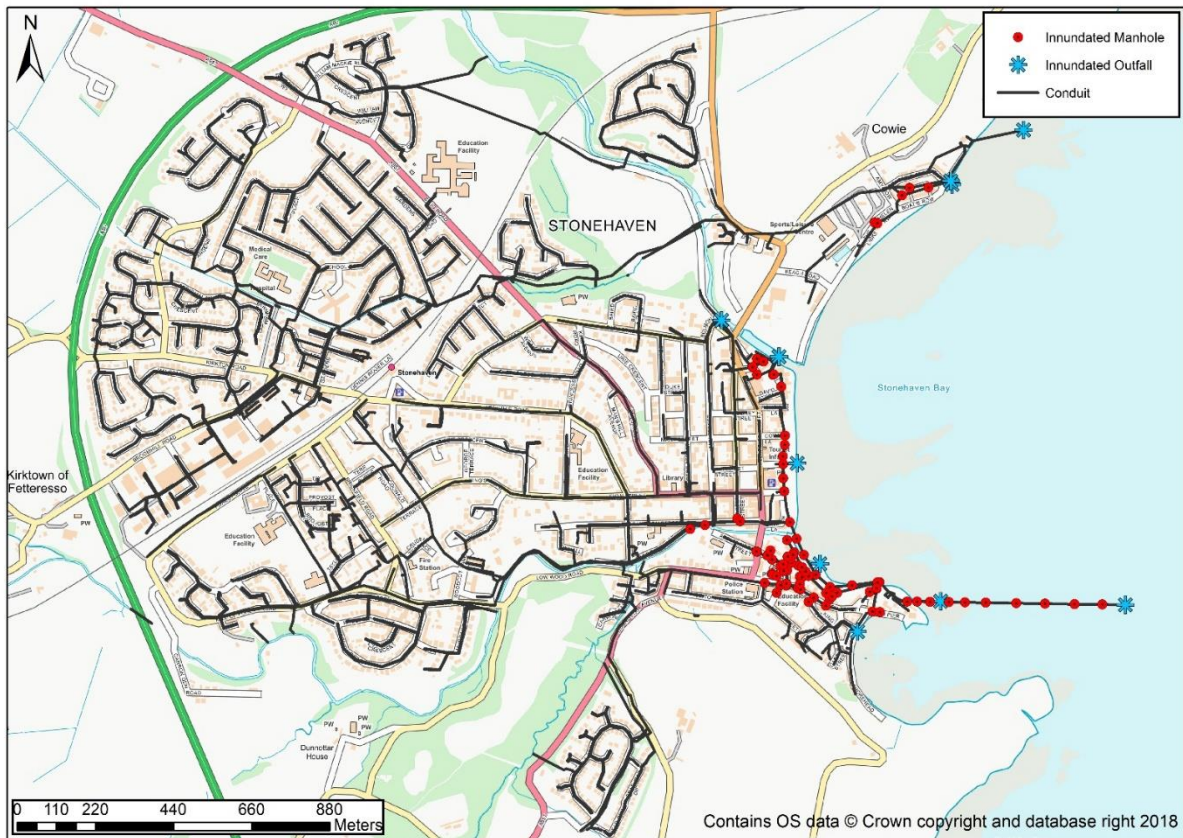


Figure 2-44: 30 year tidal flood event (2118)

During a 30-year tidal flood event which takes into consideration climate change (2118), the areas and number of drainage features identified to be 'at risk' increases. Areas located at the mouth of the Carron Water are likely to be the worst effected during a flood event of this magnitude, with risk spreading to the east along Arbuthnott Street, Arbuthnott Place, High Street, Old Pier and Cameron Street (to the west) where a number of residential properties could be impacted during surcharging of the sewer system. The number of vulnerable manholes in has also increased along The Links and Helen Row.

A summary of 'at risk' drainage features identified during a 30-year tidal flood event which takes into account climate change (2118) is provided in Table 2-18.

Table 2-18: At risk assets - 30 year, 2118

Drainage Features.	Number identified as 'at risk'.	Percentage increase from present day 30-year tidal flood event.	Percentage of drainage network considered 'at risk'.
Outfall	10	11.1%	52.6%
Manholes	90	246.2%	3.9%
Storage features	0	0%	0%

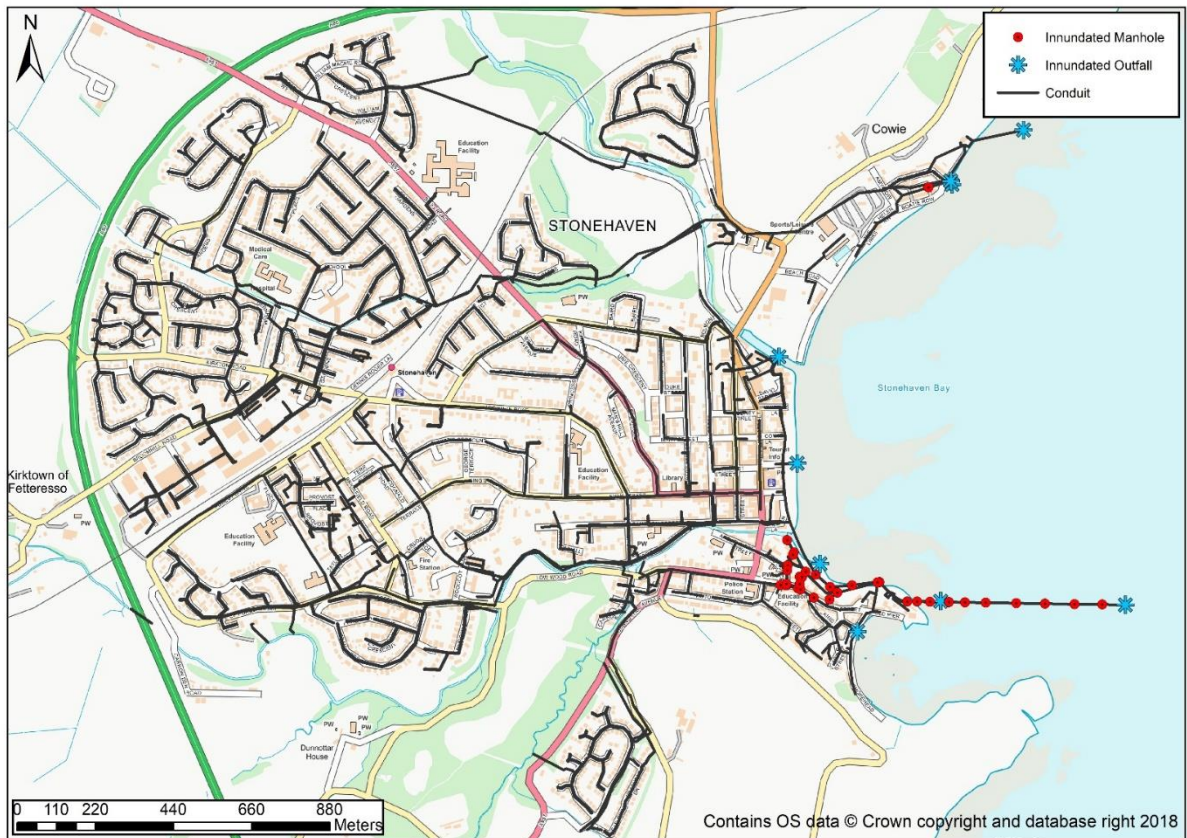


Figure 2-45: 200 year tidal flood event (2018)

During a present day 200-year tidal flood event, areas and drainage features identified to be 'at risk' largely follow the patterns identified during the present day 30-year tidal flood event scenario. The number of risk outflow locations has not changed but the number of potentially vulnerable manhole locations has increased. A summary of 'at risk' drainage features identified during a present day 200-year tidal flood event is provided in Table 2-19.

Table 2-19: At risk assets - 200 year, 2018

Drainage Features.	Number identified as 'at risk'.	Percentage increase from present day 30-year tidal flood event.	Percentage of drainage network considered 'at risk'.
Outfall	9	0%	47.4%
Manholes	34	30.1%	1.5%
Storage features	0	0%	0%

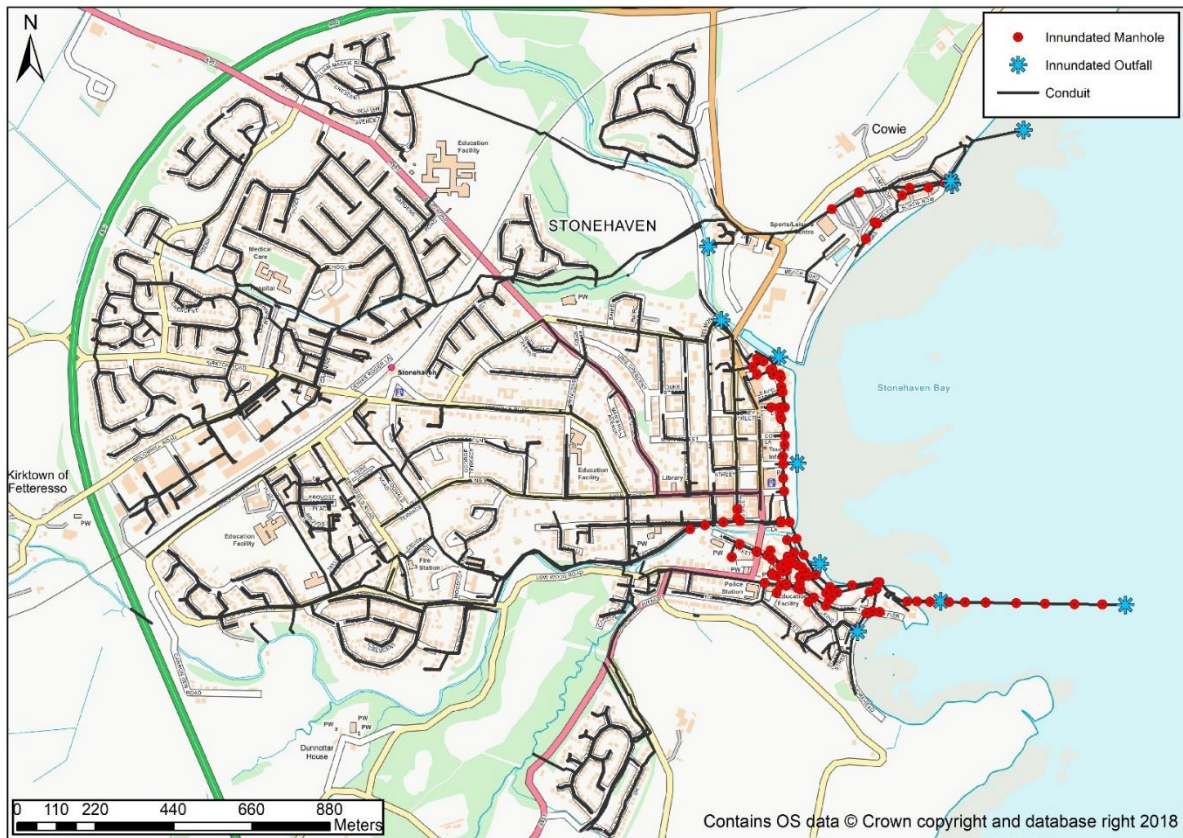


Figure 2-46: 200 year tidal flood event (2118)

During a 200-year tidal flood event which takes into consideration climate change (2118), the areas and number of drainage features identified to be 'at risk' increases. Areas located along the River Carron are likely to be the worst effected during a flood event of this magnitude, with risk spreading to the east along Arbuthnott Street, Arbuthnott Place, High Street, Old Pier and Cameron Street (to the west) where a number of residential properties could be impacted during surcharging of the sewer system. In addition, built development which back up onto the coastline to the east of Allardice Street and associated roads could also be impacted. Vulnerable manhole extents to the north have also spread to manholes along The Links and Helen Row.

A summary of 'at risk' drainage features identified within Stonehaven during a present day 200-year tidal flood event is presented in Table 2-20.

Table 2-20: At risk assets - 200 year, 2118

Drainage Features.	Number identified as 'at risk'.	Percentage increase from present day 200-year tidal flood event.	Percentage increase from 2118 30-year tidal flood event.	Percentage of Stonehaven drainage network considered 'at risk'.
Outfall	10	11.1%	0%	52.6%
Manholes	107	214.7%		4.7%
Storage features	0	0%	0%	0%

3 Geomorphology Assessment

To understand the morphological processes within the bay and how they contribute to flood risk, an assessment of the local coastal geomorphology has been undertaken. The aim of this is to evaluate the historical trends in shoreline position and beach volume, and thus provide an indication on the controlling mechanisms and influences these have on flood risk and erosion.

Assessment of future erosion is subsequently considered through numerical modelling of short-term storm response, with the objective to better understand the potential future risk to critical assets after failure of the current coastal defences.

3.1 Overview

The exposed position of Stonehaven on the coastline and the direct exposure to storm surges and extreme wave conditions historically led to the construction of multiple formal and informal coastal defences along the shore. These include a large rock armour revetment to the north of Stonehaven harbour; a boardwalk section consisting of rock armour and shingle; a concrete wall fronting the properties within the central section of the bay; stepped revetments with a small wave return wall at the crest between the mouth of the Cowie Water and the open-air pool; and sea walls along the frontage at Cowie village. All of these features enforce the current shoreline of the bay to a largely stationary position.

3.2 Geology

The arrangement of the bay and geological features has resulted in complex morphology and sediment transport patterns. The Highland Boundary Fault appears on the coastline at Stonehaven and the bedrock consists of Old Red Sandstone¹⁴ with subordinate conglomerate and siltstone formed around 420 Ma. Ice covered Stonehaven and the surrounding area from the Strathmore Ice Stream that flowed northwards depositing reddish brown deposits¹⁵. Stonehaven is built on a raised beach that was created when glaciers retreated with glacial sand and gravel dominating the superficial deposits in the area, having been reworked over time resulting in the beaches that are present today.

3.3 Sediment transport and morphology

The volume of erodible sediment in the bay is limited due to the coastal defences and underlying geology. The headlands at either end of the bay prevent continuous longshore drift, and the dominant process appears to be cross-shore movement of shingle, with the elevation of the beach varying considerably with a fluctuating wave climate. Whilst cross-shore processes dominate, there is a general north to south trend in sediment movement. This occurs due to the northern headland providing less sheltering and is exacerbated by its finer sediment and longer offshore rock platform. Transport of material to the north is constrained by the mouth of the Cowie Water and training walls which trap transported material in the channel. Periodic beach recycling of this trapped material takes place with this being deposited south of the River Carron, to minimise erosional losses here.

¹⁴ Ramsay and Brampton, 2000. Coastal Cells in Scotland: Cell 2 – Fife Ness to Cairnbulg Point. Scottish Natural Heritage Research, Survey and Monitoring Report No 144.

¹⁵ A Landscape Fashioned by Geology: Northeast Scotland. Jon Merritt and Graham Leslie.

<https://www.nature.scot/sites/default/files/2017-06/Publication%202009%20-%20Landscape%20fashioned%20by%20geology%20-%20Northeast%20Scotland.pdf>

[Accessed 28 August 2018]

AKI-JBAU-00-00-RP-HM-0002-S3-P02-Interim_Modelling_Report

3.4 Current sediment management practices

Periodic sediment recharge occurs, where sediment is removed from within the mouth of the Cowie Water and redeposited to the south of the River Carron. Table 3-1 summarises the data available from Aberdeenshire Council on previous sediment movements.

This data has been used utilised within the long term trend analysis (Section 3.5).

Table 3-1: Summary of historical beach recycling operations

Year	Collected (tonnes)		Deposited (tonnes)		
	From mouth of Cowie	From mouth of Carron	South of mouth of Carron	North of stepped seawall	South of mouth of Cowie
2001	2000	0	2000	0	0
2002	2000	0	2000	0	0
2003	2000	0	2000	0	0
2004	2000	0	2000	0	0
2005	2000	0	2000	0	0
2006	2000	0	500*	2000	0
2007	2000	150	2150	0	0
2008	2000 [†]	150	2150	0	0
2009	4350	0	4000	0	350 [‡]
2010	3000	0	3000	0	0
2011	1500	0	1500	0	0
2012	1000	0	1000	0	0
2013	0	0	0	0	0
2014	2200	0	2500	0	0
2015	0	0	0	0	0
2016	3000	0	3000	0	0
2017	3250	0	3250	0	0

Notes:

* Shingle placed over manhole cover just north of groyne at Carron.

[†] c150 tonnes of rock armour transferred from groyne at the mouth of the Cowie to improve groyne at mouth of the Carron.

[‡] Shingle placed c50m south of the mouth of the Cowie.

3.5 Long term trends

In 2015 the Scottish Government commissioned the National Coastal Change Assessment (NCCA) to provide an evidence base to understand morphological changes that have happened along the coast and how man-made interventions have shaped these changes. The datasets generated from this include historic MHWS contours from 1890s to present day and estimates of future erosion for 2050 and 2100.

The MHWS position is shown in Figure 3-1, and it can be seen that this has retreated along the northern and middle sections of the bay from 1890s to present day. Over the period the north of the bay has experienced a 10 m retreat of MHWS. The middle

of the bay, between the Cowie and Carron, has retreated ca. 40 m. Historically, the Cowie Water flowed south along the front and joined with the River Carron before discharging into the sea (Figure 3-2). The Cowie broke through the shingle bar in 1948 following a large storm event and has run its present-day course since. Additionally, this breach event coincided with an increasing loss of shingle from the beach, when it is reputed that large volumes of sediment were removed in 1940-1950. It is likely that the combination of these two processes has contributed to the retreat of MHWS observed between 1890s and 1970s.

This has potentially caused the rate of shingle loss of the main beach to increase as the river discharges towards the south east and so velocity of the river discharge contributes to the increase in velocity of the natural north to south sediment drift.

The south of the bay, at the mouth of the Carron, has experienced large fluctuations in MHWS position (Figure 3-3). In the 1890s, the larger beach width forced the river to flow further south before discharging into the sea. In the 1970s the river discharged at approximately the same location, however north of the mouth, the area of sediment had increased and caused the MHWS to advance ca. 20 m. Rock armour was put in place on each side of the River Carron mouth in 2006 to stabilise its course and reduce sediment movement across the channel, which forced the river to discharge at a more northerly location than at previous years. This explains the loss of beach observed between 1970 and present day. Beach recharge takes place south of the Carron, and has done since the early 2000s, which accounts for the increase in beach in this location compared to 1970s. At the south of the bay, north of the harbour, the MHWS has advanced since the 1890s between 40 – 50 m as land has been reclaimed, for car parking and the shoreline is now constrained.



Contains Ordnance Survey data (c) Crown copyright and database right 2018

Figure 3-1: MHWS fluctuations from NCCA data

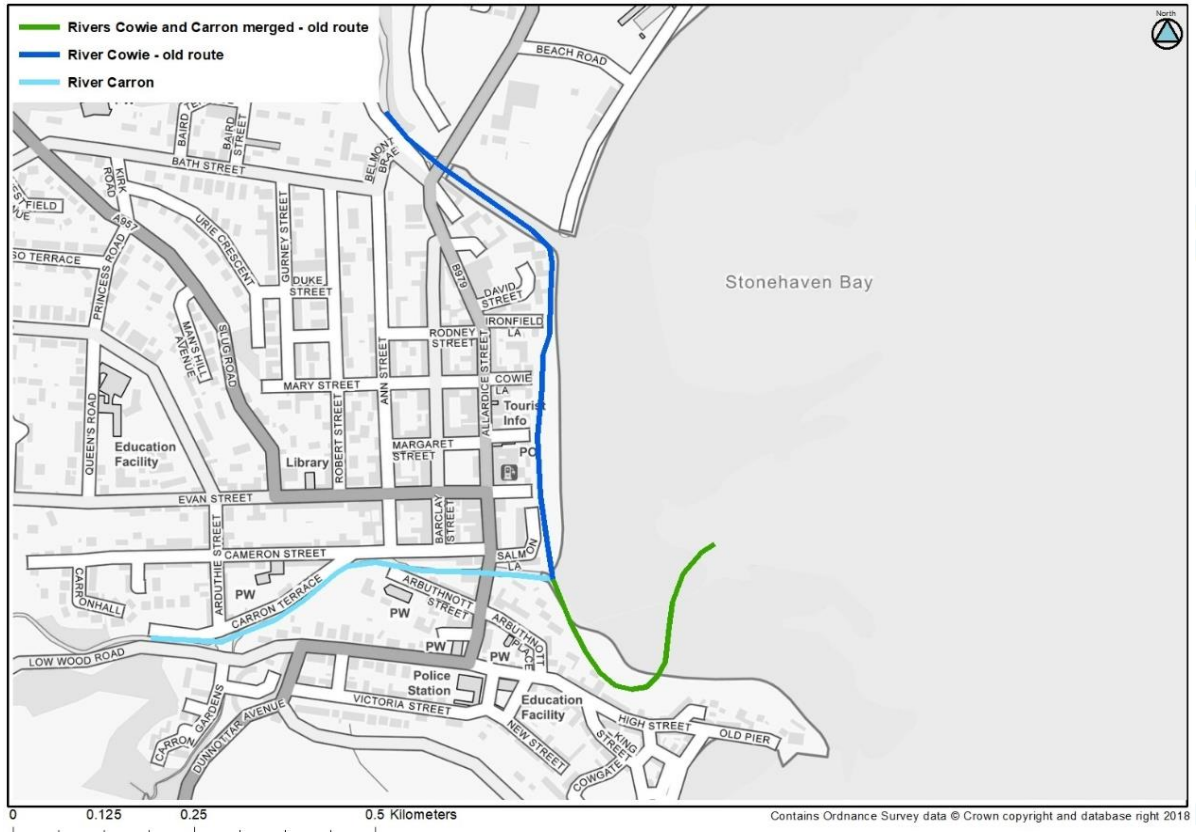


Figure 3-2: Historical fluvial flow routes

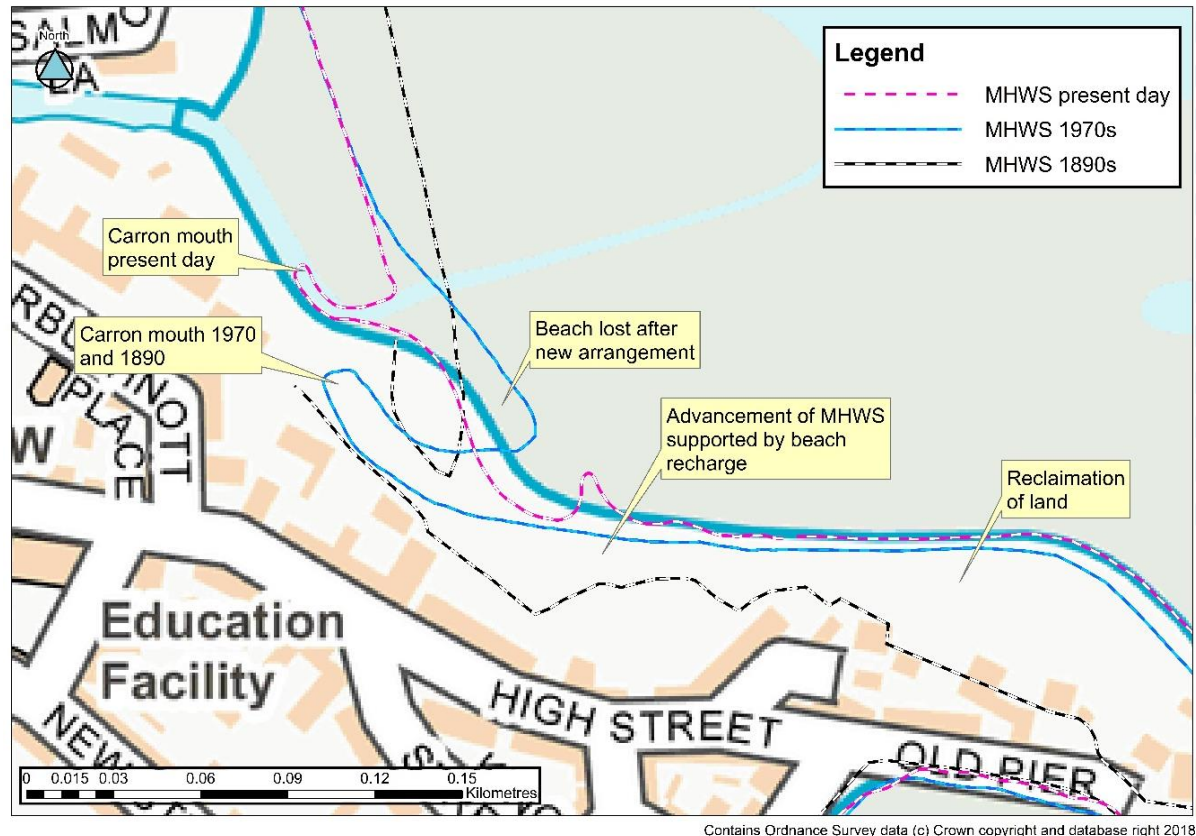


Figure 3-3: MHWS fluctuations at the mouth of the River Carron

3.6 Topographic Analysis

Topographic analysis was undertaken to understand the trends in and impacts of sediment movement in Stonehaven Bay, and to identify what controls these variations have on the coastal defences.

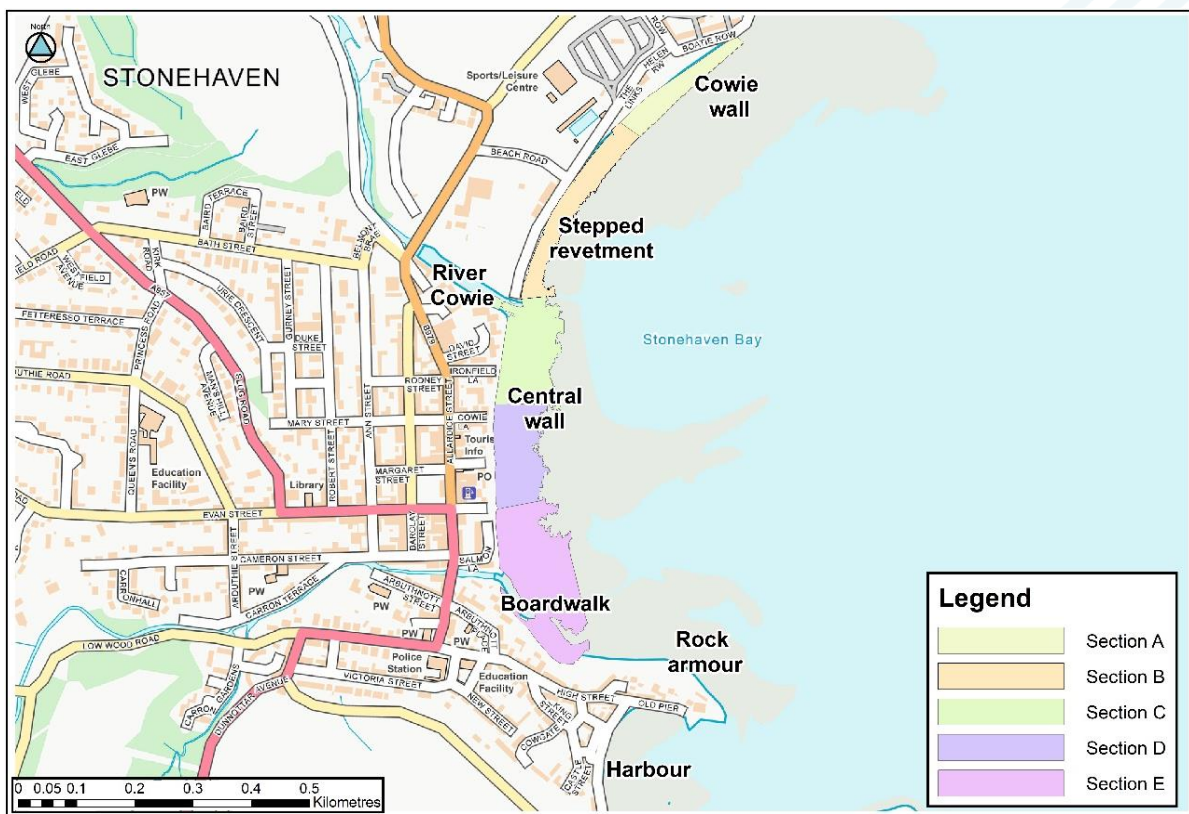
3.6.1 Data

Detailed topographic data of the beach is available for December 2008, May 2013 and May 2018 and has been used to assess the volumetric changes within the bay. A five year gap in data makes it hard to identify definitive trends. A medium term trend can be defined, however a seasonal variability trend cannot with this interval between surveys. The survey dates may also impact the analysis, as a December beach profile will be significantly different to a May beach profile. The 2013 and 2018 May beach profiles and resulting sediment budgets will reflect the previous winters' storms, whilst the 2008 December profile is pre-winter storm season and therefore will potentially show larger variations when compared with the other two datasets.

In isolation, this data is potentially insufficient to draw definitive conclusions on the erosion/accretion patterns. However, in the absence of more frequent surveys, it will be analysed with the aim of establishing medium-term beach stability.

3.6.2 Sections

There is considerable variability in both the defence types and sediment characteristics within Stonehaven Bay. To effectively manage the analysis, the length of the beach was divided into a number of sections based on the defence and sediment type. It was decided that five different sections best described Stonehaven Bay (Figure 3-4) and allows variation in erosion and sediment movement to be identified along the beach.



Contains Ordnance Survey data © Crown copyright and database right 2018

Figure 3-4: Division of Stonehaven Bay into sections

Table 3-2: Stonehaven Bay sections summary

Section	Defence type	Predominant sediment type	Approx. D50 (mm)	Offshore platform
A	Vertical wall	Coarse sand	1	Yes
B	Stepped revetment	Coarse sand/shingle	10	No
C	Buried revetment	Shingle	50	No
D	Buried revetment	Shingle	50	Yes
E	Shingle beach	Shingle	50	No

The general characteristics of the beach and defences at each section are shown in the figures below.



Figure 3-5: Section A/XS08: Vertical sea wall and sandy beach

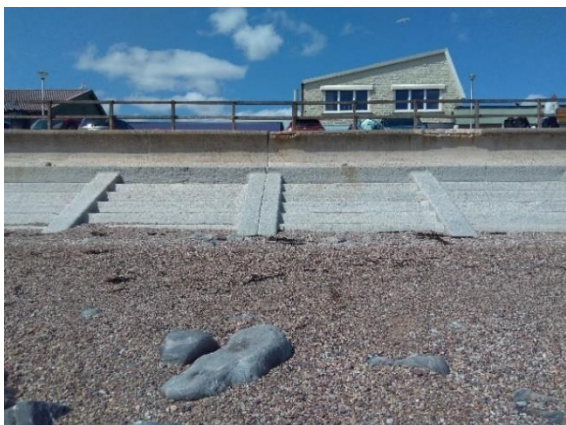


Figure 3-6: Section B/XS12: Stepped revetment and shingle beach



Figure 3-7: Cowie Water estuary from the south with sediment accumulation

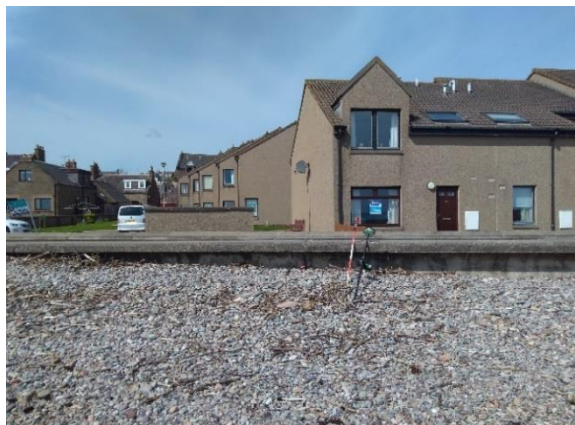


Figure 3-8: Section C/XS17: Seawall with sediment build up and shingle beach



Figure 3-9: Section D/XS20: Seawall with sediment build up. Shingle and coarse sand beach.



Figure 3-10: Section E/XS26: Boardwalk at the top of the beach; River Carron discharging into the sea across the beach

3.6.3 MHWS variations

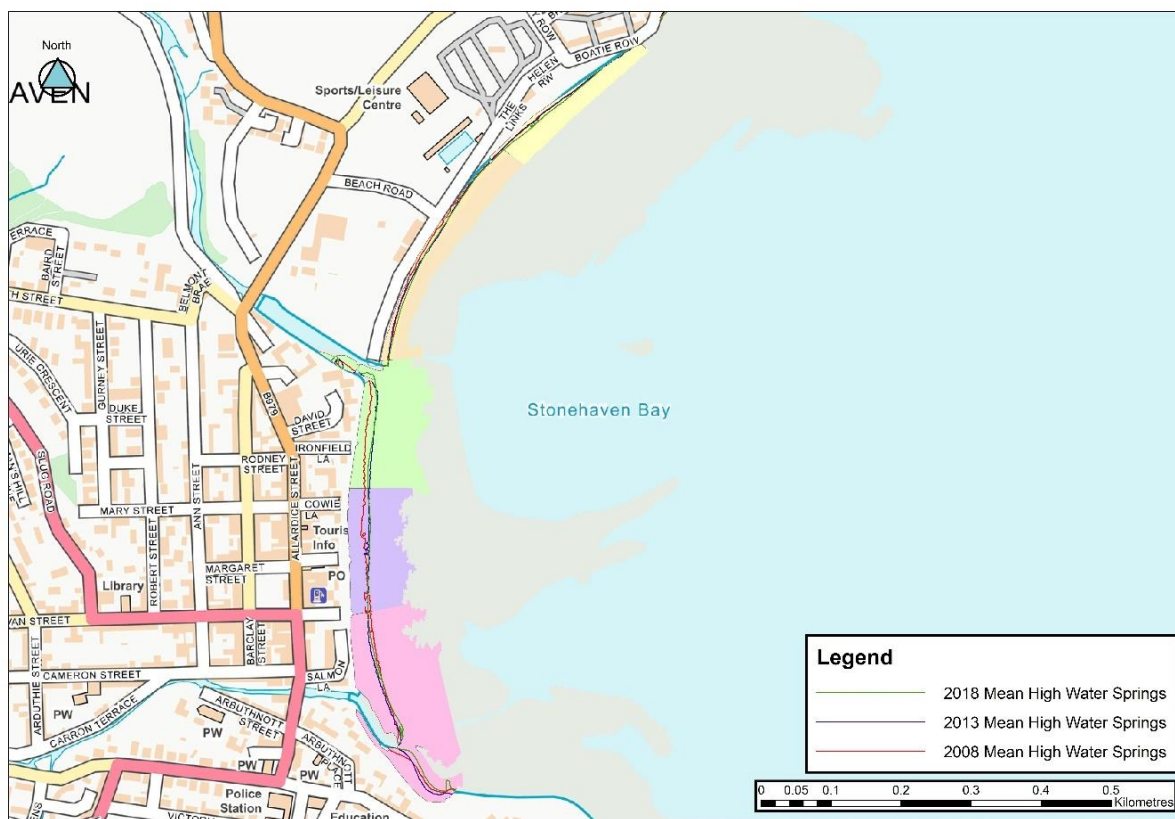
The MHWS contour line (2.07 mAOD) was extracted as a contour for each of the three datasets to track shoreline movement over the last 10 years (Figure 3-11). The showed MHWS has advanced in Section A by 5 m from 2008 to 2018.

Section B also sees an advance of the MHWS by an average of 3 m along the section. Within Section C, the 2013 MHWS position is the most seaward, 3 m beyond the position of the 2018 MHWS. However, from 2008 to 2018, the MHWS has advanced 8 m within this section.

The MHWS in Section D has advanced at the north, by over 12 m, whilst it has retreated at the south by 3 m.

In Section E this has retreated at the north by 3 m, and advanced in the south by 5 m.

The overall trend is that of MHWS advancement, and therefore sediment accumulation in the upper beach.



Contains Ordnance Survey data (c) Crown copyright and database right 2018

Figure 3-11: MHWS fluctuations from 2008, 2013 and 2018

3.6.4 Volumetric Analysis

Within each section of the beach, overall volume change and volume change above and below the MHW (1.17mODN) was calculated between 2008, 2013 and 2018 in ArcGIS. It should be noted that MHW was chosen over MHWS as the proximity of MHWS to the existing defences made it unsuitable for establishing volumetric changes. The results are presented in Table 3-3, Table 3-4 and Table 3-5.

Table 3-3: Volumetric changes within each section (2008 to 2013)

Section	Volume change above MHWN (m ³)	Volume change below MHWN (m ³)	Net Sediment Budget (m ³)
A	436	659	1095
B	1198	1319	2517
C	2868	-3092	-230
D	1881	-2964	-1083
E	-1129	-2328	-3457

Table 3-4: Volumetric changes within each section (2013 to 2018)

Section	Volume change above MHWN (m ³)	Volume change below MHWN (m ³)	Net Sediment Budget (m ³)
A	666	194	860
B	329	-314	15
C	708	-296	412
D	1842	-1866	-24
E	3466	-780	2686

Table 3-5: Volumetric changes within each section (2008 to 2018)

Section	Volume change above MHWN (m ³)	Volume change below MHWN (m ³)	Net Sediment Budget (m ³)
A	1102	854	1956
B	1527	1019	2546
C	3663	-3386	277
D	3725	-4807	-1082
E	2332	-3103	-771

Section A

A steady increase in volume across the whole beach, both above and below MHWN, of 1,956 m³ was seen in Section A from 2008 to 2018. The section contains the lowest volume of active sediment across the bay.

Section B

A large increase in volume of 2,517 m³ above and below the MHWN is observed in Section B between 2008-2013 (Table 3-3). However, although the overall change is positive, there is an area of significant sediment loss north of the Cowie Water training wall. Whilst longshore drift is north to south, cross-shore sediment movement is likely to dominate the beach profile, and the training wall appears to interfere with the natural sediment movement patterns. Between 2013-2018, the volume of sediment transported is much reduced to 300 m³ (Table 3-4). Volume increases above MHWN and decreases below MHWN resulting in a negligible net sediment budget of 15 m³. Overall, there is a significant sediment gain across the section over the period (Table 3-5).

Section C

Sediment volume within Section C is very variable, and much larger than at the two northern sections. Whilst there is a large gain above MHWN, there is also a significant loss below MHWN, making the overall volume change within the cell negative between 2008 – 2013 (Table 3-3). Between 2013-2018, sediment gain above MHWN outweighs the sediment loss happening below MHWN and so the overall change is positive (Table 3-4).

South of the Cowie Water training wall (Figure 3-14), there is a large accumulation of sediment building up both within the river channel and south along the main beach. This indicates the current training wall arrangement is insufficient for sediment retention in Section B.

Across the 10-year time period, Section C experiences a very large gain above MHWN, 3,663 m³, and a very large loss below MHWN, -3,386 m³, (Table 3-5), leading to only a slight increase in sediment across the section overall.

Section D

Section D experiences a significant gain of sediment above MHWN between 2008 and 2013, however a large loss below MHWN is seen, making the overall sediment budget negative (Table 3-3). The same pattern is seen between 2013- 2018 (Table 3-4) meaning the overall change in sediment within this cell from 2008 – 2018 is negative: -1,082 m³ (Table 3-5). The positive gain above MHWN is also significant (3,725 m³), however does not outweigh the large amount of sediment that is lost from the lower beach.

Section E

Section E covers the mouth of the River Carron and experiences negative sediment movement, both above and below the MHWN from 2008 – 2013 (Table 3-3). Between 2013-2018, a significant sediment gain within the cell is seen, caused by a large increase in sediment above MHWN of 3,466 m³ (Table 3-4). Section E has seen an overall loss in sediment from 2008 – 2018 (Table 3-5), despite the large accumulation observed between 2013 and 2018, potentially following a recharge event. The River Carron is partially responsible for the large fluctuations in sediment balance at the south of the bay. Whilst beach recharge takes place within this cell, the sediment deposited does not accumulate further and is slowly lost offshore due to combined river and wave processes. The sediment accumulation seen in Figure 3-14 may be due to a combination of sediment within the watercourse being flushed down during high flows, creating a bar across the beach, and the rock armour arrangement directing flow further south.

Overall, there was a net sediment gain in the north of the bay (Sections A – C), and a net sediment loss in the south (Sections D and E). Each section of the beach experienced sediment accumulation above MHWN, and the three southern sections (C – E) experienced sediment erosion below MHWN. The changes seen between 2013 – 2018 were much smaller in volume than those seen the previous 5 years, which could be due to the survey dates as the difference between 2008 December and 2013 May beach profiles are more significant than differences between May 2013 May and May 2018 beach profiles.

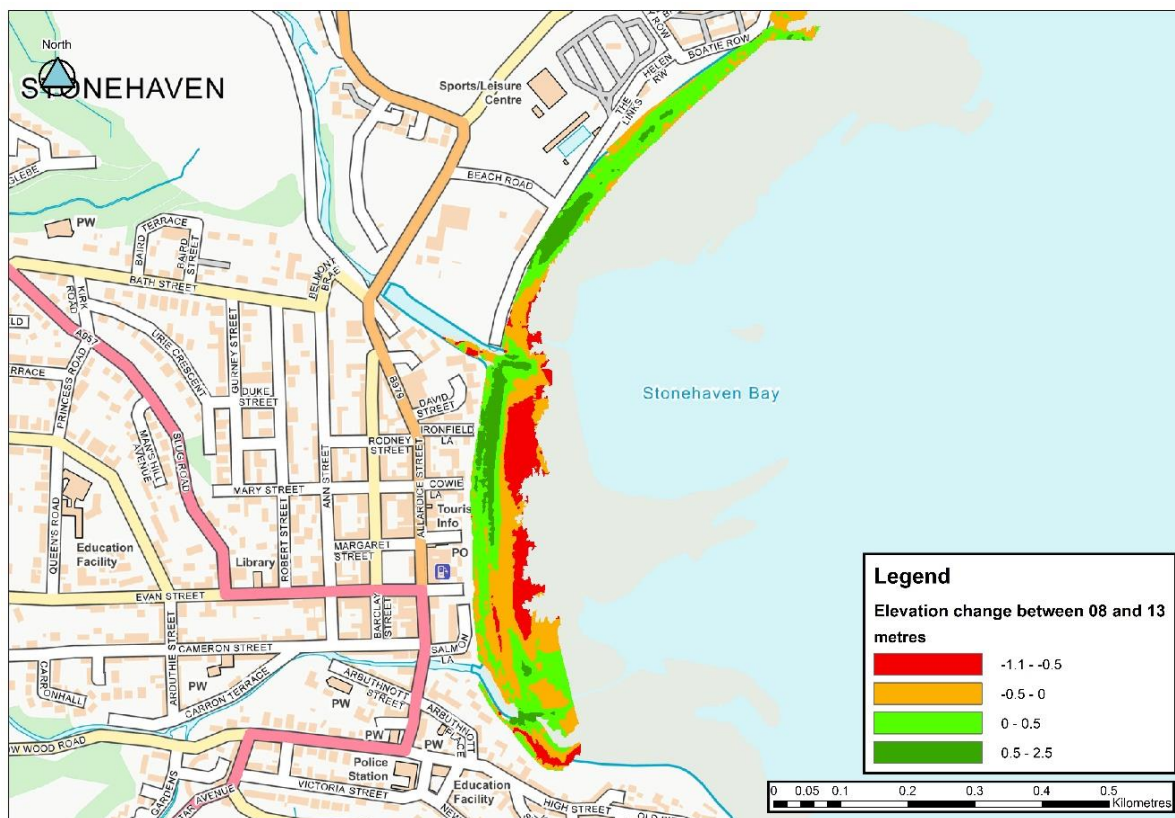


Figure 3-12: Elevation change from 2008 to 2013 across Stonehaven Bay

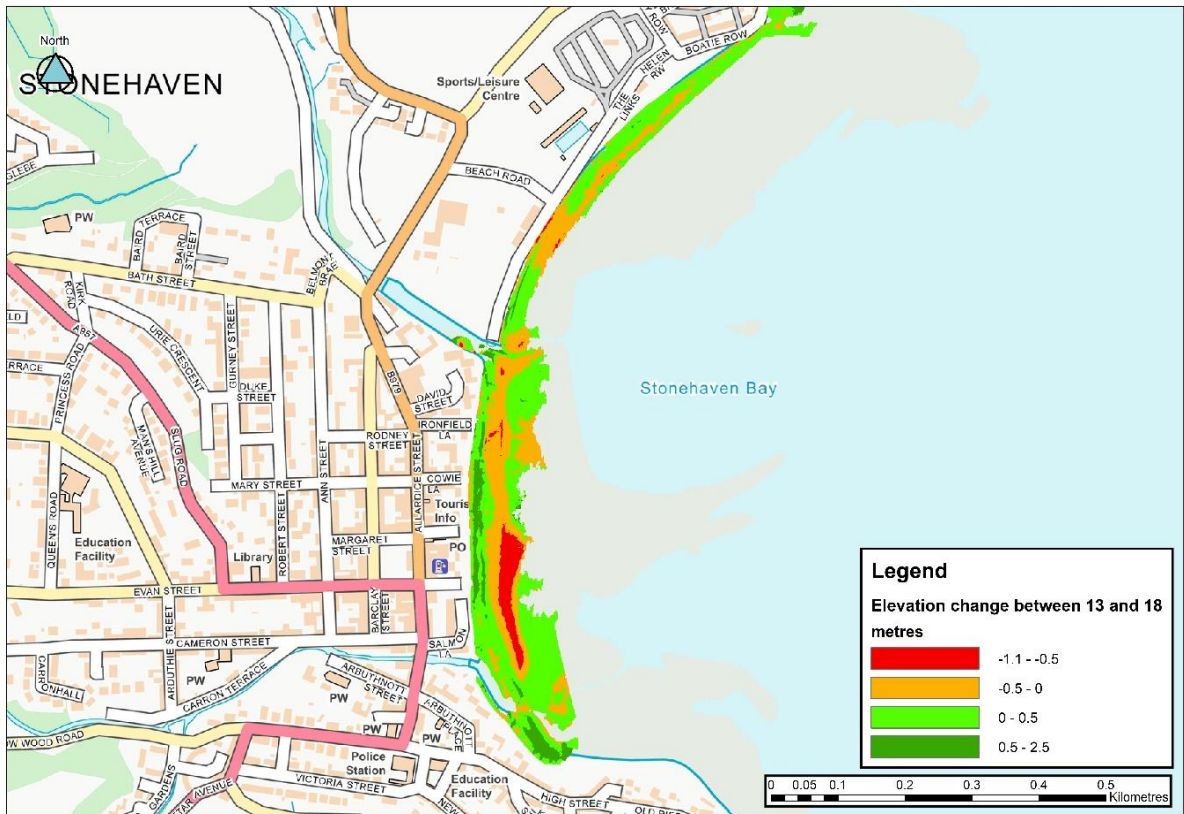


Figure 3-13: Elevation change from 2013 to 2018 across Stonehaven Bay

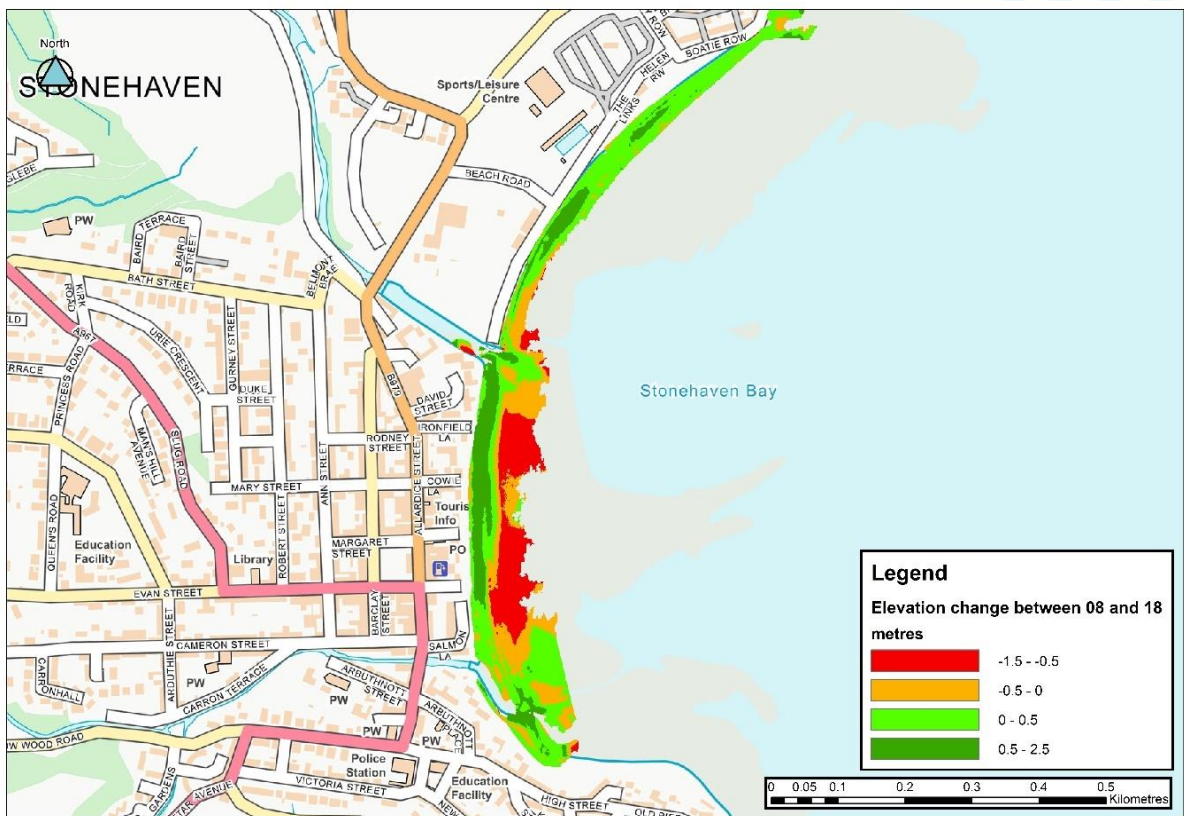


Figure 3-14: Elevation change from 2008 to 2018 across Stonehaven Bay

3.6.5 Cross sectional analysis

As part of the earlier surveys, cross-sectional profiles were taken at 26 locations along the beach (Figure 3-15).

These were replicated for the May 2018 survey and have been used to provide additional analysis of the volumetric changes in the beach.



Figure 3-15: Cross sections at Stonehaven Bay

Figure 3-16 shows a general increase in sediment volume from 2008 to 2018 above MHW. An overall summary of volume changes is provided in Appendix B, with profile plots from each year in Appendix D. Between 2008 and 2013, the majority of cross sections gained volume, with the largest volume gain seen between XS15-XS20. Between 2013 and 2018, the volume variations are much smaller and more varied, with some sections that had been gaining volume previously seeing a loss in volume, e.g. XS15 and XS17. The cross sections with the largest variability from 2008 to 2018 are XS14 - XS21 and XS26. Overall, there is a general increase in sediment volume towards the south of the bay (Figure 3-16) and significant volume losses are present predominantly north of the River Carron estuary (XS22-XS24), whilst the most significant volume gains are south of the Cowie Water estuary in the middle of the bay (XS15-XS21). XS04, XS05, XS07, XS08, XS09, XS19, XS20, XS21, XS25 and XS26 are always gaining sediment above MHW whilst XS22, XS23 and XS24 are consistently losing sediment.

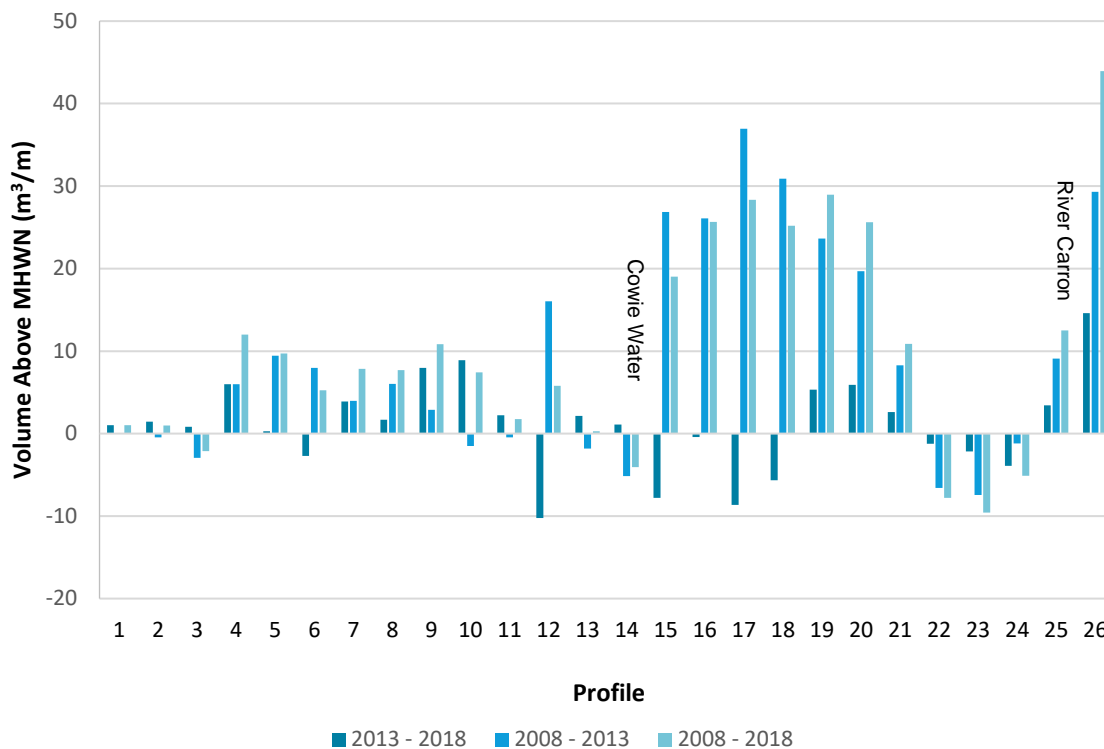


Figure 3-16: Sediment volume below MHWN from 2008 to 2018

3.6.6 Volumetric trends

Overall, the volume above MHWN increases north to south due to the increasing width of the beach and therefore sediment available. This supports the predominant sediment movement findings from previous studies.

Generally, variations between 2008 and 2013 are larger than those between 2013 and 2018. It is hypothesised that this is primarily due to the timings of the surveys with the 2008 being undertaken before the storm season, and the 2013 and 2018, after.

To support this, an analysis of “storm” event frequency was undertaken. This was based on the emulated hindcast dataset at the buoy location and an Hs threshold of the 99th percentile. Independent events were generated when Hs exceeded this threshold, assuming a 24-hour independence. This resulted in 21 events for 2008-2013, and 20 events for 2013-2018.

This supports the fact that there is no physical reason for such large variation between 2008-2013 and 2013-2018 and the date of the survey, may heavily influence the trends evident in the data.

The three northern sections are experiencing a net volume gain, whilst southern sections have experienced a net loss of volume. The composition of the beach and presence of a rock platform varies throughout the bay, explaining the different patterns seen. The Cowie Water supplies fine sediment to Section C, within the river channel and to the beach to the south of the watercourse. An overall gain of sediment is seen within the cell, and across the profiles in the area, which is inconsistent with the volume of sediment removed periodically through recharge.

The largest variation is seen in the sections south of the Cowie Water and the beach is seen to accumulate near the defences and erode near the sea, leading to a steepening of the whole beach. This eroded sediment contributes to the increase in

volume above MHWN. This is typical of a storm response in gravel beaches and is more pronounced between 2008 and 2013.

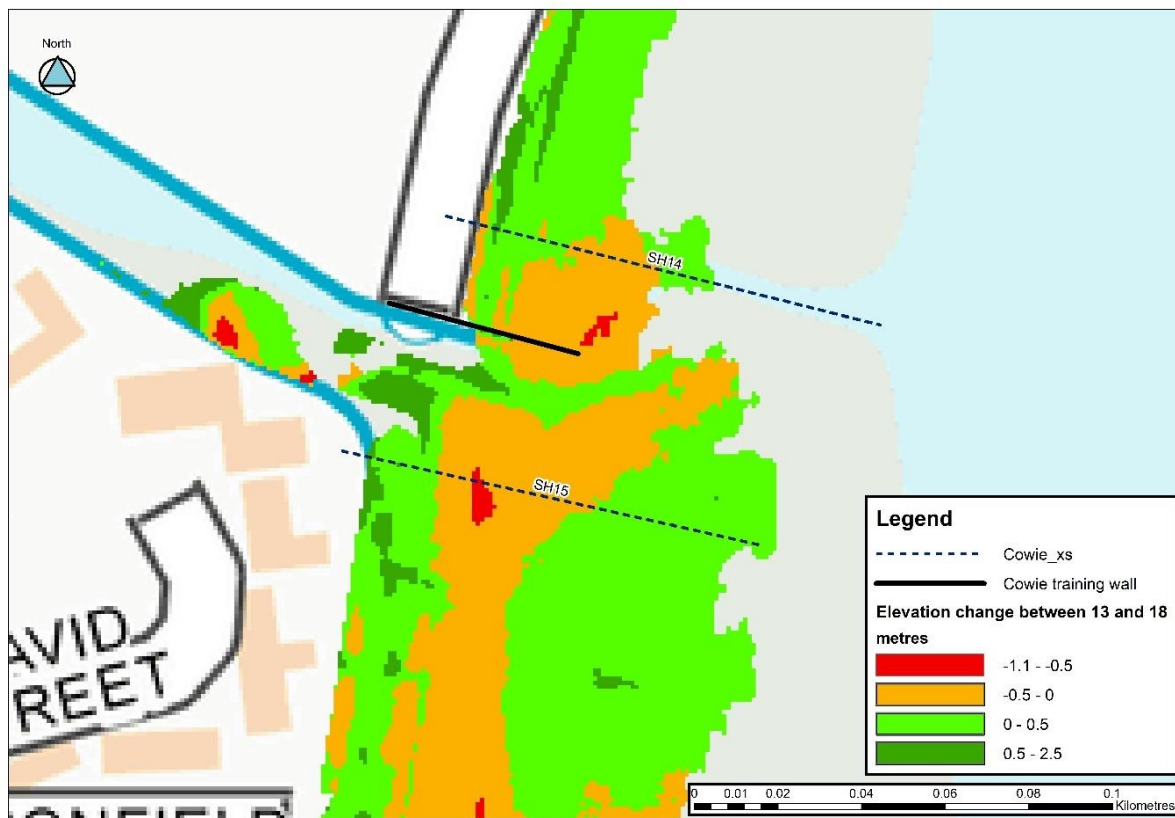
3.6.7 Coastal structure performance

Cowie Water training wall

The sediment bar within the Cowie Water channel has considerably increased in volume since 2013 and significant sediment build up within the channel at the mouth of the Cowie Water is also present (Figure 3-17). The Cowie runs along the south of the training wall in a narrowed channel before discharging into the sea. The training wall was installed to prevent sediment from the north blocking the mouth of the Cowie and help maintains beach volume to the north.

Table 3-6: Volumetric changes above the toe of the Cowie training wall

Profile	2008	2013	2018
Volume above toe of the wall (m ³ /m)			
14	65.44	60.38	60.74
15	68.25	87.39	76.89



Contains Ordnance Survey data (c) Crown copyright and database right 2018

Figure 3-17: Cowie Water: elevation change from 2013 to 2018

In an attempt to assess the performance of the structure a refined topographic and profile analysis was undertaken.

The wall ends at approximately 0.55 mAOD in 2018, and volume change was analysed above and below this level.

Between 2008 and 2013, the volume at Profile 14 decreased from 65.44 m³ to 60.38 m³ (Table 3-6). Between 2013 and 2018, the volume change was very little, gaining

only 0.4 m³/m. In both time periods an area of significant sediment loss is present behind the training wall (Figure 3-18) suggesting the north to south longshore drift movement of sediment is not the dominant process at this location. It is possible that cross-shore transport during extreme events dominates here and is responsible for the erosion at the structure.

Profile 15 experienced the opposite sediment patterns to those at Profile 14, increasing in volume from 2008 to 2013, from 68.25 m³ to 87.39 m³. Between 2013 and 2018, the volume change was less and a loss of 10 m³ was evident.

The highest volume at Profile 14 was experienced in 2008, which is the same year that Profile 15 experienced its lowest sediment volume (Table 3-6 and Figure 3-16). The lowest volume at Profile 14 coincided with the highest volume at Profile 15, in 2013. The largest volume change at both profiles occurred in the period between 2008 – 2013, and the following five years experienced less sediment variation. It may be that Profile 14 is more prone to erosion from extremes when the training wall is at full capacity, and additional sediment bypasses the wall and accumulates within the Cowie channel.

Removal of sediment through beach recycling in this area does not appear to have a large influence on the overall sediment budget of this section, or the flood risk to assets shoreward, as the beach is naturally replenished from river discharge and longshore sediment movement.

The training wall at the Cowie is effective at reducing sediment transport south to an extent, however when it is at full capacity, sediment bypasses it and contributes to build up in the Cowie Water channel.

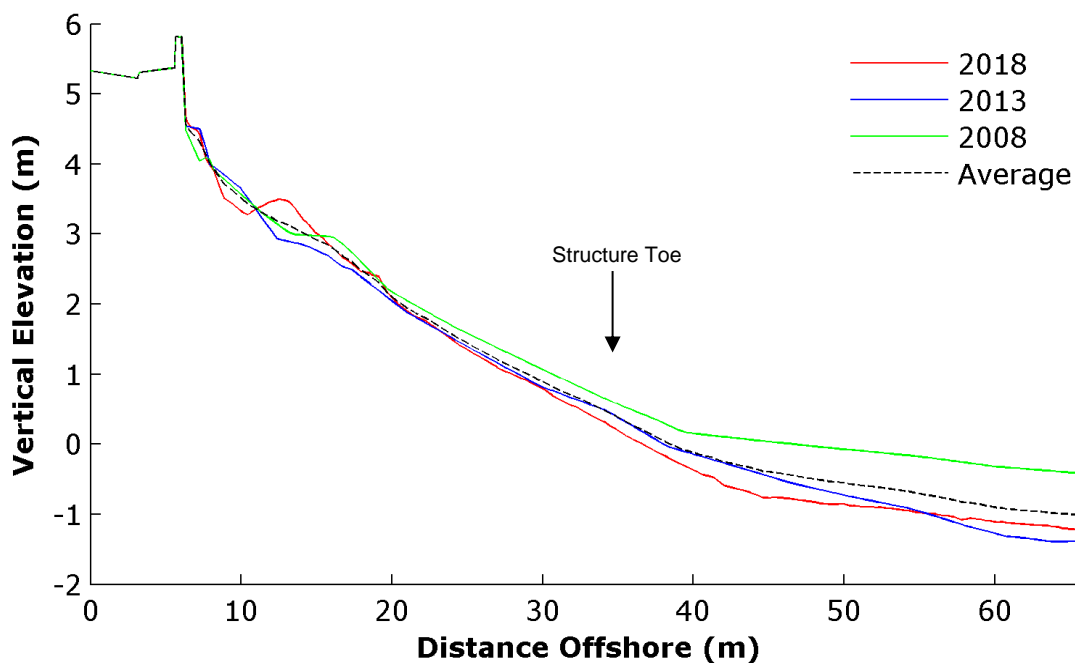


Figure 3-18: Profile 14

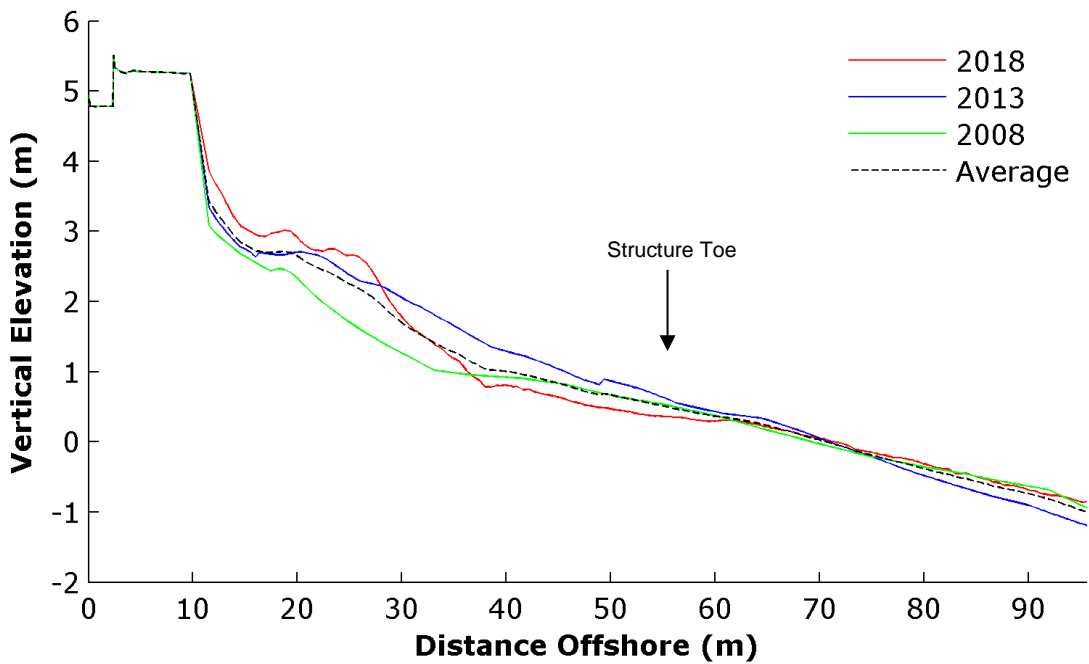


Figure 3-19: Profile 15

River Carron rock armour

Figure 3-20 shows the area considered for detailed analysis and this shows while sediment has eroded at the mouth of the river, there are large areas of accumulation present to the north and south. North of the mouth, significant erosion in the middle beach is seen. The lower beach of both profiles has consistently gained sediment throughout the time period. The overall volume above MHWN has steadily increased from 2013 to 2018, following a decrease from the previous 5 years. Profile 25 (Figure 3-21) remains relatively steady, with a slight increase in volume across the profile, from 66.4 m³ to 78.9 m³. Profile 26 (Figure 3-22) also sees accumulation of sediment almost throughout the profile, which may be explained by deposition from the River Carron, or as a result of the sediment recharge that takes place.

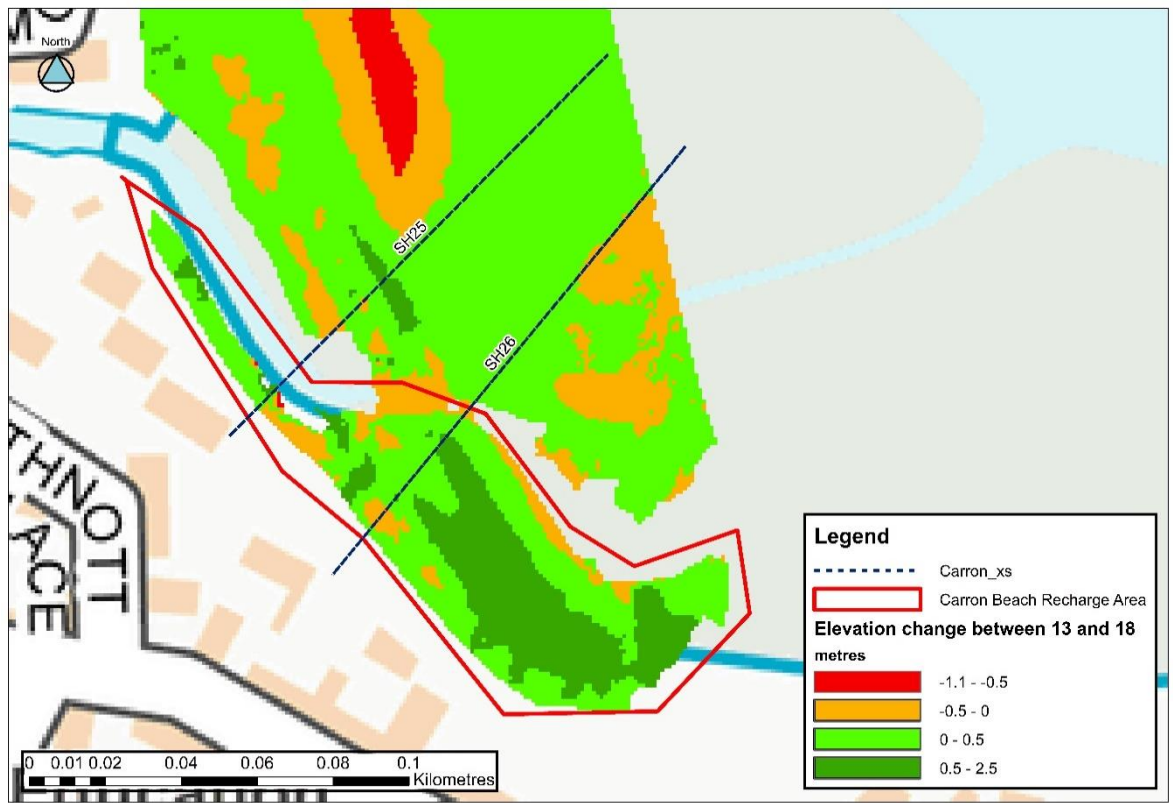


Figure 3-20: River Carron: Elevation change from 2013 to 2018 (NB: the area of no data is the current course of the River Carron which was not included in the topographic survey from 2018.)

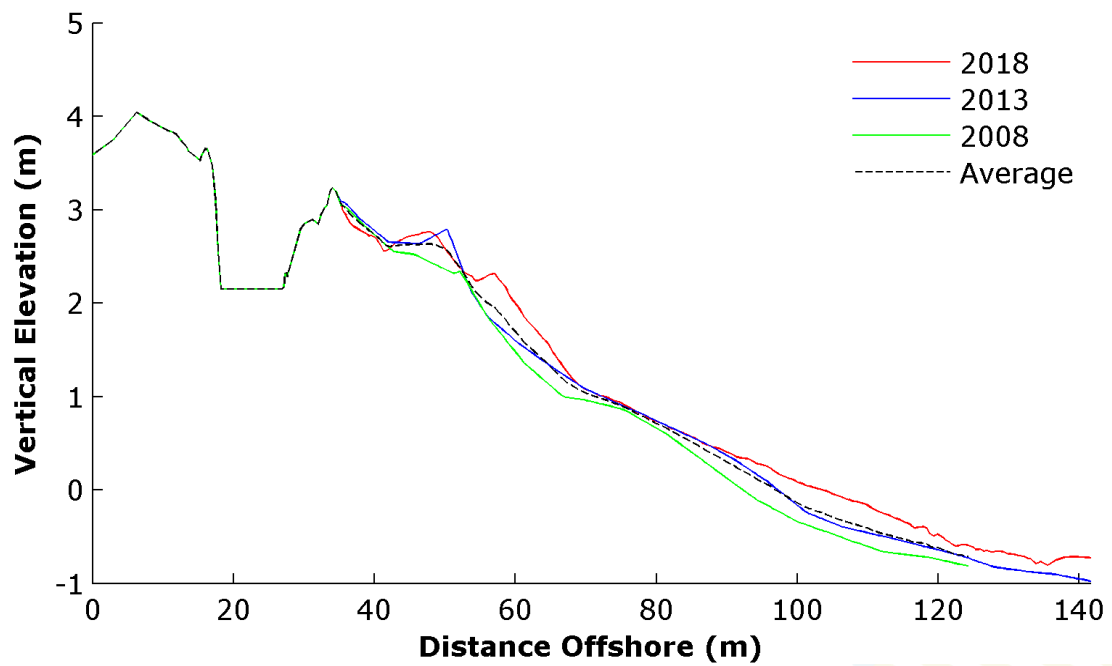


Figure 3-21: Profile 25

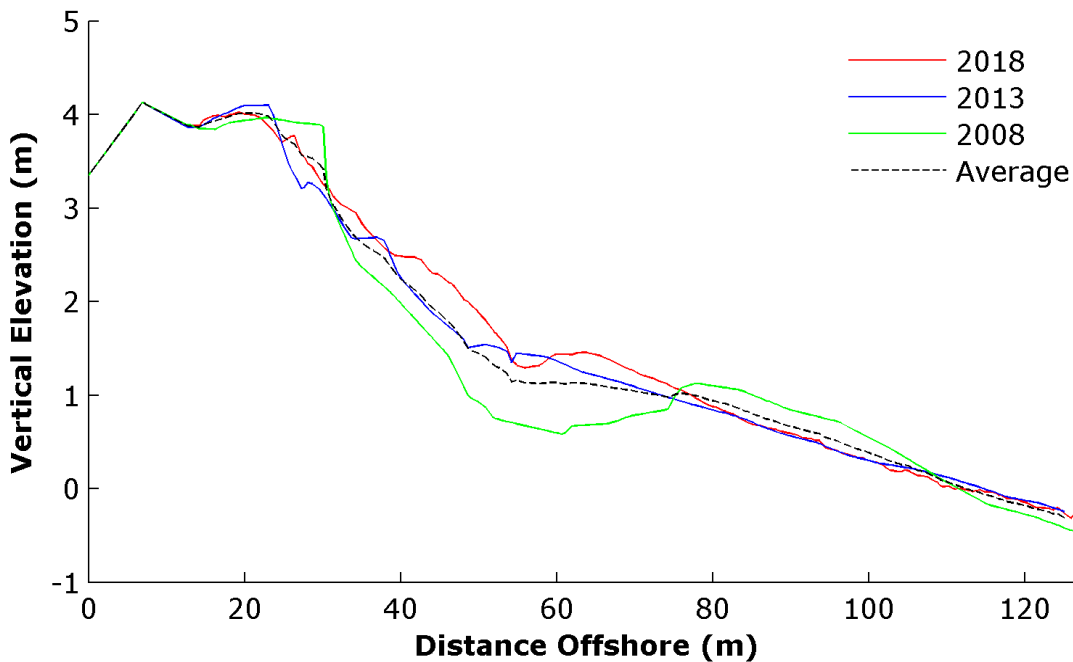


Figure 3-22: Profile 26

Specific analysis of the area of beach recharge (south of the Carron estuary outlined in Figure 3-20) undertaken and the overall volume change from 2008 to 2018 was calculated (Table 3-7). The first five years analysed return a negative value of -810 m³. During this time period, 5,825 m³ (11650 tonnes, converted at 2000kg/m³) of sediment was deposited in this area, and this analysis supports the observations that sediment from the beach recycling is consistently being lost from this area. From 2013 to 2018, the topographic analysis estimated a volume gain of 2,101 m³, which is less than was deposited during the period (4,375 m³). This again supports observations that sediment is lost offshore from this area, despite the ongoing beach recharge.

Table 3-7: Volumetric changes within Carron recharge area

	2008 - 2013	2013 - 2018	2008 - 2018
Volume change within Carron recharge area (m ³)	-810	2101	1291
Volume deposited through beach recycling (m ³)	5,825	4,375	10,200
% sediment retained from recharge	-13.9%	48%	12.7%

Although there is a high degree of uncertainty in the analysis (both in survey data and extent), this demonstrates that the current practice is ineffective. Despite sediment being lost from the recharged area, the overall analysis shows that it may not be completely lost from the Stonehaven Bay sediment cell and is rather redistributed within the bay. To better understand this redistribution, detailed monitoring (e.g. tracers) or 2D modelling of combined waves and currents, would be required.

3.7 Erosion modelling

To better understand the morphological response of the beach during extreme conditions, a numerical modelling assessment was undertaken. This used the XBeach suite of morphodynamic models and will be used to:

- Provide an understanding of storm responses;
- Identify critical assets at risk of erosion.

The division of the beach presented previously was retained for the XBeach modelling, leading to the creation of five 1D models. These were extended offshore to the approximate location of the buoy.

The details of the models are explained in the following sections, with each being set up to best represent the characteristics of the section of the beach being modelled.

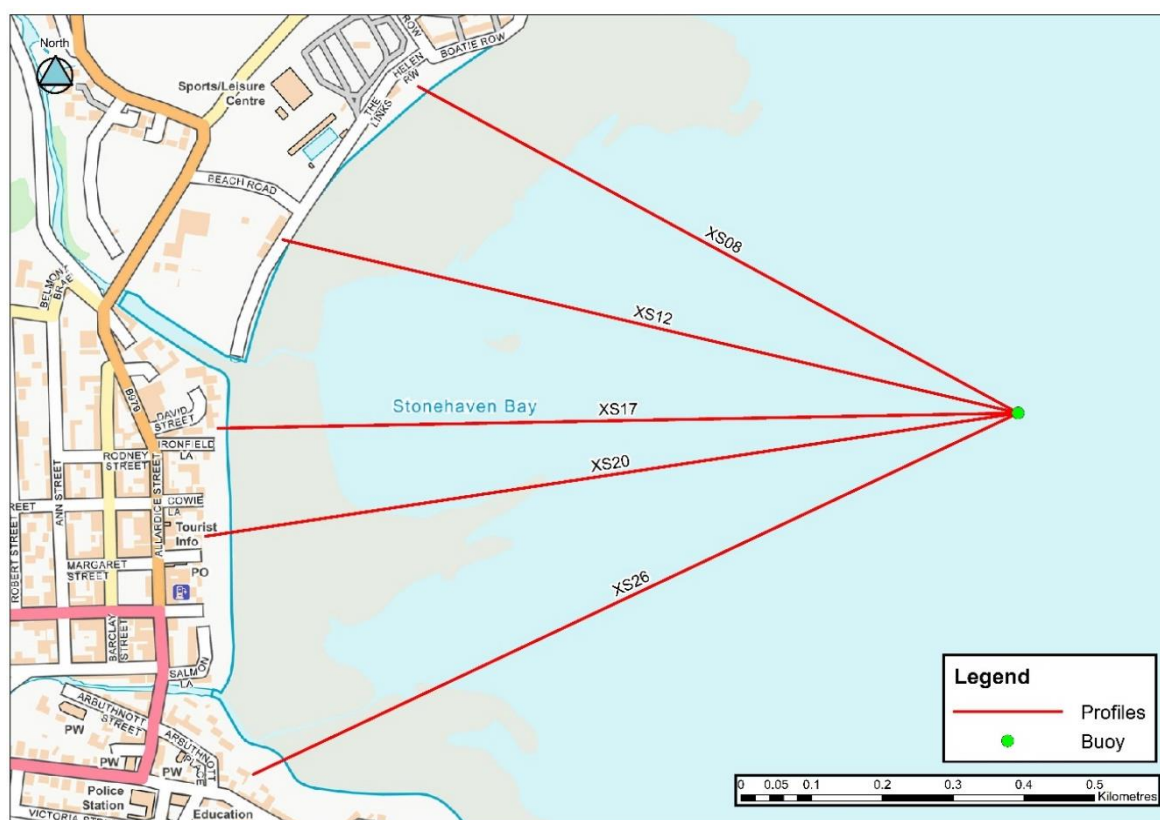


Figure 3-23: Topographic profiles extended to nearest wave buoy

3.7.1 XBeach requirements

Bathymetry and beach profiles

The full cross-section profiles were compiled using the topographic data from the 2018 survey and OceanWise data to extend them to wave buoy.

The location of any structures and offshore rock platforms were identified and included in the model bathymetry as unerodable sections.

Section A/XS08

This location is characterised by a small sandy beach fronted by a large rock platform that protrudes over 100 metres into the bay, protecting the shore from erosion to some extent. There is a vertical seawall at the top of the beach, landward of which is a grass bank leading to properties at a lower level. Figure 3-24 shows a schematised cross section of the profile.

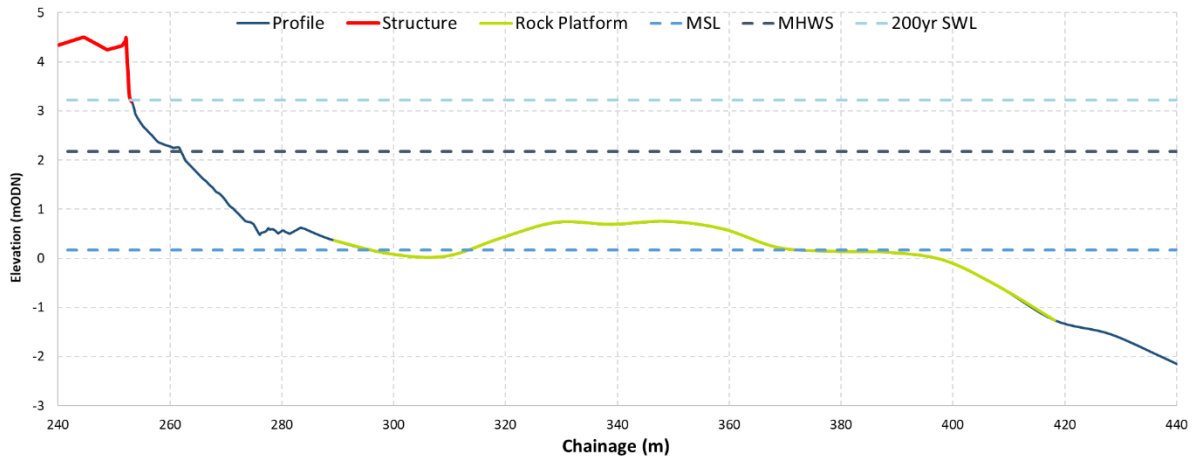


Figure 3-24: XS08 topographic profile

Section B/XS12

This location is predominantly shingle but mixed with coarser sand lower on the beach. There is no offshore rock platform. A stepped revetment with recurve wall is present at the top of the beach (Figure 3-25) which backs directly onto the Links esplanade.

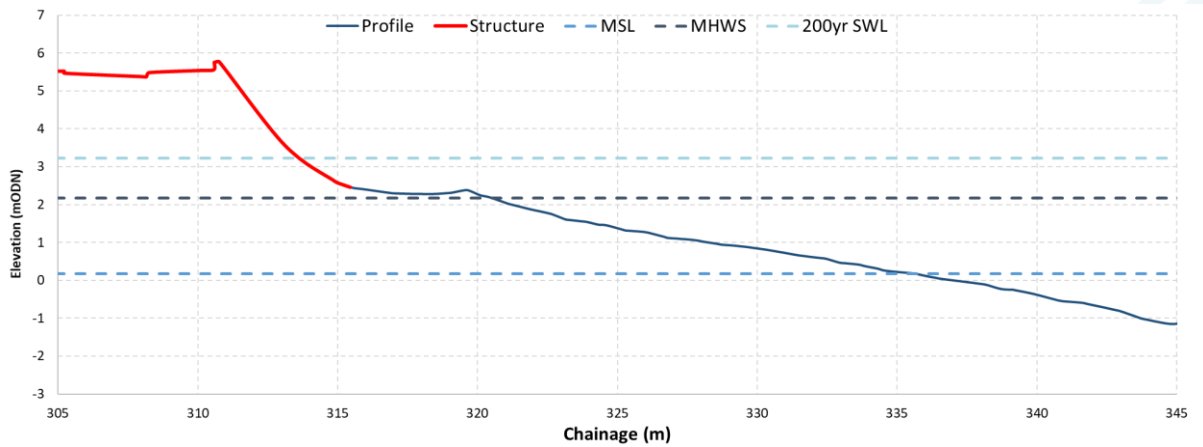


Figure 3-25: XS12 topographic profile

Section C/XS17

The beach at this location is again a mix of coarse sand and shingle and is much wider than the previous two sections. The seawall present (Figure 3-26) is becoming buried underneath accumulated beach sediment from the predominant landward movement of the beach.

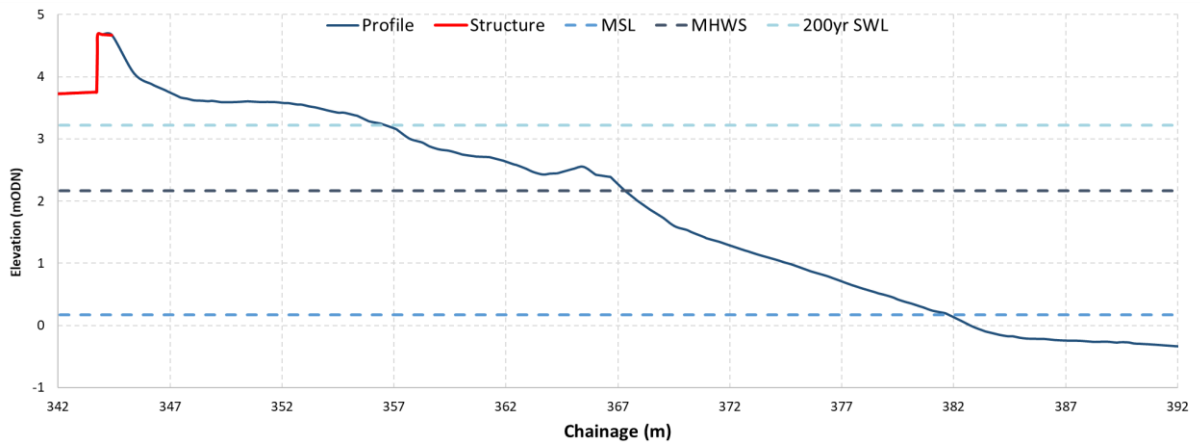


Figure 3-26: XS17 topographic profile

Section D/XS20

The beach at this location is similar to Section C, however the seawall is more visible from the shore. There are multiple rock platforms present offshore of this profile just below MSL (Figure 3-27). It is likely that these will dissipate wave energy, explaining why less accumulation of sediment has occurred compared to Section C.

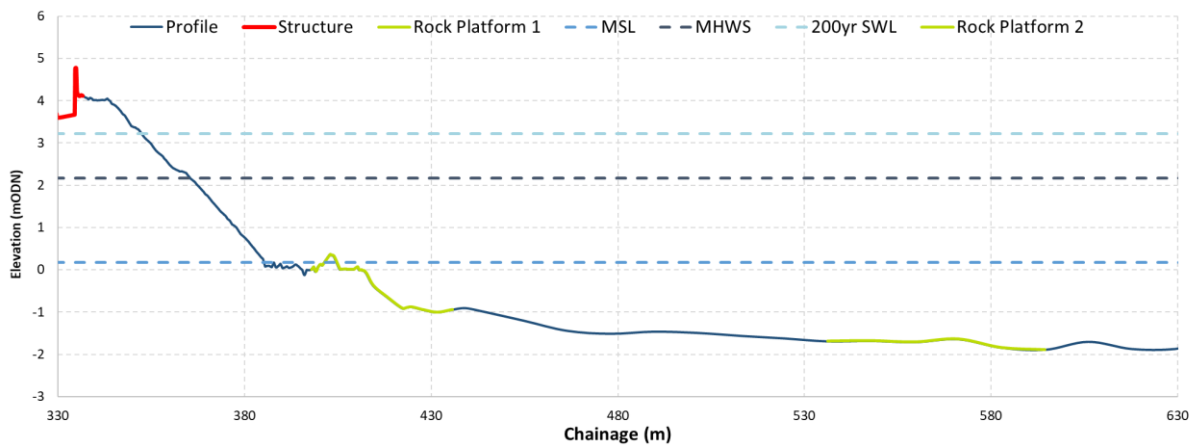


Figure 3-27: XS20 topographic profile

Section E/XS26

There are no defences in place at this location, and there is a boardwalk at the crest of the beach (Figure 3-28). The beach is predominantly shingle with sand present where the River Carron discharges into the sea.

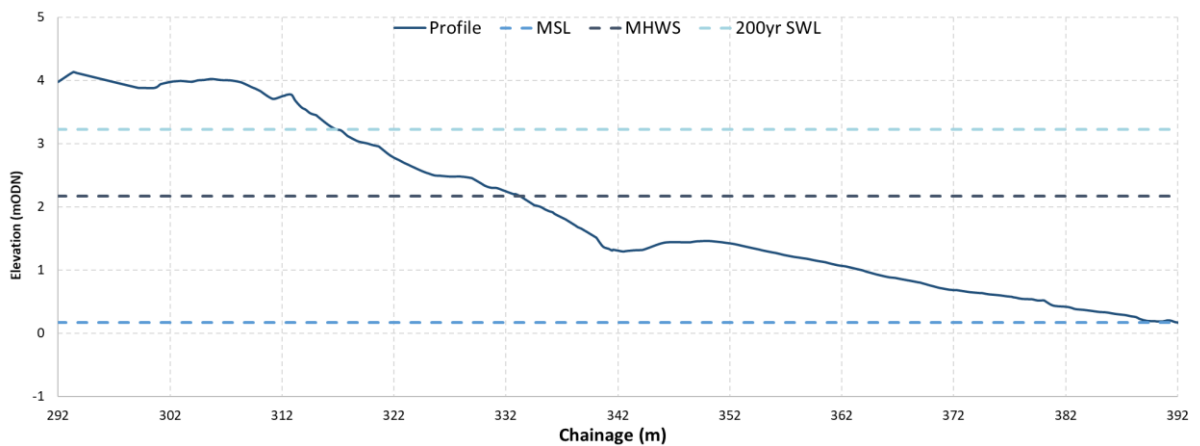


Figure 3-28: XS26 topographic profile

Sediment availability

The quantity and depth of erodible material present across the section is required for XBeach modelling to be realistic. The majority of the profile was set to 10 metres of erodible material, except for the rock platform and coastal defences which had 0 metres of erodible material. Depth was transitioned between 0 and 10 to create a smooth slope. The hardbed locations were identified from aerial imagery and topographic data.

Sediment size was estimated through aerial imagery and photographs and is outlined in Table 3-2.

3.7.2 Modelling of the 2017 event

Morphodynamic modelling of beaches is an extremely complex process with a high degree of uncertainty. To have greatest confidence in model outputs and behaviour it is preferable to have pre- and post-event profiles to calibrate and validate the model. In the absence of this here, the models have been sense checked based on the predicted behaviour during the peak of the highest recorded wave event in the offshore buoy record (February 2017).

The XBeach suite of models consists of XBeach (for sandy beaches) and XBeach-G (for gravel beaches). These represent the key physical process that control morphology (e.g. hydrodynamics, undertow, groundwater flow and sediment transport) on different beach types using different numerical approximations.

Based on the characteristics of each section, the most appropriate model was determined and set up accordingly (Table 3-8).

Table 3-8: Preferred model setups for each section

Section	Model	Wave solver
A / X08	XBeach	Non-hydrostatic
B / XS12	XBeach-G	Non-hydrostatic
C / XS17	XBeach-G	Non-hydrostatic
D / XS20	XBeach-G	Non-hydrostatic
E / XS26	XBeach-G	Non-hydrostatic

The non-hydrostatic wave solver allows for the estimation of the short-wave shape and runup. This is used as default in XBeach-G as it is the short waves that are responsible for shaping the morphology.

However, by default the XBeach models uses a surfbeat wave solver, where the infragravity wave shape is fully solved and the short-wave component estimated through energy balance. For exposed sandy beaches with wide surf zones, infragravity waves are the predominant control on erosion. This approach allows for the approximation of wave undertow and will always result in a net offshore movement of sediment.

To provide a comparison to the preferred model setup, a second model using the original XBeach in surfbeat mode was made. This is used to highlight the differences between approaches and give confidence that the preferred set-up is appropriately replicating the expected morphological response.

Boundary Conditions

The event on the 7th February 2017 was identified as the largest in the wave buoy record and was extracted from the data. This was combined with the recorded water level at the Class-A tidal gauge at Aberdeen to form the boundary conditions for the modelling. The dominant wave direction within the event was from the east, $\sim 107^\circ$, with wave heights exceeding 5m, and periods over 10s. The 12 hours encompassing high tide was used in the modelling (Figure 3-29); with the waves assumed to be approaching each profile perpendicularly.

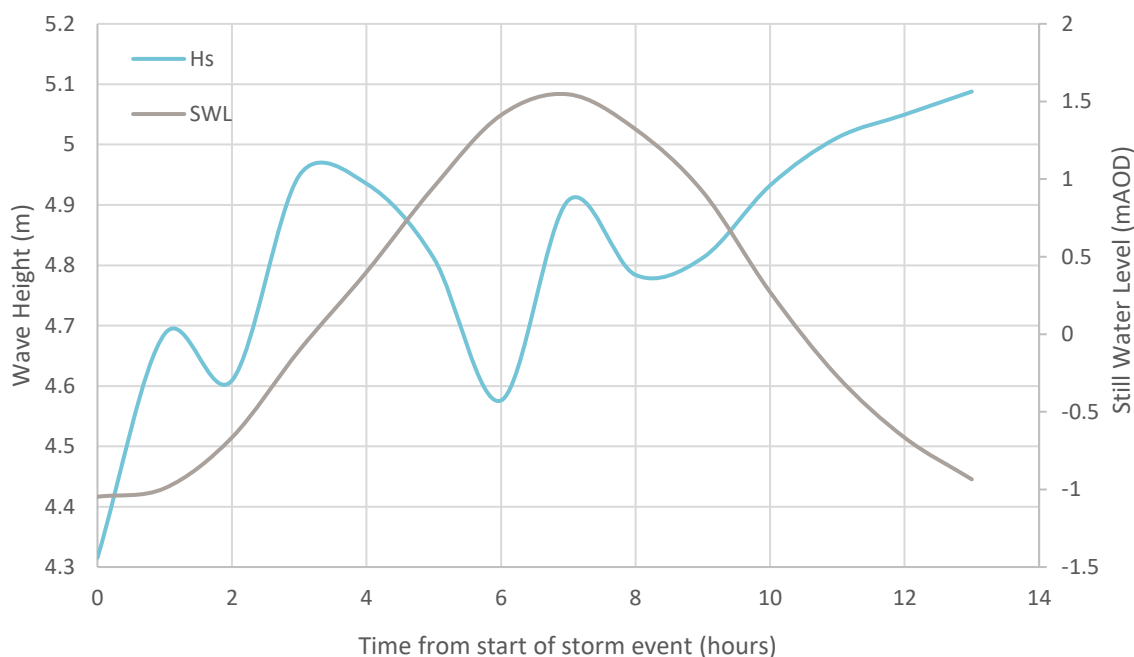


Figure 3-29: February 2017 event Wave Height and SWL

Results

The results from the modelling of the February 2017 event are provided in the following sections. These present the estimated change in the beach profile post-event and the change in level at the defence toe level throughout the event.

XS08

The preferred model setup demonstrates accumulation of sediment at the toe of the defences and an overall landward movement of the beach.

As a comparison the default surfbeat model predicts significant erosion at the toe and offshore deposition.

At the peak water level recorded in the event (~1.5mODN) the rock platform is likely to provide substantial sheltering from the larger offshore waves. It is likely that this would influence sediment movement at this location, with the smaller waves in the lee of the platform promoting onshore transport of the beach sediment.

While scour at the toe of the defences has been observed in the past, it is likely that this is attributed to events with larger SWL.

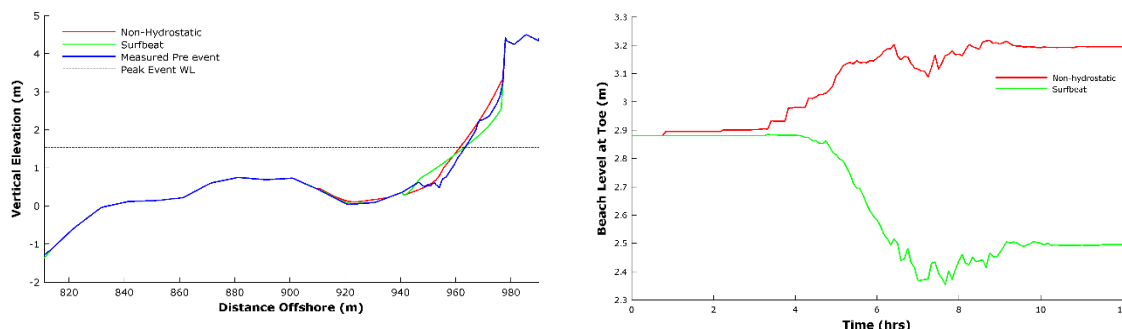


Figure 3-30: XS08 modelled profile and beach level at the defence toe

XS12

The level at the toe stays similar in the preferred model setup, as accumulation of the beach takes place predominantly below the toe level.

In the XBeach surfbeat model a substantial portion of the beach below the defence becomes eroded and is deposited offshore.

The beach here is predominantly gravel meaning the use of XBeach is inappropriate and the predicted erosion is unrealistic.

Given the peak water level of the event, the modelled accumulation of the beach using the preferred model setup is considered realistic.

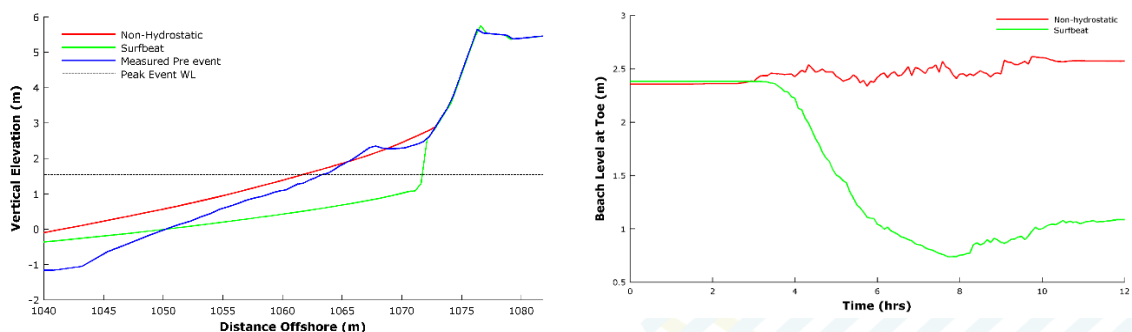


Figure 3-31: XS12 modelled profile and beach level at the defence toe

XS17

Accumulation of sediment is predicted across the whole beach at XS17 for the preferred model setup, as well as some sediment depositing landward of the defences.

Modelling erosion with surfbeat shows unrealistic erosion of the beach above SWL.

These sediment changes are mirrored in the change in beach level at the defence toe; taken as the crest of the beach in front of the sea wall.

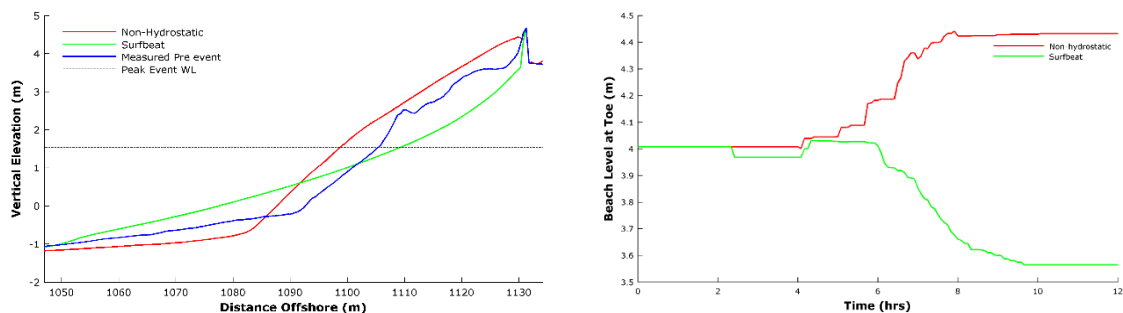


Figure 3-32: XS17 modelled profile and beach level at defence toe

XS20

Accumulation of sediment is predicted across the whole beach at XS20 for the preferred model setup, as well as some sediment depositing landward of the defences.

The XBeach surfbeat model results in unrealistic erosion of the beach.

Compared to XS17, the sheltering provided by the rock platform reduces wave energy resulting in less accumulation.

The level at the toe (taken as the top of the beach at the sea wall) varies very slightly with preferred model setup. Again, this is a reflection in the reduction in wave energy and runup attributed to the rock platform. The XBeach surfbeat model estimates a greater level of deposition at the toe, primarily due to the sediment size and the undertow being insufficient to return all transported material offshore.

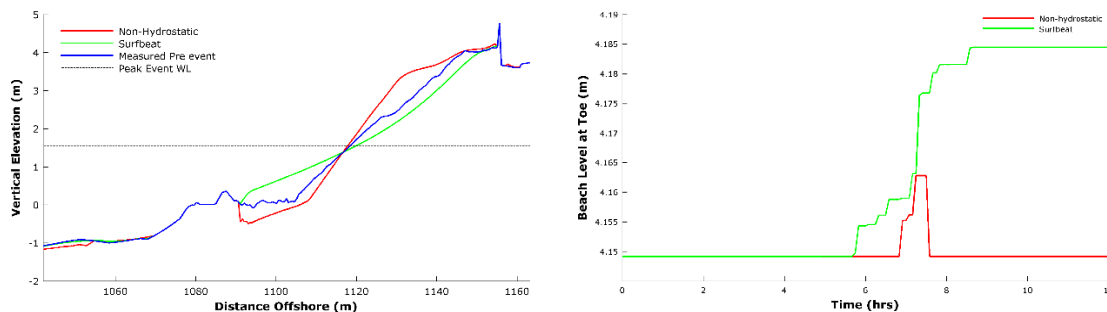


Figure 3-33: XS20 modelled profile and beach level at toe

XS26

Accumulation of a large amount of sediment above the high tide level is predicted by the preferred model setup. Given the coarseness of the beach material, and the relatively low SWL, this behaviour is expected. Shingle is also deposited landward of the boardwalk.

Little to no erosion is predicted by the XBeach surfbeat model as the undertow is insufficient to transport such large shingle.

The level of the beach crest decreases slightly in both models.

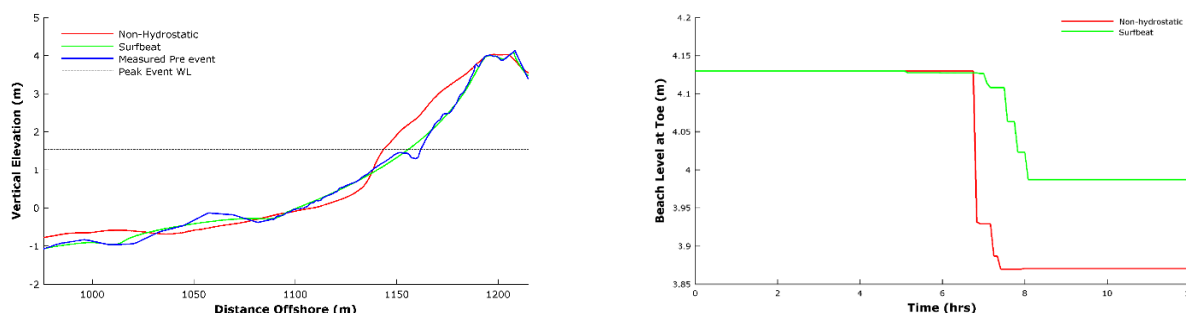


Figure 3-34: XS26 modelled profile and beach level at defence toe

Summary

Historical data in the form of photographs and topographic survey has shown that sediment moves steadily shoreward and the upper beach builds.

While there is anecdotal evidence of scour at defence toes, this suggest that predominantly the nearshore beach steepens and the upper beach gains in volume during extreme events.

During the February 2017 event, it is likely that the low water level was the controlling mechanism on the beach morphology, and during such conditions the predicted net movement of sediment would be landward, resulting in an increase in volume of the upper beach and deposition at defence toes.

It is proposed that the preferred model setups replicate this expected behaviour and are suitable for use in the more detailed erosion modelling.

3.8 undefended erosion modelling

In Stonehaven Bay, the coastal defences are critical to preventing the exposure and damage of key infrastructure. Should these defences fail, the land behind will be exposed to direct wave attack resulting in erosion and associated economic damage. To estimate the likely assets at risk of erosion throughout the appraisal period, undefended modelling will be undertaken.

The complex nature of the morphological response of beaches (particularly shingle) means that no model (empirical or numerical) has been developed or tested for long-term profile response with most focusing on estimating response to individual events. While certain attempts have been made to use XBeach (Original) for long-term simulations, these have been met with varying success and are limited both by computational effort and the accumulation of errors through time.

It is therefore proposed that the following methodology be used to establish future erosion scenarios:

- Create XBeach models with defence structures removed to replicate failure of the defences;
- Generate joint-probability extreme boundary conditions for a range of events (1yr to 1000yr RPs);
- Model profile response for each event and establish an "average" eroded profile for each RP;
- Estimate the retreat of the HAT (Highest Astronomical Tide, 2.57m) for each from the "average" profile response;
- Use these to establish and Annual Average Retreat (m/year);
- Identify the failure year of the defences;

- Based on the failure year, project HAT at 2050, 2080 and 2118 to estimate potential erosion and assets at risk.

Different profiles will respond differently to different forcing conditions and it was therefore decided that the change in HAT was most appropriate for use here. This is consistent with what has been used in the National Coastal Change Assessment and prevents unrealistic erosive response during the highest wave events, particularly at the finer sediment profiles in Cowie.

It should be acknowledged that this type of analysis is highly uncertain and that progression of erosion, in the event of defence failure, will likely occur at different rates along the front. None-the-less, the analysis presented here is useful in that it helps identify the potential risk of unchecked erosion which can be carried forward to develop the business case for investment in the frontage.

Given the inherent uncertainty of the method, attempts to include climate change in the analysis will have no additional benefit.

3.8.1 Coastal defence conditions and residual life

The coastal defences' lifespan and condition were assessed in a separate report (Coastal Asset Condition Survey Report¹⁶). The defences were all graded at CG3 as some defects were present. It was predicted that within 30 years, the defences present at XS08, XS12, XS17 and XS20 will have degraded to CG5, which results in complete failure of the defences. The wall north of Section A, at profiles 1-4, was graded at a CG4, indicating failure is predicted within 15 years. As there is no beach present here, the results from XS08 will be applied to this location. As no defences were in place at XS26, a condition assessment had not been undertaken at this location and the beach is free to advance and retreat from the present day.

3.8.2 2017 event

To demonstrate the concept, the models were run again for the 2017 event to simulate a situation where all the coastal defences have failed, to demonstrate the extent of erosion/sediment movement that may occur.

The movement of the MHWS was analysed by identifying the corresponding chainage of the 2.17mODN contour (MHWS for Stonehaven) at the start and end of the simulation.

The results are presented in the following section.

¹⁶ JBA Consulting. Coastal Asset Condition Survey Report. Final Report. July 2018.
AKI-JBAU-00-00-RP-HM-0002-S3-P02-Interim_Modelling_Report

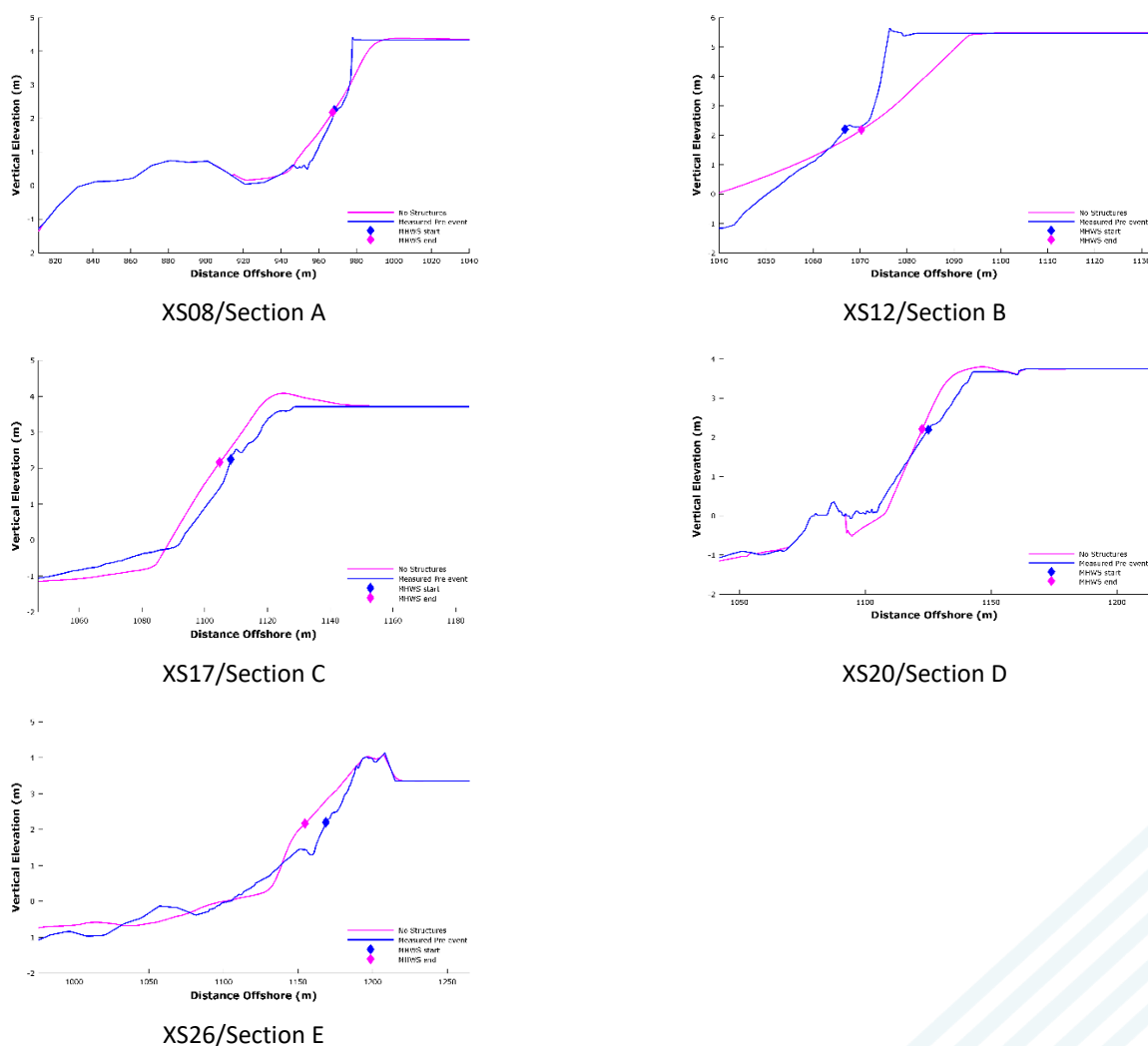


Figure 3-35: Undefined modelled profiles

- At XS08, the coastal defences erode whilst the lower half of the beach accumulates sediment. The MHWS line moves 1m towards the sea due to accumulation of sediment.
- At XS12, similarly to XS08, the defences get completely eroded away, and the MHWS line moves 3.5m landward.
- XS17 is subject to further accumulation across the whole beach, and erosion of the small seawall. The MHWS line moved 3.5m seaward.
- At XS20, without the seawall, erosion has little effect on the assets behind the defences however the beach advances, as seen by the 3.5m advance of the MHWS line.
- At XS26, given that no defences or hardbed was present, the sediment movement profile is identical to the original non-hydrostatic mode model run and the MHWS line advances by 14m.

Summary

At XS08 and XS12, the coastal defences are predicted to erode, which differs from the sediment patterns seen in the modelled scenario (Figure 3-30 and Figure 3-31) and in the topographic analysis (Section 3.6) that see accumulation of sediment above the MHWN. The defences in this location are preventing the landward erosion of sediment, holding the beach in place.

Without defences in place at XS17, XS20 and XS26, the upper beach is predicted to accumulate sediment, with some beach erosion occurring below MHWN. This is similar to the sediment trends seen from topographic analysis (Section 3.6) and the modelling of the February 2017 event, suggesting the defences are not playing a major role in controlling sediment movement.

3.8.3 Design Events

Boundary conditions

For the wave overtopping analysis SEPA’s offshore multivariate dataset has been used. This involves the modelling and emulation of a dataset containing approximately 2 million “events”. As part of this process the dataset was emulated at the buoy location for use in the erosion modelling.

Analysis of this dataset allows for the generation of joint-dependency curves of any variable at any return period. Here we have used this to estimate joint-dependency Hs and SWL for 1yr, 2yr, 10yr, 30yr, 50yr, 100yr, 200yr and 1000yr events. This is like the standard DEFRA 2003 joint-probability methodology but makes use of the modelled dependency between the parameters from the analysis undertaken to develop the MV data.

The wave period was estimated based on developing a relationship of the average value within ranges of Hs in the emulated MV data. This relationship is shown below and was used to estimate T_p for the design events.

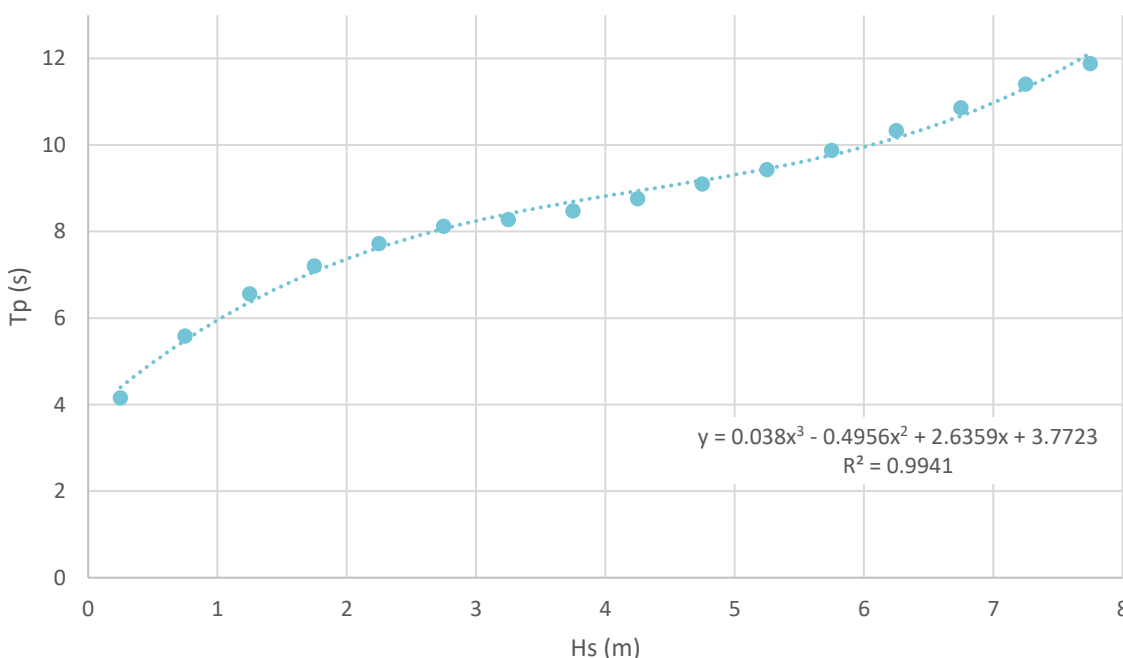


Figure 3-36: Relationship between Hs and T_p

Events have been modelled for the 12 hours encompassing high tide, with the offshore wave conditions assumed to stay constant throughout. The combinations of Hs, T_p and SWL for all events are presented in Appendix C.

Results

The input files for the design events were the same as for the undefended runs above, however 150m of LiDAR data behind the coastal defences was added onto the profiles to estimate realistic sediment movement at different return periods.

The movement of the HAT for the average eroded profile for each return period at each cross section was estimated.

Overall, the amount of potential sediment movement increases with increasing return period. Cross sections 08 and 12 have the potential to be subject to significant erosion, including erosion of the crest of the defence, whilst the other three cross sections are predicted to experience accumulation, especially at the crest of the beach.

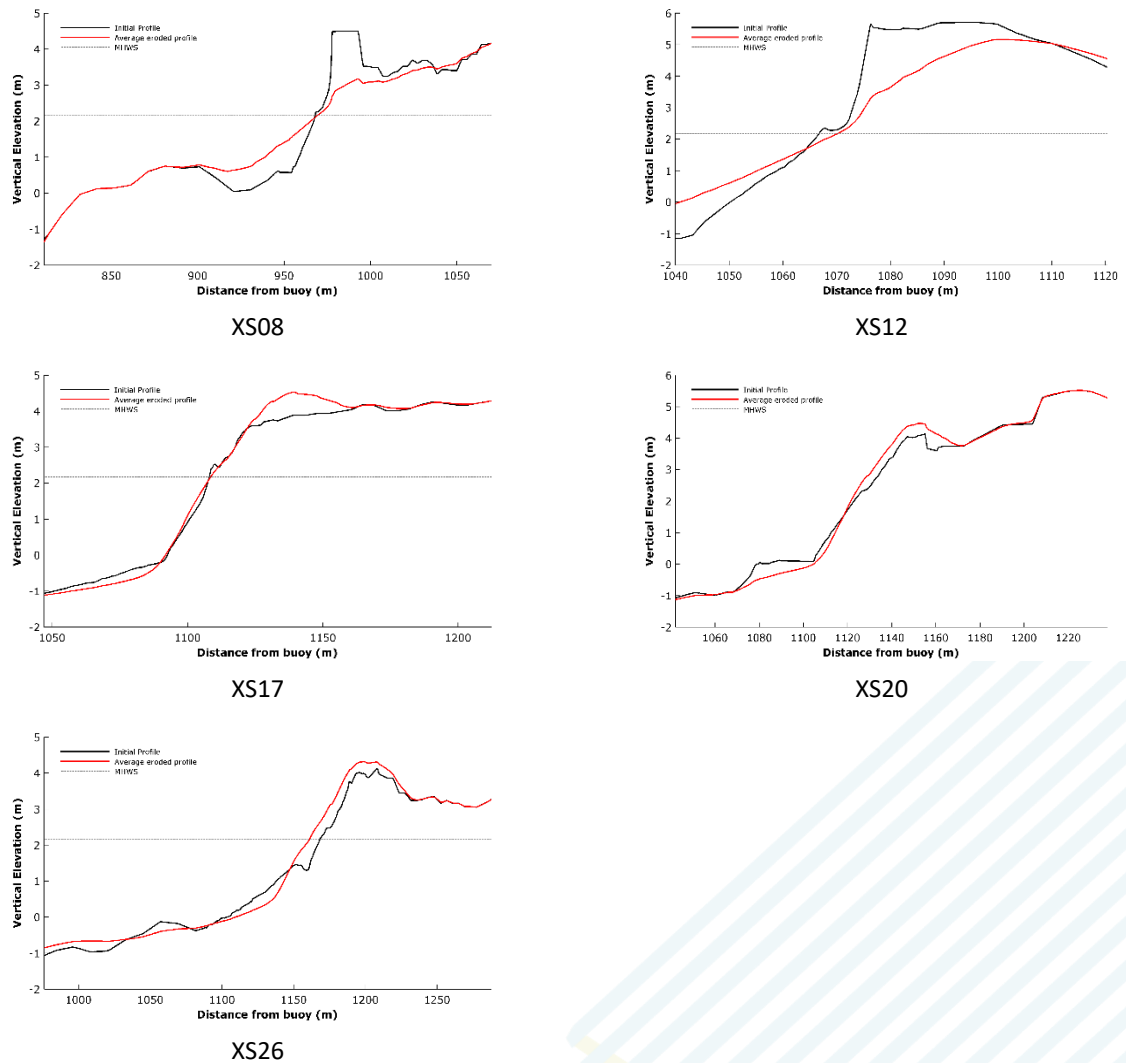


Figure 3-37: 0.5% AP (200 year) profiles

HAT movement

Movement of the HAT contour was estimated by annualising the average profile movement for each return period. For profiles where advancement of the beach was seen, the minimum values from each event were analysed to model the maximum extent of landward erosion. The results of this are provided in Table 3-9.

Table 3-9: Annual Average Retreat (m/year) for each profile

Profile	Annual Average Retreat (m/year)
XS08	1.66
XS12	1.59
XS17	0.36
XS20	0.50
XS26	0.27

In the northern section of Stonehaven Bay (Cowie), sediments are predicted to significantly erode, and therefore a retreat of the HAT line will be seen. The HAT average retreat near the Cowie Water has been identified as c. 50 metres by 2080, and c. 110 metres by 2118. The shaded area highlights the maximum area at risk of erosion between 2018, 2080 and 2118 (Figure 3-38), if all defences were to fail at the end of their given lifespan. Assuming a similar erosion pattern at XS01-04 as at XS08, and given the failure of the defences 15 years earlier, by 2080 a retreat of c. 75 metres is seen and by 2118, a retreat of c. 138 metres at the north of the bay is predicted. The assets within this erosional zone are therefore potentially at risk.

The southern end of Stonehaven Bay is predicted to experience little retreat of the HAT position, with a maximum retreat of 15 metres by 2080, and 34 metres by 2118, within section D. The number of assets within the erosion zone here is significantly less than in the north of the bay. It is more likely that the southern end of the bay will experience HAT advancement.

Events with lower water level and high wave heights cause the largest erosion.

An A3 figure of HAT predictions is in Appendix F.

This modelling and analysis approach have an extremely high degree of uncertainty and assumes that the backshore consist of fill material similar to the beach. In reality, the: slow failure of the defences, man-made surfaces, buildings and other materials will significantly influence the erosion rates.

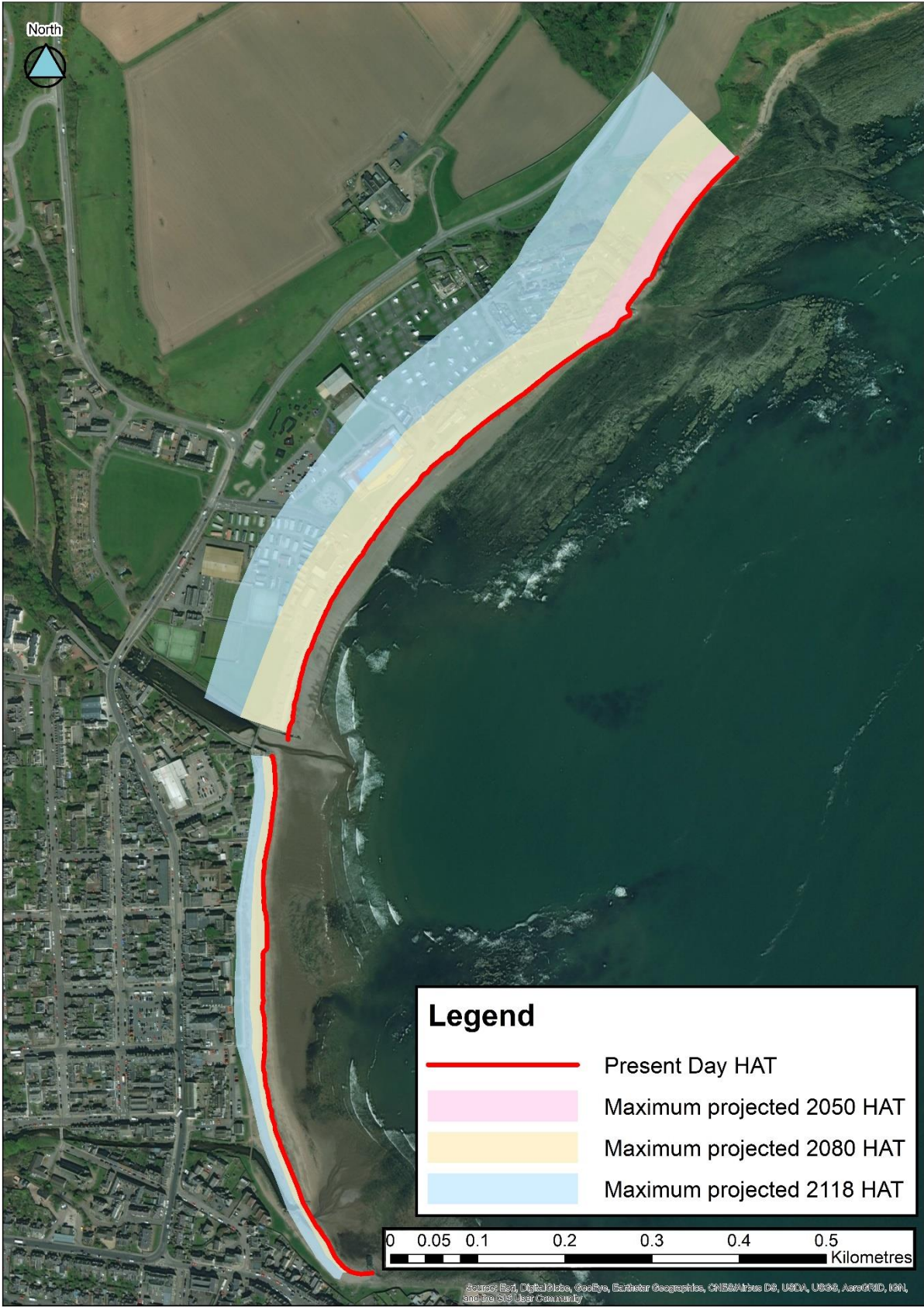


Figure 3-38: Projected HAT retreat by 2050, 2080 and 2118.

Erosion enhanced flooding

North of the Cowie Water, the Promenade and Links area provide a high ground buffer to the lower areas to the rear. Should defences fail, erosion of these “buffer” area will result in significant exposure to the lower lying areas to inundation from future extreme sea levels.

To provide an indicative assessment of this future risk, crest elevation changes, predicted by XBeach, were annualised, to establish when these low-lying areas would become at risk from SWL flooding.

The crest was taken as the top of the coastal defence and compared to the highest elevation point on the eroded profile, not including the ground beyond the defence. Crest elevation drop is shown in Figure 3-39 and analysed further in Table 3-11.

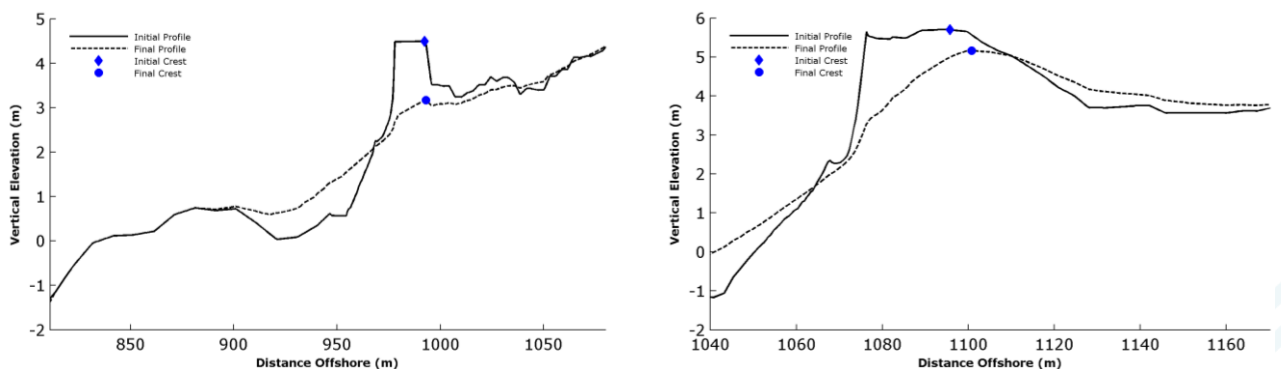


Figure 3-39: Crest changes from the 200-year event (XS08 on left, XS12 on right)

Table 3-10: Extreme Sea Levels from UKCP18

RP	2080	2118
30	3.51	3.83
200	3.71	4.03

Table 3-11: Crest elevation variation

	Crest Level	Ground Level	2080	2118
XS08	4.49	3.49	Crest < Ground Ground < 30yr and 200yr	Crest < Ground Ground < 30yr and 200yr
XS12	5.65	3.75	Crest < Ground Ground > 30yr and 200yr	Crest < Ground Ground < 30yr and 200yr

At XS08, a drop of 0.77m/year is estimated. The top of the coastal defence is 4.5 mAOD and the ground level behind the defences is 3.49 mAOD. Following the predicted degradation of the defences in 2050 at this profile, and assuming the crest level would not drop below ground level, by 2052, the crest level would be at ground

level and the area would be at risk of flooding from SWLs. In 2080 and 2118 at both the 30-year and 200-year return periods (Table 3-10).

At XS12, the estimated crest elevation drop is 0.14m/year. The crest of the defences at this location is 5.65 mAOD with ground level of 3.75 mAOD. The defences are predicted to have degraded by 2050, and by 2064 the crest level would be at ground level of the backshore, and the area would be at risk from SWL. The 2080 SWLs are not sufficient to inundate but at 2118 the 30-year and 200-year return periods (Table 3-10) will flood the backshore area.

To estimate flooding impacts of this erosion, these "buffers" were removed from the TUFLOW model and simulations of the 30 and 200-year events at 2118 were undertaken. The results of these are presented in Appendix F and show the predicted extent of SWL flooding alone for these events.

It should be noted that, a comparison between the defended 2118 extents (Appendix E) shows less inundation occurring for the erosion enhance maps. This is a product of the modelling method and occurs for the following reasons:

- No wave action has been accounted for in the erosion enhanced flooding;
- SWLs alone do not exceed the average backshore level to the north (XS08).

3.9 Erosion assessment summary

North of the Cowie Water the sediment is fine sand, and a rock platform is present. The beach is subject to large variations in volume, however the topographic surveys indicate that the upper beach has accumulated in the past 10 years. Given the uncertainty in the analysis due to the survey frequency, it is not possible to say whether this demonstrates long-term accretion or is a product of short-term fluctuations captured by the survey. Anecdotal evidence and local observations suggest extreme short-term fluctuations in beach levels exist here, and that the frequency of the survey is unable to capture this behaviour. The analysis does however show that the sediment balance within the bay can be considered relatively stable over this period. This is supported by the long-term MHWS analysis which shows minimal variation.

Modelling has shown this area has a tendency to accumulate across the upper beach and erode at the lower beach during small storm events such as the February 2017 event, however in a scenario without coastal defences in place, this area is projected to significantly erode, leading to a retreat of the HAT location. The lower beach is predicted to increase in volume from the eroded sediment further up the profile, in a scenario with no coastal defences, demonstrating the opposite trend to normal conditions. Coastal defences are playing a role in holding the line, preventing loss of assets and restricting sediment movement landward. South of the Cowie Water, sediment increases in diameter, and therefore behaves differently. The general pattern is a steeping of the beach, through accumulation near the defences and erosion of the lower beach. This dynamic response during extreme events will have implications on the wave overtopping rates along the front. Considerations of the impacts and management of this response will be investigated during the concept design of the preferred option.

Modelling of the February 2017 event in this area mirrors the general sediment movement patterns over the past 10 years. Without defences, the beach is predicted to accumulate sediment across the whole profile, causing a seaward movement of HAT. The defences do not appear to be influencing the general sediment movement trends in the lower three sections of the beach. The beach recycling that takes place annually does not appear to have a large influence in the overall sediment budget of

the beach as sediment is naturally replenished near the Cowie Water and sediment is consistently lost offshore south of the River Carron.

3.10 Erosion assessment recommendations

Morphodynamic modelling is attributed with a high degree of uncertainty and so recommendations are proposed to increase certainty of future analysis. Better topographic data is recommended, both at more frequent intervals and from the same time of year so post-storm analysis can be made. If possible, this should be targeted to capture pre- post-storm changes in beach levels to allow for quantification of anecdotal evidence of rapidly varying beach levels in the bay.

Monitoring of the gravel bar within the Cowie would allow for detailed analysis of sediment recycling to be made. Data regarding the volume of shingle “cleaned up” following storm events from the coastal footpath and other areas would allow for a more accurate analysis.

4 Baseline economic assessment

To assess the present-day economic impact for coastal flood events a baseline economic assessment was undertaken. These results, presented above, are used to estimate the damage associated with given coastal events at specified return periods.

It should be noted that, although the available modelling results have been utilised in the most appropriate manner, the representation of the baseline scenario may change through consultation with stakeholders, and the monetary values presented here may change as the project develops. Attention should therefore primarily be focused on the approach that is being recommended to ensure there is agreement going forward.

4.1 Estimation of flood damages

4.1.1 Damage calculations

The SEPA receptor dataset has been used in this initial economic assessment to give an estimate of flood damages. At this stage, only corrections have been applied to the floor areas of properties. Prior to the full options appraisal, a detailed analysis (including ground truthing) will be undertaken to assess the quality of this receptor database. This will include:

- Checking of property types against MCM code;
- Checking for basements;
- Assessment of vulnerability.

Flood damages were estimated by linking the receptor points to the building footprints and estimating the water depth at each from flood extents generated by TUFLOW model. These analyses use 2017 depth-damage curves from the Multi-Coloured Handbook (MCM) associated with coastal flooding.

The above determines the direct damages due to property inundation. In addition to these further indirect damages were added to the total. Below is a summary of all damage and additional benefits considered here.

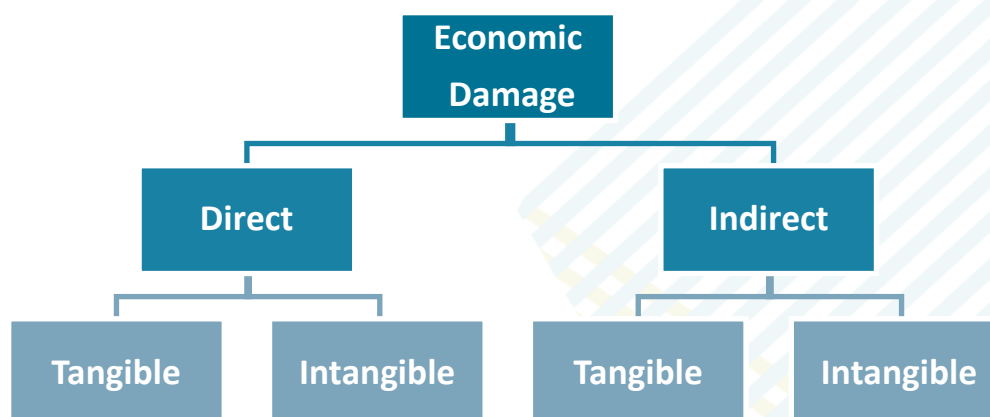


Figure 4-1: Aspects of flood damage

- Direct damages due to property inundation
- Indirect non-residential damages at 3% of direct damages

Evacuation and temporary accommodation costs

- Emergency services costs at 5.6% of total residential direct damages
- Intangible damages (e.g. health)

For calculation of damages the analyses consider a building threshold level for each property, derived from surveyed levels, which is common in FCERM appraisals and provides an accurate assessment of property inundation depths at each return period.

The following assumptions and additional data were used to improve and provide the necessary information to supplement the above datasets. Comments on the quality of the data have also been listed.

Should the ground truthing exercise not support of these assumptions, the options appraisal analysis will be adapted as required.

Table 4-1: Direct flood damage assumptions

Data type	Data and any assumptions used
Depth Damage data	Long Duration Multi-Coloured Manual for coastal (wave damage) sources used.
Flood levels	Flood levels derived from inundation modelling for the 2, 5, 10, 50, 100, 200 and 1000 year return periods for present day.
Threshold level	Threshold levels used where available. Remaining data taken from LiDAR. Visual assessment using Google Streetview conducted.
Basements	Not considered
Residential property types	Defined by property types (Detached, Semi-Detached, Terraced, Flat).
Non-residential property types	Defined by SEPA Receptor Database. Assumed as sector average where no data available
Property areas	Defined by SEPA Receptor Database or as building areas
Residential market values for capping	Zoopla market values used.
Non-residential market values for capping	Market values determined from bulk class rateable values per m ² . uplifted to 2018 by CPI
Flood duration	Assumed to be more than 12 hours as overtopping occurs over at least a single tidal cycle
Updating of MCM damage data	2017/18 damage data used. No updating necessary.

4.1.2 Depth damage curve

The FHRC MCM provides standard flood depth/direct damage datasets for a range of property types, both residential and commercial. This standard depth/damage data for direct and indirect damages has been utilised in this study to assess the potential damages that could occur under each of the options. Flood depths within each property have been calculated from the inundation modelling by comparing predicted water depths at each property to threshold levels.

The following FHRC depth damage curve was selected for this baseline assessment: Long Duration with Warning (Without Cellar), Wave and Salt Water Damage

4.1.3 Threshold levels

Threshold levels used within the damage calculations were obtained from topographic survey available and from LiDAR levels (as outlined in TuFlow modelling, Section 2.9.2) and applied to building footprint in modelling as well as to the receptor points for estimating flood depths in the damage calculations.

4.1.4 Residential property capping

In line with the guidance in the MCM, the property damages are capped to market value. For residential properties, the capped values have been taken from Zoopla and are presented in Table 4-2.

Table 4-2: Average property for Stonehaven (prices taken from Zoopla, Sept. 2018)

Property	Market Value
Detached	£302,671
Semi-detached	£214,556
Terraced	£227,140
Flat	£140,938

4.1.5 Non-residential property capping

Market values for non-residential properties can be estimated from a properties rateable value. The rateable value is used, together with an equivalent yield to estimate market value for damage capping using the following relationship:

$$\text{Estimated Capital Valuation} = \text{Factor} \times \text{Rateable Value}$$

The 'Factor' reflects the added value or percentage rental yield from that property. This is typically recommended to be a value of 10-12.5 for flood defence purposes¹⁷, although the MCH recommends a value of 16.7¹⁸. A value of 16.7 was used.

Non-residential properties have been capped based on the Valuation Office Agency rateable values (RV) for bulk classes. These have been assigned to non-residential receptors within the study area and vary between properties. Table 4-3 summarises the rateable values used for the non-residential within Stonehaven these have been uplifted from 2008 to 2018 using the CPI (Consumer Price Index)

17 Environment Agency (2009). Flood and Coastal Erosion Risk Management - Appraisal Guidance.

Table 4-3: Rateable values applied to non-residential receptors

Bulk Class	2018 CPI (£/m ²)
All Bulk Classes	83
Retail premises	164
Total Offices	153
Commercial Offices	162
'Other' Offices	107
Factories ³	37
Warehouses ³	50
Other bulk premises	40
Non-bulk premises	-
Non-bulk premises with floorspace	59

The capped value for non-residential properties was therefore determined from the following relationship in line with the MCH guidance:

$$Value = Floor\ area \times RV \times 16.7$$

4.1.6 Intangible damages (Health)

Intangible damages for each property, and each return period have been estimated using the following equation¹⁹

$$Damages\ (\text{£ per yr per household}) = 286 \times \{1.026 - (1/(1 + 37.5e^{-0.06/APP})\}$$

Typically, a value of £286 is used in the calculations. For assessment of baseline damages and to appraise the damage associated with given options at a later stage this approach is used.

However, there is debate as to whether the methodology used to determine this value underestimates the adverse health impacts of flooding. This may be particularly relevant in Stonehaven where there is high risk of flooding combined with a high concentration of vulnerable people.

Through consultation with SEPA, it has been agreed that the typical value (£286) be applied as part of the appraisal to allow for consistent national comparison of economic viability of proposed FPSs. This value has therefore been used for the calculations presented here and will be carried forward to the appraisal.

None-the-less, the vulnerability of the local community at risk of flooding is extremely important in Stonehaven. To emphasise this when developing the business case for the preferred option, we will test the sensitivity of the Benefit Cost Ratio by assigning a "vulnerability index" to each receptor based on the information

¹⁹ Environment Agency, 2004, The Appraisal of Human Related Intangible Impacts of flood, R&D Technical Report FD2005/TR, Environment Agency
AKI-JBAU-00-00-RP-HM-0002-S3-P02-Interim_Modelling_Report

available in the SEPA's strategic receptor dataset. This combines over 75 and vulnerable people scores, with higher scores indicating higher levels of vulnerability. The average vulnerability index for residential properties within 20m of the present day 1,000-year coastal inundation extent was found to be 38.8, significantly greater than the average score within Stonehaven (14.63). The classification of vulnerable properties at risk of flooding from the present-day 1000-year event in Figure 4-2.

For the inclusion of vulnerability, we will use the average vulnerability index of 38.8 to determine a cut off, above which a higher monetary value has been applied.

This will likely be taken as £1,340/yr/household based on the typical (£286) and higher (£2513) values presented in the MCM.



Figure 4-2: Property vulnerability index for properties in Stonehaven

4.2 Indirect damages

4.2.1 Local authority and emergency services losses

The multi coloured manual provides guidance on the assessment of indirect damages for emergency services and other third party costs. It recommends that a value between 5.6% and 10.7% of the direct property damages is used to represent emergency costs. These include the response and recovery costs incurred by organisations such as the emergency services, the Local Authority and SEPA.

The 5.6% value is more representative of flooding to a smaller community, whereas the 10.7% value is more representative of a more widespread regional flood scenario. This led to a value of 5.6% being considered most appropriate Indirect commercial damages

Obtaining accurate data on indirect flood losses is difficult. Indirect losses are of two kinds:

- losses of business to overseas competitors, and
- the additional costs of seeking to respond to the threat of disruption or to disruption itself which fall upon firms when flooded.

The first of these losses is unusual and is limited to highly specialised companies which are unable to transfer their productive activities to a branch site in this country, and which therefore lose to overseas competitors. The second type of loss is likely to be incurred by most Non-residential Properties (NRPs) which are flooded. They exclude post-flood clean-up costs but include the cost of additional work and other costs associated with inevitable efforts to minimise or avoid disruption. These costs include costs of moving inventories, hiring vehicles and costs of overtime working. These costs also include the costs of moving operations to an alternative site or branch and may include additional transport costs.

Chapter 5, Section 5.7 of the MCM²⁰ recommends estimating and including potential indirect costs where these are the additional costs associated with trying to minimise indirect losses. This is assessed by calculating total indirect losses as an uplift factor of 3% of estimated total direct NRP losses at each return period included within the damage estimation process.

4.2.2 Evacuation losses

The MCM (2013) provides guidance on the losses associated with evacuation (getting people safely out of homes during an event and temporary accommodation costs whilst properties are repaired). Costs recommended are based on flood depths and property type.

4.3 Modelling Results

To inform the baseline assessment, only present day flood extents have been used. The water surface was used in conjunction with the receptor dataset and threshold datasets to identify the properties inundated (i.e. water level above threshold) at each return period. These are presented in Table 4-4. A total of 68 properties are expected to be inundated during a 200-year event. Most of these properties are situated to the South of the River Cowie, in Stonehaven and Boatie Row.

Table 4-4: Count of inundated properties for Present day scenarios

Event	2yr	5yr	10yr	30yr	50yr	100yr	200yr	1000 yr
Residential	14	21	29	37	48	54	57	64
Commercial	2	2	3	6	7	9	11	19
Total	16	23	32	43	55	63	68	83



Figure 4-3: Two year flood extent with impacted properties



Figure 4-4: 200 year flood extent with impacted properties

4.3.1 Flood damages

Baseline flood damage calculations were undertaken following the methodology defined in the previous sections. This has assumed a 100-year appraisal period using the standard Treasury discount rates outlined in the Green Book.

This results in a total estimate of Present Value Damages (PvD) of £12.6 million. Table 4-5 and Figure 4-5 provide a breakdown of the contribution from each component considered at this stage, both in terms of Annual Average Damages (AAD) and PvD.

Table 4-5: Breakdown of 2018 flood damages

Component	AAD (£k)	PvD (£k)
Direct Residential	£261.86	£7,806.79
Direct Commercial	£84.81	£2,528.36
Indirect Commercial	£2.54	£75.85
Emergency Services	£20.80	£620.11
Evac. And Temp Accom	£28.87	£860.81
Intangibles (Health)	£20.38	£607.70
Vehicles	£3.47	£103.30
Total	£422.73	£12,602.92

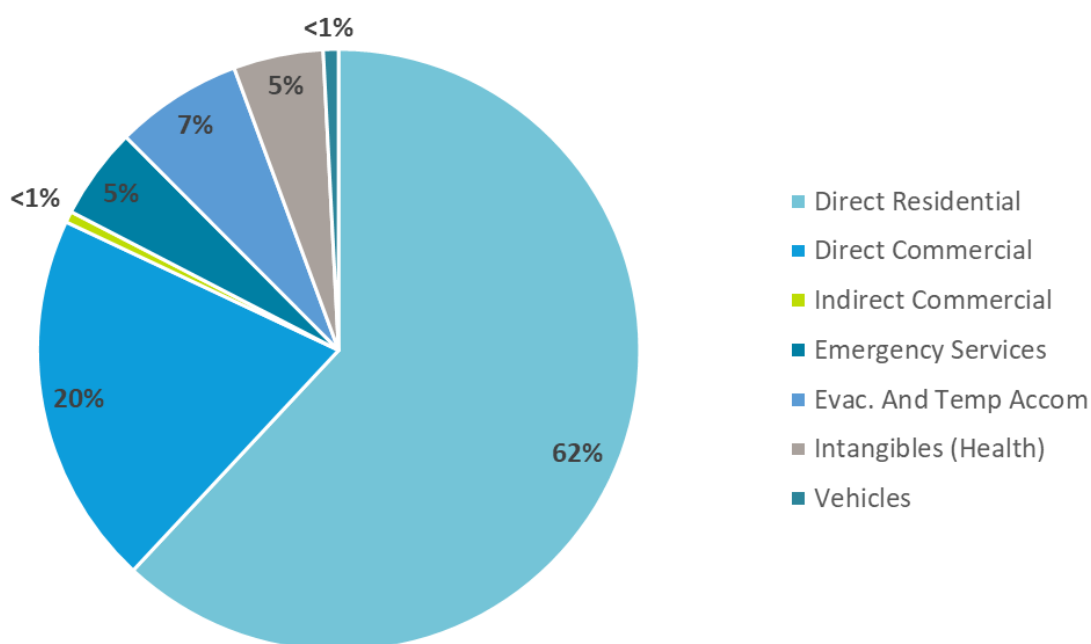


Figure 4-5: Proportion of components contributing to 2018 flood damages

It should be noted that, given the high risk of flooding and large depth that can accumulate behind the defences, the values reported above are significantly influenced by the capping of PvD to property values. Out of all the properties flooded, 55% of residential, and 21% of non-residential properties have their AAD capped at market value. If no capping was considered, the total PvD would increase to £54.7 million.

5 Conclusions and recommendations

5.1 Flood modelling

The methodology for developing and assessing flood risk has been demonstrated and shown to have the following phases:

- Processing of SEPA's offshore multivariate data into an MDA sample;
- Wave transformation modelling of the MDA sample to provide nearshore conditions;
- Fitting of emulators to the wave transformation results;
- Emulation for the entire multivariate dataset and corresponding WaveWatch III hindcast data;
- Estimation of overtopping for hindcast wave conditions using EurOtop Neural Network 2;
- Calibration and sense checking of overtopping schematisations using historic flood information;
- Estimation of extreme overtopping rates using the full multivariate dataset and EurOtop Neural Network 2;
- TUFLOW inundation modelling of the December 2012 event as a validation of the entire modelling framework;
- TUFLOW inundation modelling of extreme events to inform baseline flood damage calculations.

The results presented, and checks undertaken have demonstrated that the methodology is robust and effectively captures the baseline flood risk to Stonehaven from wave overtopping and extreme sea levels.

As part of this interim reporting, baseline flood risk has been considered. This assessment will be used to inform the options appraisal, allowing for a managed adaptive approach to flood risk for Stonehaven to be undertaken.

The main source of uncertainty in the results has been shown to be within the harbour where the SWAN modelling and emulators have the largest errors. While, the methodology presented is considered sufficient to estimate flood risk as part of this study, should the outcomes demonstrate the requirement for the re-design of defences at the rear of the harbour, it is recommended that more detailed (phase-resolving) wave modelling be considered at a later stage.

It has been shown that, sea level rise due to climate change has the potential to significantly affect additional parts of the drainage network. This is primarily concentrated on assets south of the Carron.

The increase in flood risk on the watercourses has not been considered at this stage. This will be assessed throughout the options appraisal to make sure that any alterations to the banks and defences include sufficient levels and freeboard, given the combined fluvial-coastal risk.

5.2 Erosion Modelling

The erosion risk at Stonehaven has been analysed and assessed using the following steps:

- Review of the baseline processes that influence sediment transport and erosion;
- Analysis of national datasets (NCCA) to establish the long-term trends in shoreline position;

- Analysis of available topographic survey data to establish medium-term term (10 year) volumetric variations in the beach;
- Numerical modelling of the beach to estimate erosion rates after defence failure and identify any critical assets at risk.

The results presented show that there is a high level of variability in the beach levels and volumes. The primary control mechanism is cross-shore transport during extreme events which lead to berm building and burying of the defences. This particularly evident south of the River Cowie, where the revetment is almost completely buried, and the beach now forms the primary defence to the properties behind. Anecdotal evidence from local residences suggests that this improves dissipation of wave energy further offshore, reducing overtopping. This will be considered further during the option development.

Although the cross-shore processes are thought to dominate, a longshore gradient exists. This is likely to do with the higher exposure of the northern section of the bay (Cowie) and explains the increase in beach width from north-to south.

The assessment of the performance of the control structures at the Cowie and Carron mouths have shown them to be inefficient at retaining beach sediment, with the Carron mouth arrangement possibly exacerbating the loss of sediment that is recycled to the area. Overall, the volume increase around the Carron mouth, is less than the volume placed by Aberdeenshire Council.

While the analysis undertaken has been useful to give an overall picture of the changes in the beach, these are not available at the frequency required to fully understand the performance and changes in the beach during extreme conditions. This is exacerbated by the trends potentially being skewed by the timing of the surveys undertaken (i.e. 2008 was before/during the storm season and 2013 and 2018 were after). These data are insufficient to fully understand the morphological behaviour of the system and to assess the implications that these changes may have on flood risk (i.e. there is no evidence of toe scour in the available data, which has been discussed in previous studies). Although, the numerical modelling undertaken in XBeach helps to understand the short-term changes during storms, this is again limited with a lack of recorded pre-storm profiles to give confidence that the range of processes are adequately captured.

The morphology of the beach is clearly a key component in the protection against, and exacerbation of, flood risk within the bay. Should the study undertaken here lead to the design and construction of a new FPS, it is recommended that regular beach monitoring and survey be undertaken in the intervening period to support the management decisions and ongoing processes.

The area south of the Carron mouth is a key area of interest in terms of erosion and morphological change. While it has been hypothesised that the discharge from the river increases erosion in this location by altering the longshore gradient this is only anecdotal. Some further detailed modelling of 2D velocity gradients and vectors within the bay (including river discharges) should be considered in the future to better understand the overall processes during extreme events.

5.3 Baseline economic appraisal

The results from the baseline economic appraisal has shown that the present-day damages have a present value of approximately £12.6 million. The main contribution to this is through direct residential property damages. The high frequency of flooding and number of properties at risk during low return periods has resulted in significant capping of the damages to market value. Without this capping

the present value damages are estimated to be £54.7 million, further highlighting the high level of risk at lower return periods.

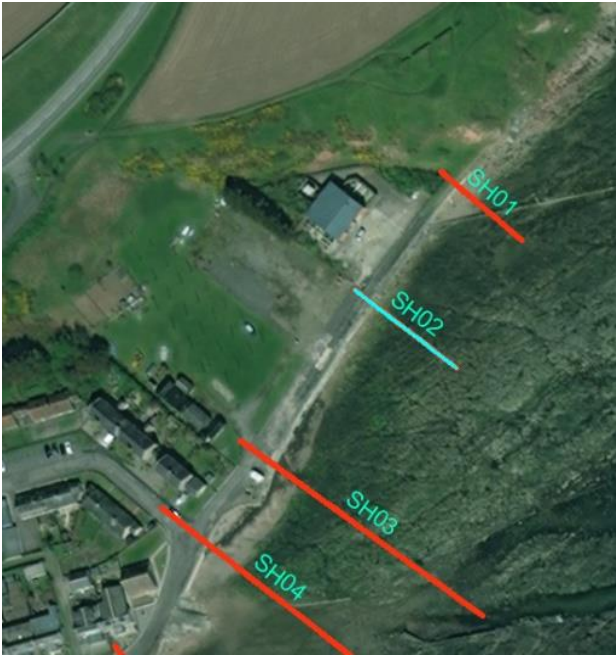
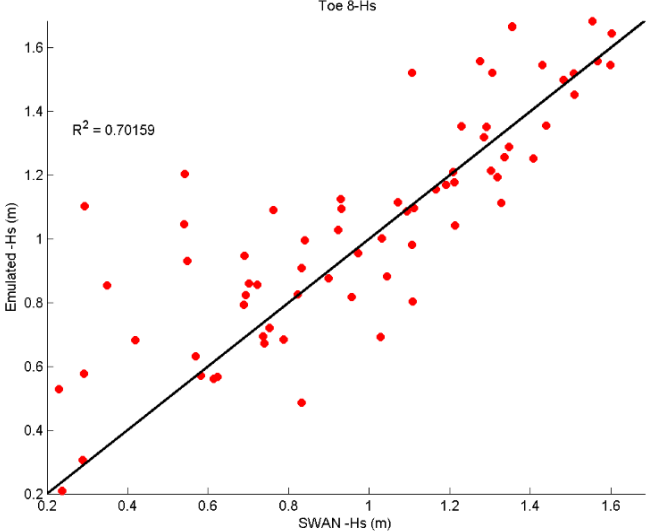
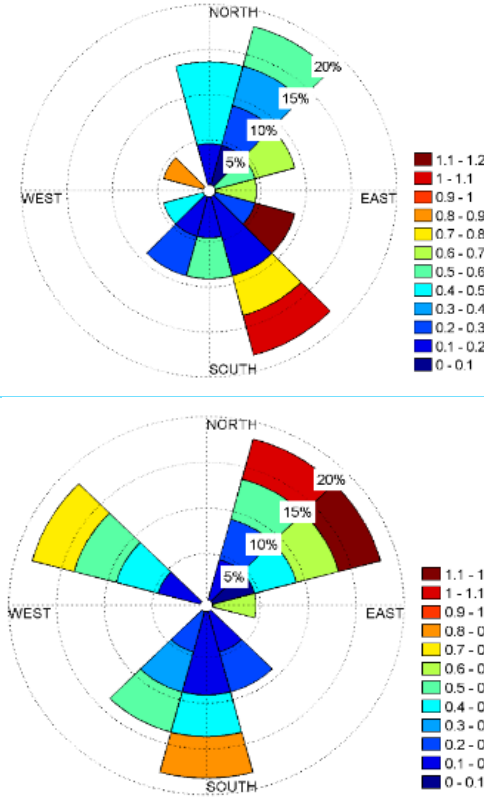
Prior to full options appraisal the following will be incorporated into the damage assessment:

- Recreational losses through erosion of the beach;
- Risk-to-life from wave overtopping;
- Critical infrastructure at risk from erosion;
- Sea level rise and climate change.

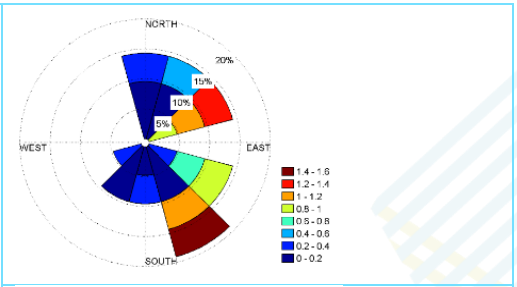
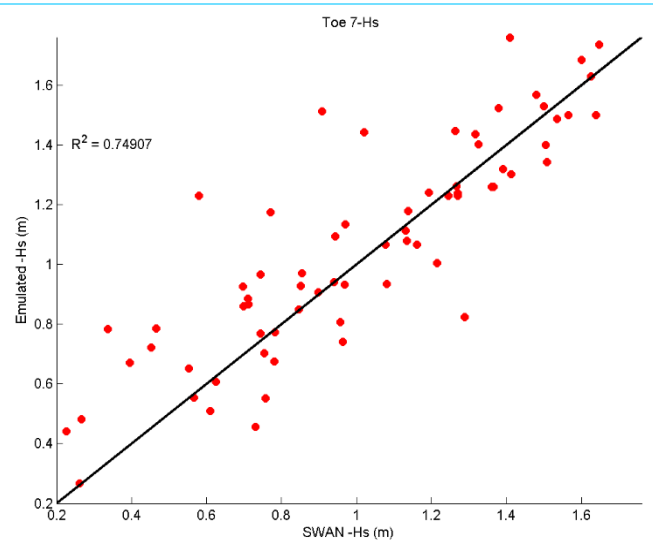
Inclusion of these will increase the overall present value damages for the appraisal period.

Appendices

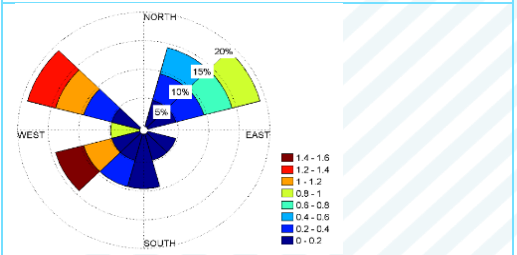
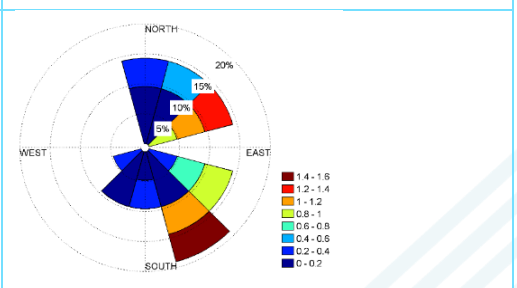
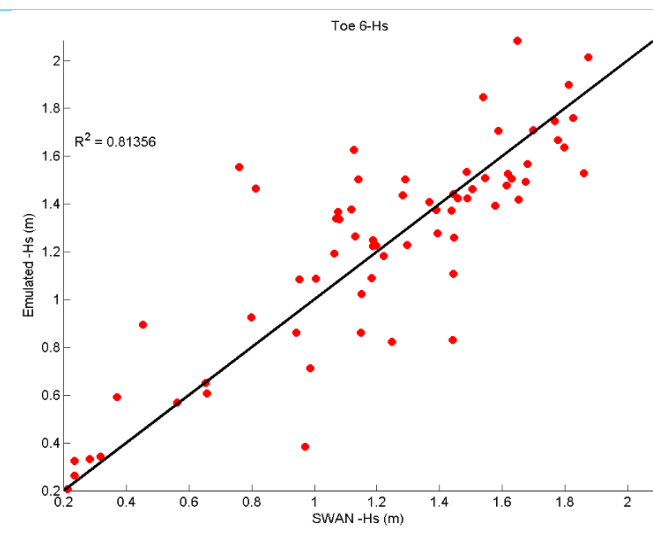
A Emulator function diagnostics

Output Location	Function scores (top) and chosen function Hs prediction (bottom)	Hs errors for offshore wind direction (top) and wave direction (bottom)
<p>SH_02</p> 	<p>Toe 8-Hs</p> 	

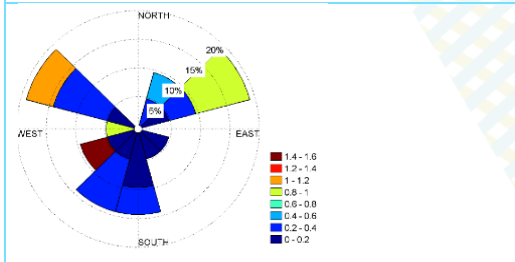
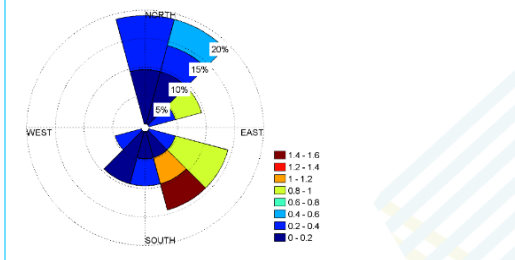
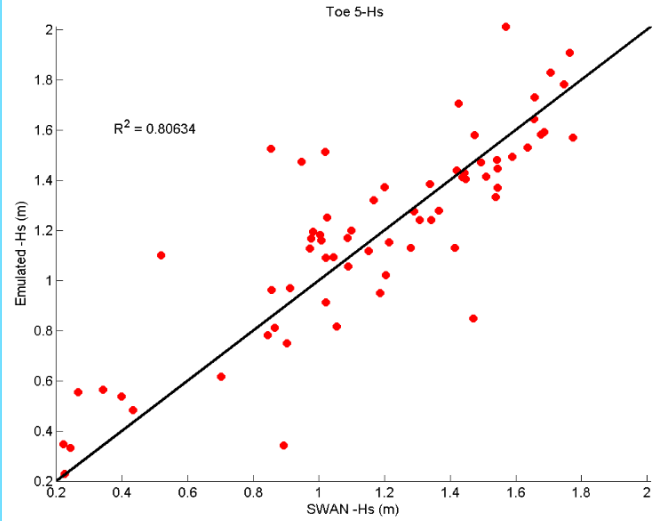
SH_06



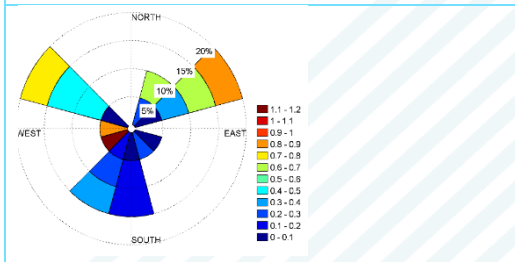
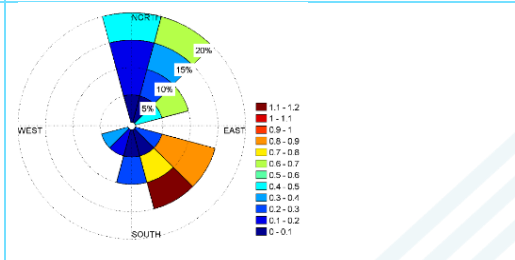
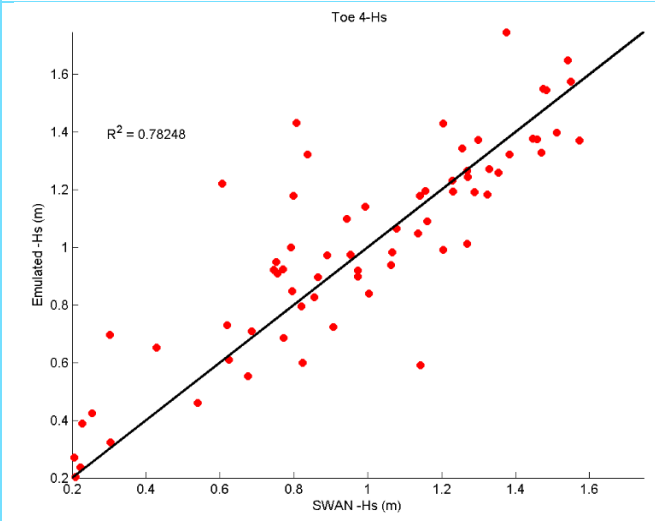
SH_12



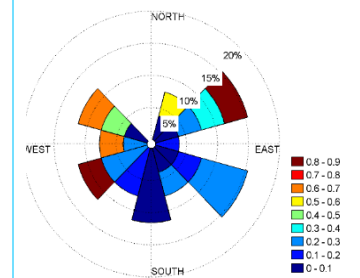
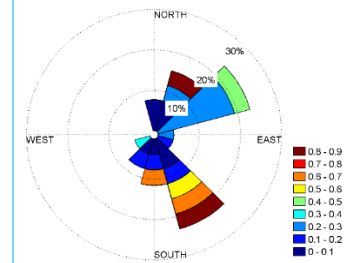
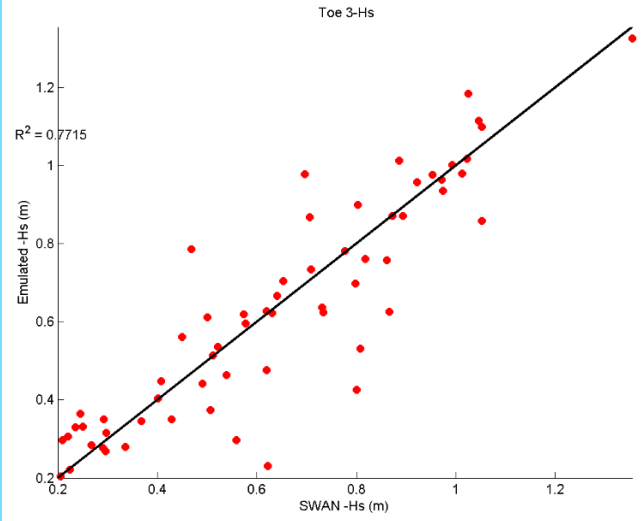
SH_17



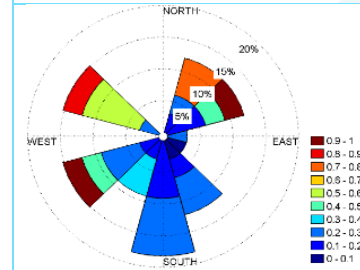
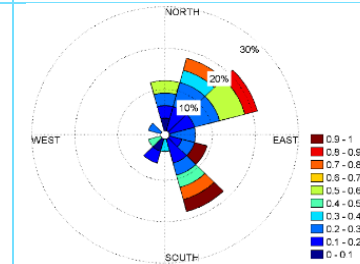
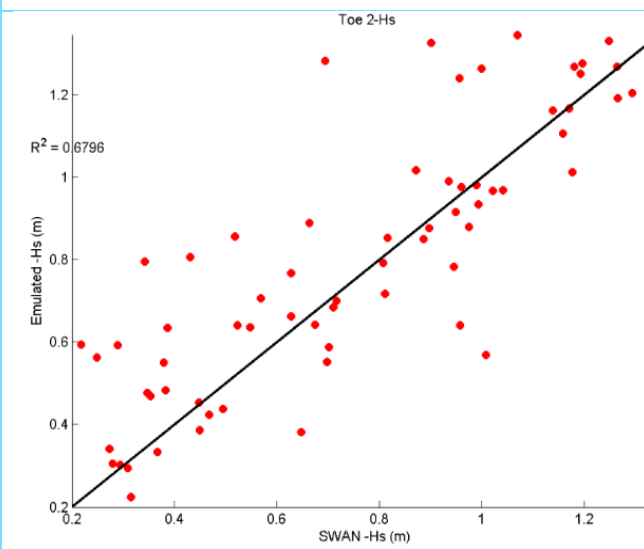
SH_20



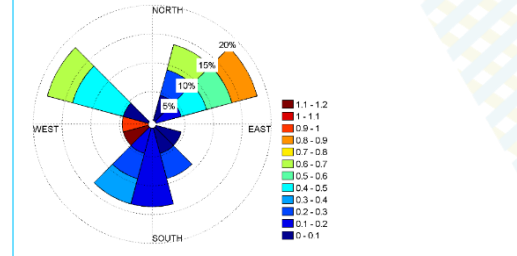
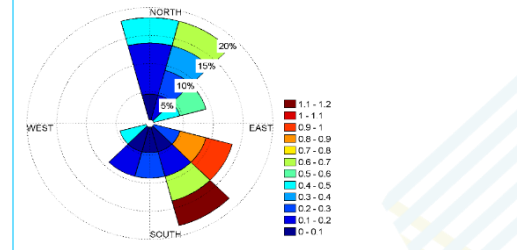
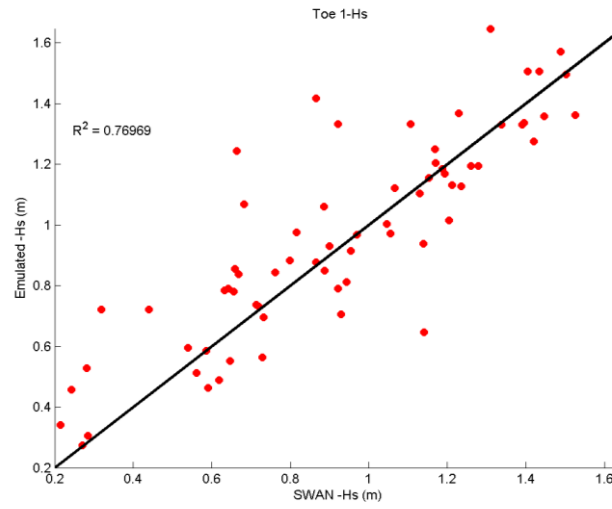
SH_25



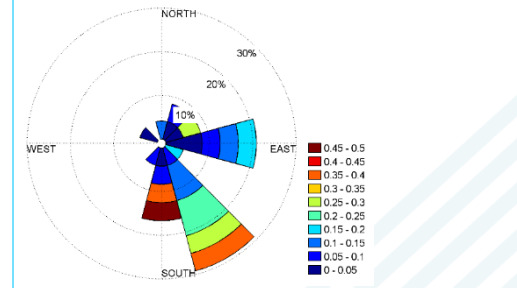
SH_28



SH_29

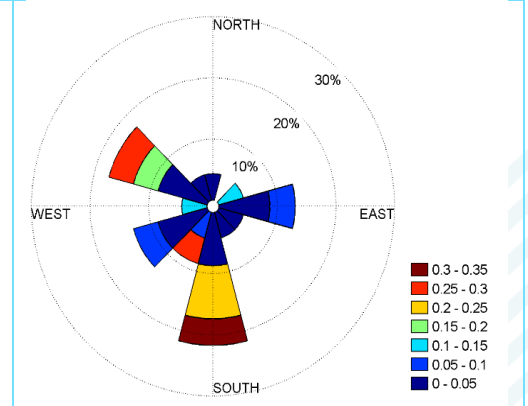
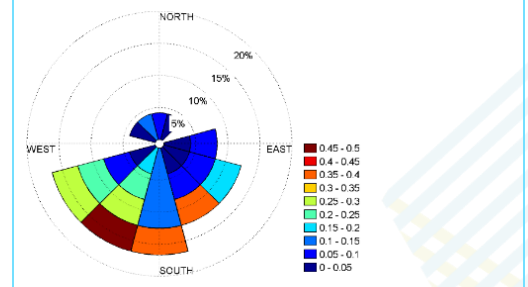
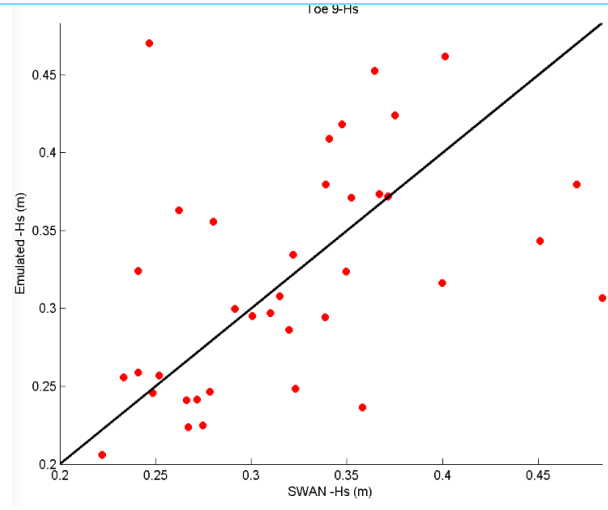


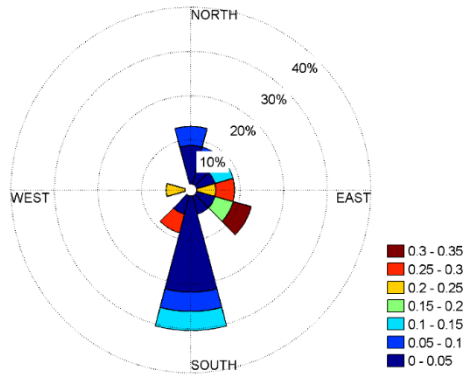
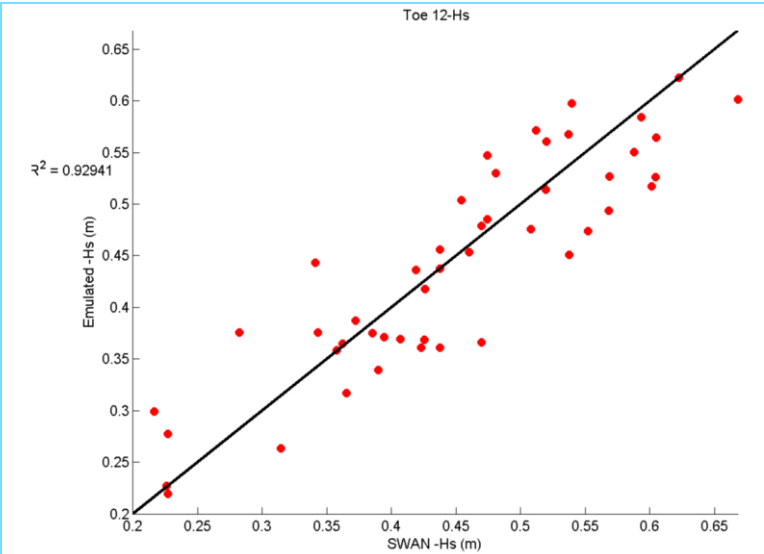
SH_H_01



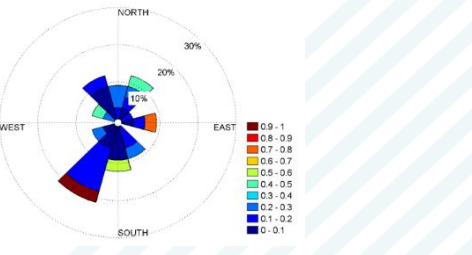
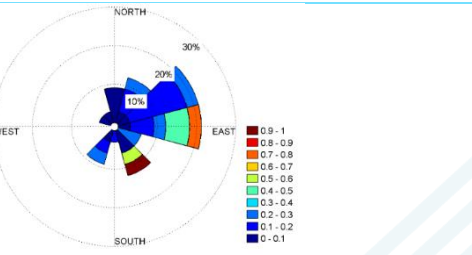
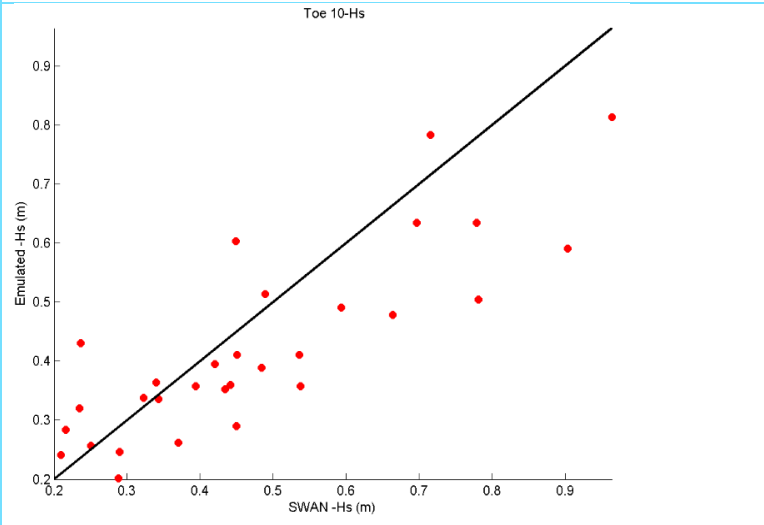


SH_H_01b

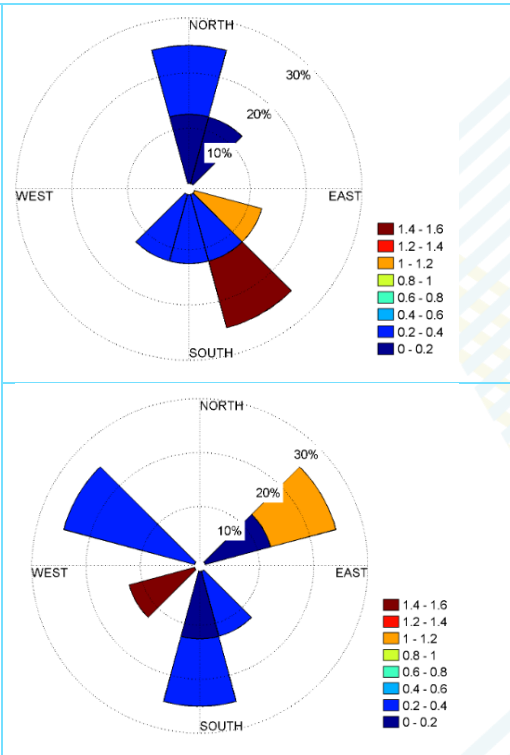
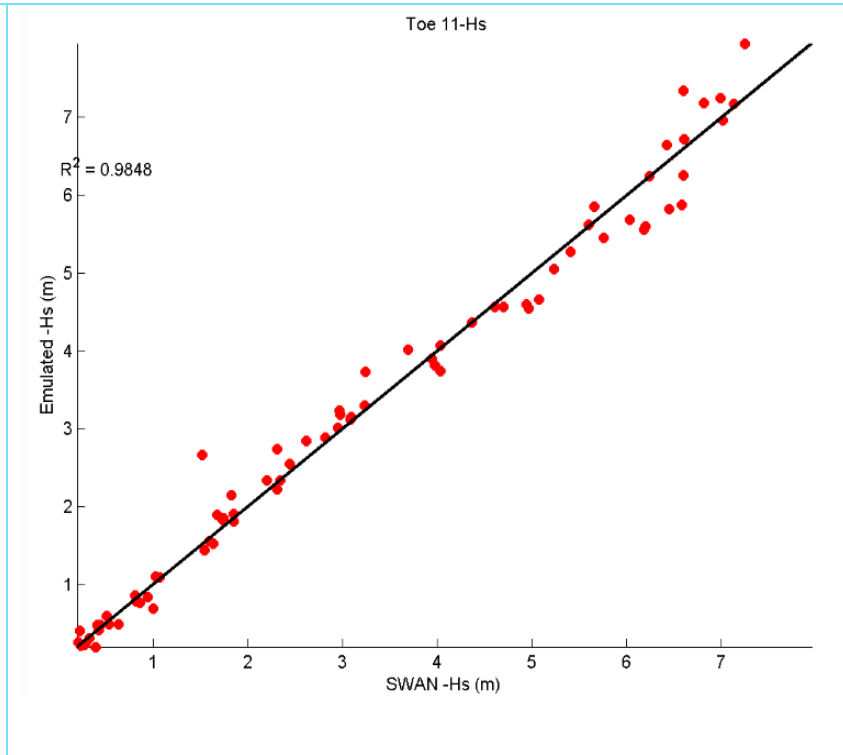




SH_H_02



Calibration Buoy (Cal_buoy)



B Volumetric Analysis

Table B-1: Volumetric changes above MHW in Stonehaven Bay

Profile	Volume in 2008 (m3/m)	Volume in 2013 (m3/m)	Volume in 2018 (m3/m)	Volume change 2008-2013 (m3/m)	Volume change 2013-2018 (m3/m)	Total volume change 2008-2018 (m3/m)
1	34.06	34.06	35.07	0.00	1.01	1.01
2	20.72	20.26	21.72	-0.46	1.46	1.00
3	32.31	29.38	30.19	-2.93	0.81	-2.12
4	43.76	49.76	55.74	6.00	5.99	11.99
5	16.22	25.65	25.93	9.43	0.28	9.71
6	18.87	26.82	24.10	7.95	-2.71	5.24
7	24.47	28.42	32.32	3.95	3.90	7.85
8	31.26	37.29	38.95	6.03	1.66	7.69
9	32.78	35.65	43.61	2.87	7.97	10.84
10	28.38	26.88	35.78	-1.50	8.90	7.41
11	39.01	38.56	40.78	-0.45	2.22	1.77
12	33.67	49.70	39.45	16.03	-10.24	5.78
13	41.05	39.22	41.35	-1.83	2.14	0.30
14	60.09	54.93	56.02	-5.16	1.10	-4.06
15	48.78	75.63	67.82	26.85	-7.80	19.04
16	50.87	76.94	76.54	26.07	-0.40	25.66
17	53.85	90.80	82.17	36.95	-8.63	28.32
18	73.22	104.10	98.43	30.88	-5.67	25.21
19	96.65	120.29	125.62	23.64	5.33	28.97
20	94.21	113.91	119.83	19.70	5.92	25.62
21	94.35	102.62	105.23	8.27	2.61	10.88
22	135.81	129.24	128.01	-6.57	-1.23	-7.80
23	99.27	91.83	89.68	-7.44	-2.15	-9.58
24	103.71	102.50	98.61	-1.21	-3.90	-5.10
25	66.40	75.49	78.91	9.08	3.42	12.50
26	127.40	156.72	171.32	29.32	14.60	43.92

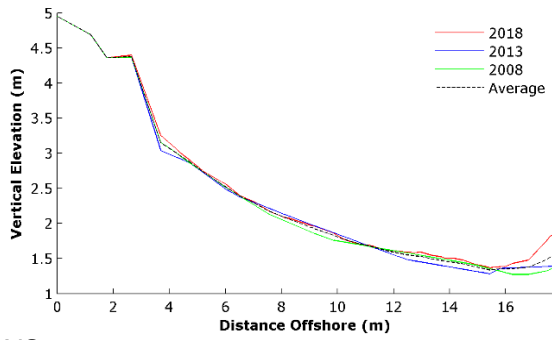
C XBeach Joint Probability Runs

Table C-1: Joint probability boundary conditions for XBeach modelling

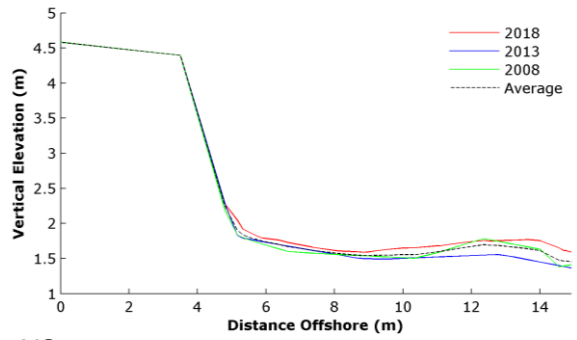
Event	1 year	2 year	10 year	30 year	50 year	100 year	200 year	1000 year
1								
Hs (m)	0.617	0.653	0.716	0.753	0.768	0.785	0.802	0.859
SWL (mAOD)	2.859	2.859	2.859	2.859	2.859	2.859	2.859	2.859
Tp (s)	5.741	5.822	5.964	6.041	6.074	6.110	6.147	6.264
2								
Hs (m)	1.234	1.306	1.434	1.505	1.537	1.570	1.605	1.7176
SWL (mAOD)	2.764	2.835	2.999	3.107	3.156	3.226	3.282	3.449
Tp (s)	6.976	7.099	7.310	7.422	7.469	7.520	7.571	7.733
3								
Hs (m)	1.851	1.958	2.151	2.258	2.305	2.355	2.407	2.576
SWL (mAOD)	2.680	2.747	2.151	3.027	3.070	3.146	3.209	3.354
Tp (s)	7.914	8.051	2.151	8.399	8.448	8.501	8.553	8.716
4								
Hs (m)	2.468	2.611	2.868	3.011	3.073	3.141	3.209	3.435
SWL (mAOD)	2.594	2.659	2.822	2.935	2.987	3.056	3.132	3.273
Tp (s)	8.613	8.748	8.967	9.078	9.125	9.173	9.222	9.371
5								
Hs (m)	3.085	3.264	3.585	3.764	3.841	3.926	4.012	4.294
SWL (mAOD)	2.477	2.558	2.701	2.814	2.863	2.941	3.034	3.133
Tp (s)	9.134	9.259	9.464	9.568	9.612	9.659	9.707	9.857
6								
Hs (m)	5.554	3.917	4.302	4.516	4.610	4.711	4.814	5.153
SWL (mAOD)	2.35	2.388	2.576	2.666	2.707	2.763	2.849	2.950
Tp (s)	10.59	9.655	9.862	9.975	10.02	10.08	10.13	10.33
7								
Hs (m)		3.976	4.621	4.777	4.853	4.942	5.046	5.369
SWL (mAOD)		2.370	2.514	2.610	2.654	2.713	2.770	2.900
Tp (s)		9.687	10.03	10.11	10.15	10.20	10.27	10.471
8								
Hs (m)		5.873	5.019	5.269	5.378	5.496	5.617	6.011
SWL (mAOD)		2.35	2.386	2.526	2.566	2.611	2.649	2.712

TP (s)		10.84 ₂	10.25 ₄	10.40 ₇	10.47 ₇	10.55 ₇	10.64 ₃	10.960
9								
Hs (m)			6.453	6.776	6.914	7.068	6.419	6.870
SWL (mAOD)			2.35	2.35	2.35	2.35	2.395	2.518
TP (s)			11.39 ₁	11.77 ₀	11.95 ₂	12.16 ₃	11.35 ₄	11.893
10								
Hs (m)							7.224	7.738
SWL (mAOD)							2.35	2.35
TP (s)							12.40 ₄	13.310

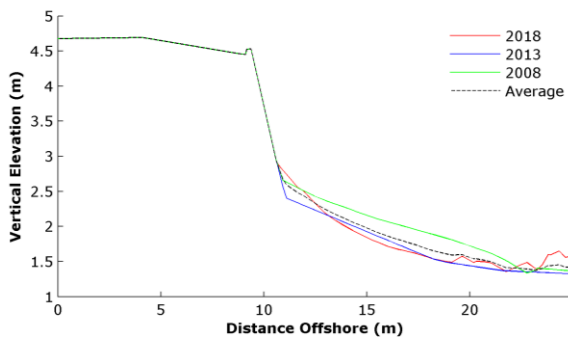
D Profile Plots



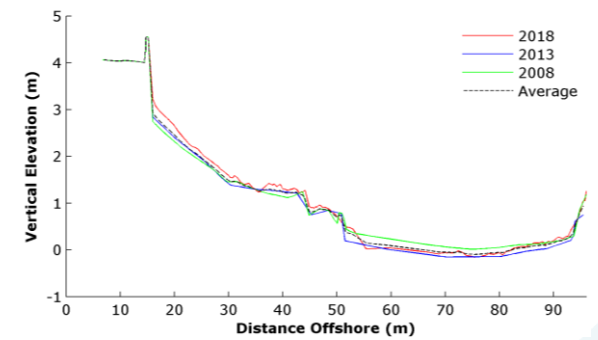
XS01



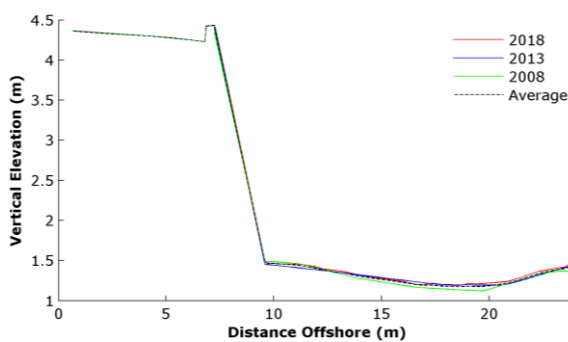
XS02



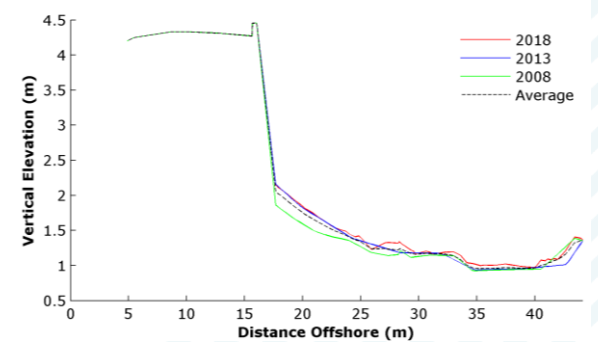
XS03



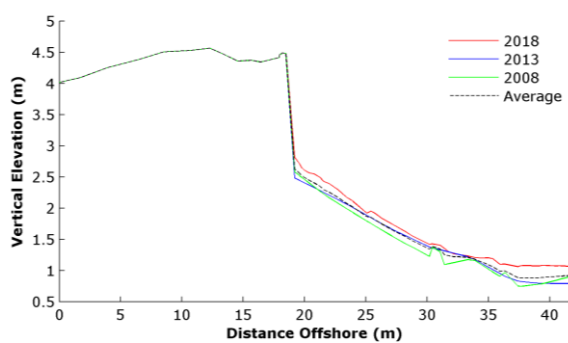
XS04



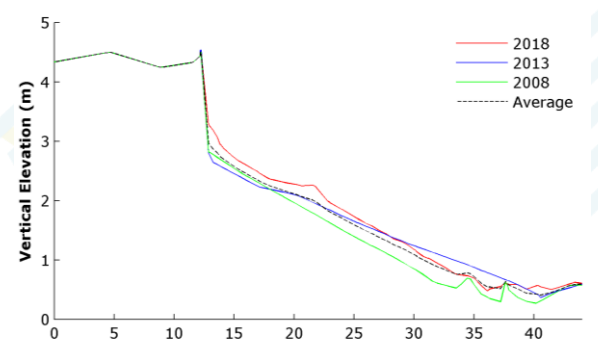
XS05



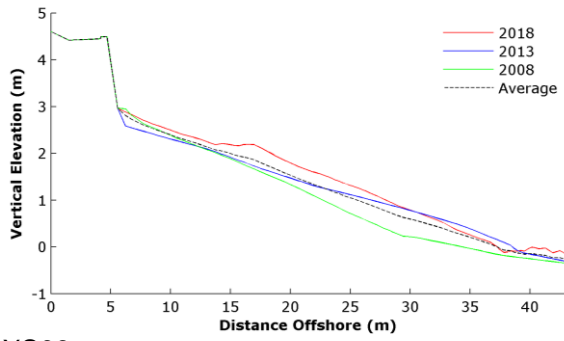
XS06



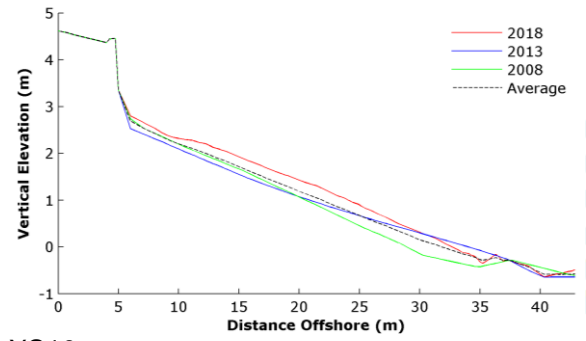
XS07



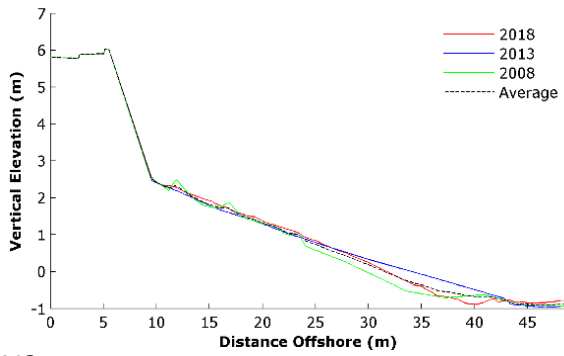
XS08



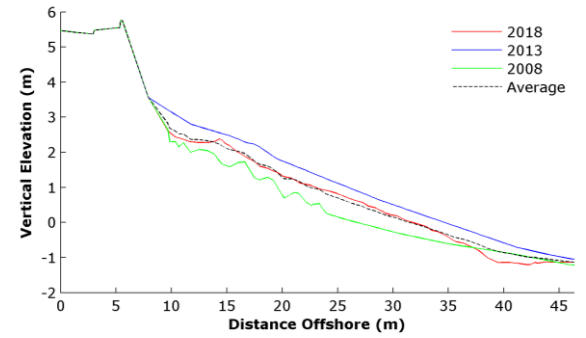
XS09



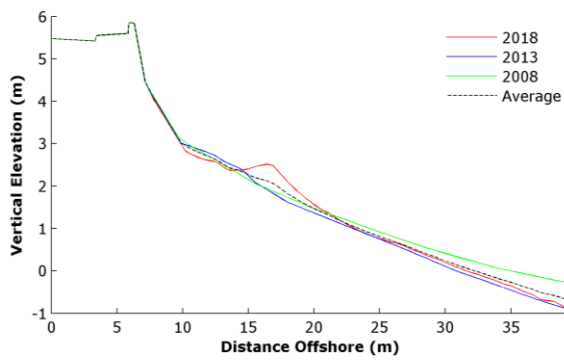
XS10



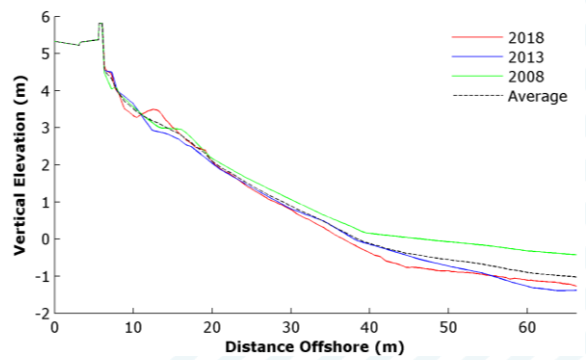
XS11



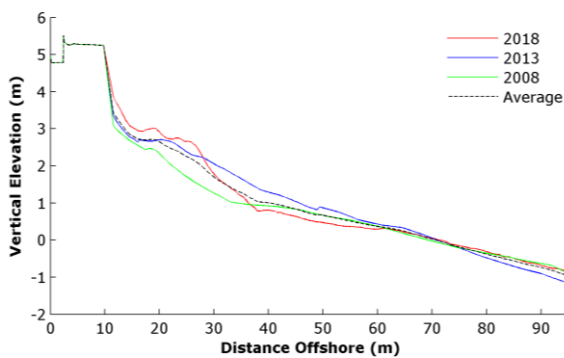
XS12



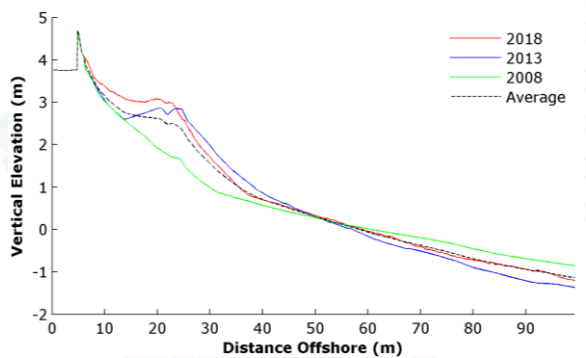
XS13



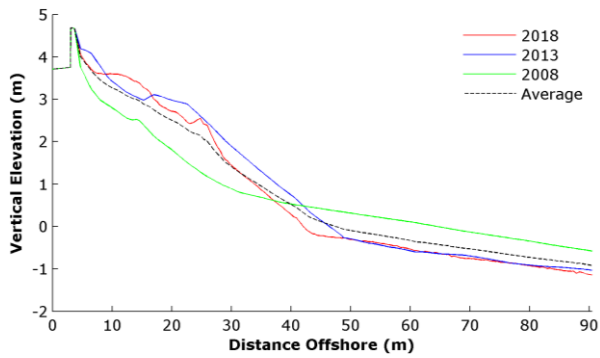
XS14



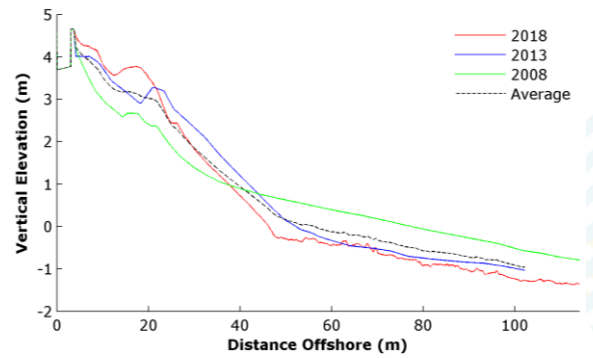
XS15



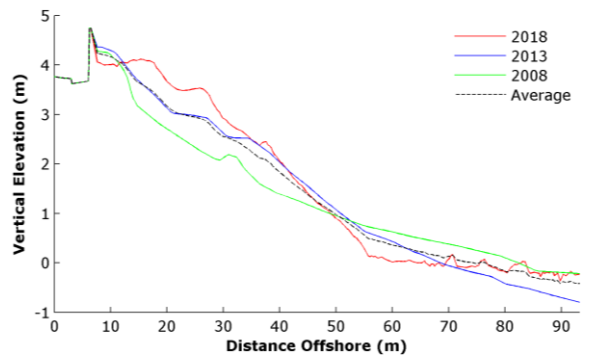
XS16



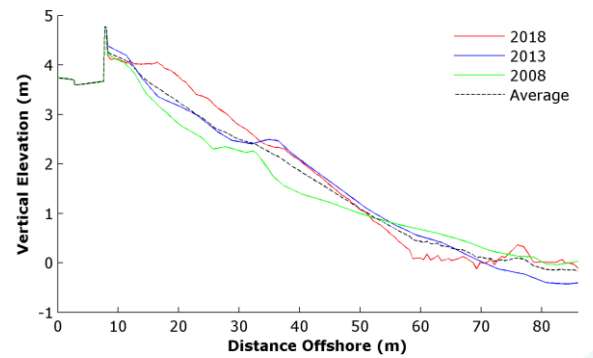
XS17



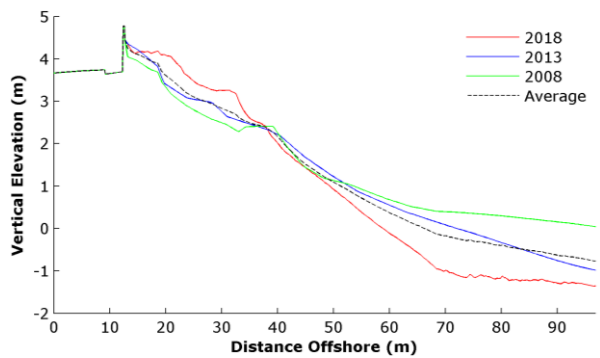
XS18



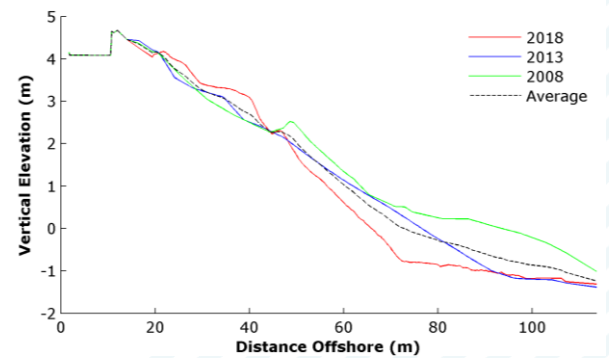
XS19



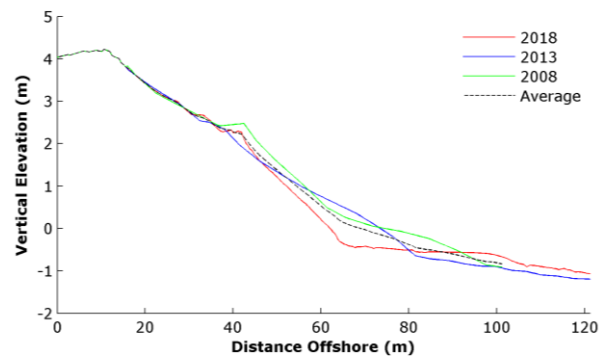
XS20



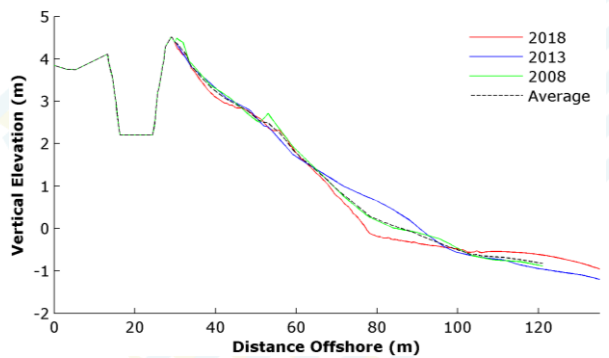
XS21



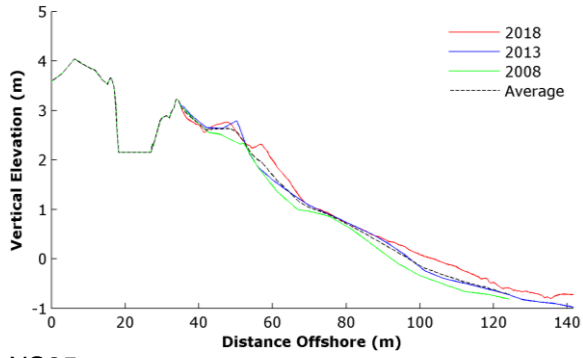
XS22



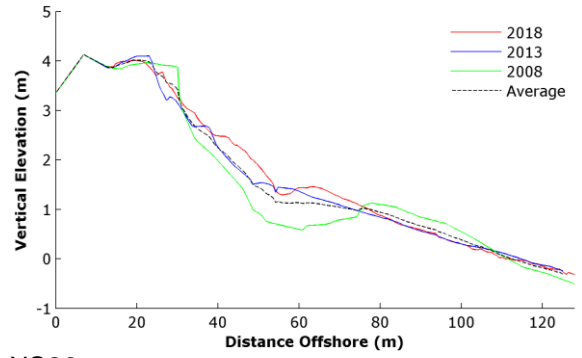
XS23



XS24



XS25



XS26

E Inundation extent



Present Day 2 year flood extent



Legend

 Present Day 2 year flood extent

Source: Esri, DigitalGlobe, GeoEye, Earthstar Geographics, CNES/Airbus DS, USDA, USGS, AeroGRID, IGN, and the GIS User Community



Contains OS data © Crown copyright and database right 2018



Present Day 30 year flood extent



Legend

 Present Day 30 year flood extent

Source: Esri, DigitalGlobe, GeoEye, Earthstar Geographics, CNES/Airbus DS, USDA, USGS, AeroGRID, IGN, and the GIS User Community



Contains OS data © Crown copyright and database right 2018



Present Day 100 year flood extent



Legend

 Present Day 100 year flood extent

Source: Esri, DigitalGlobe, GeoEye, Earthstar Geographics, CNES/Airbus DS, USDA, USGS, AeroGRID, IGN, and the GIS User Community



Contains OS data © Crown copyright and database right 2018



Present Day 200 year flood extent



Legend

 Present Day 200 year flood extent

Source: Esri, DigitalGlobe, GeoEye, Earthstar Geographics, CNES/Airbus DS, USDA, USGS, AeroGRID, IGN, and the GIS User Community



Contains OS data © Crown copyright and database right 2018



2118 - 30 year flood extent



Legend

 2118 - 30 year flood extent

Source: Esri, DigitalGlobe, GeoEye, Earthstar Geographics, CNES/Airbus DS, USDA, USGS, AeroGRID, IGN, and the GIS User Community



Contains OS data © Crown copyright and database right 2018



2118 - 200 year flood extent



Legend

 2118 - 200 year flood extent

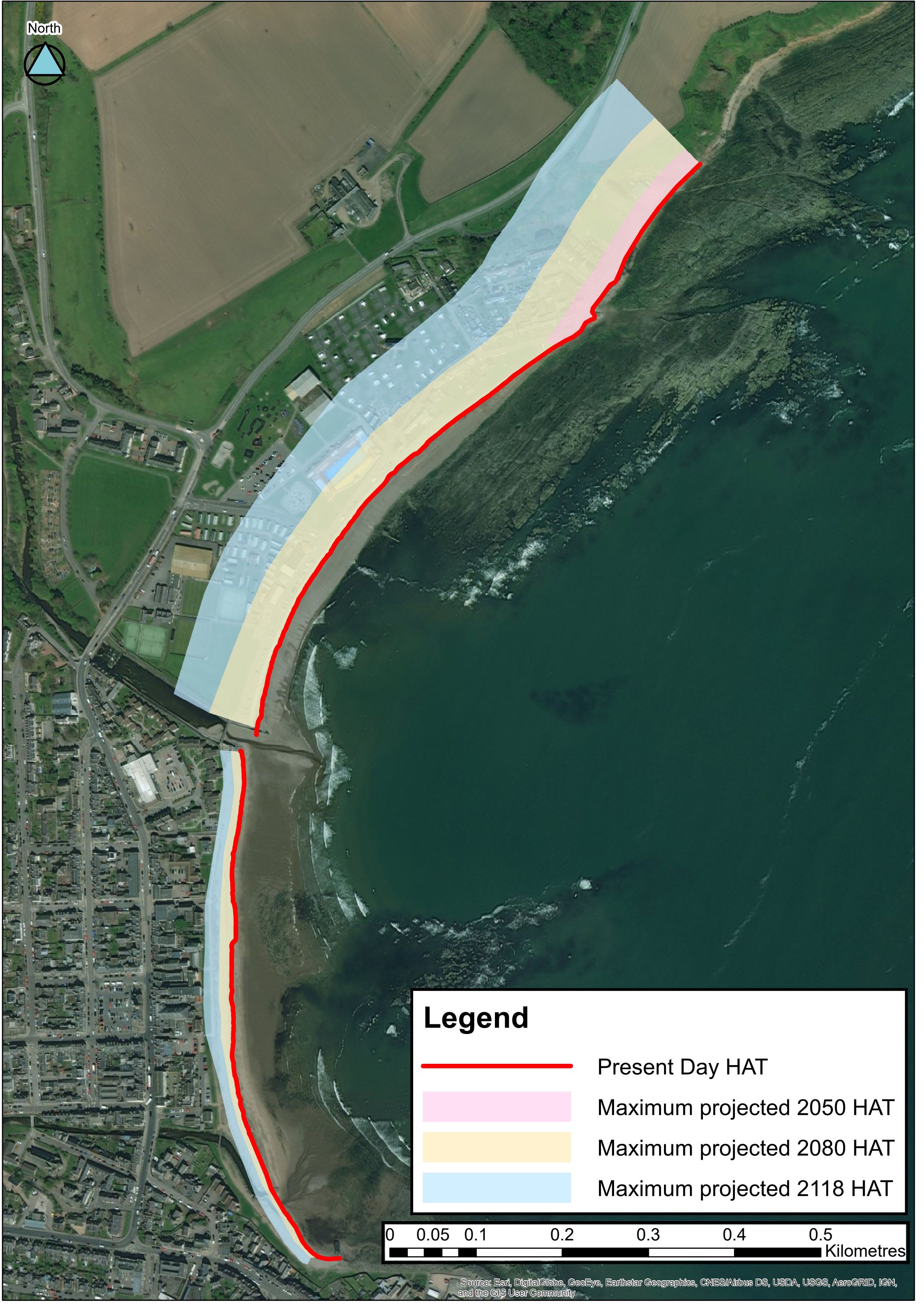
Source: Esri, DigitalGlobe, GeoEye, Earthstar Geographics, CNES/Airbus DS, USDA, USGS, AeroGRID, IGN, and the GIS User Community



Contains OS data © Crown copyright and database right 2018

F Erosion map

North



Legend

- Present Day HAT
- Maximum projected 2050 HAT
- Maximum projected 2080 HAT
- Maximum projected 2118 HAT

0 0.05 0.1 0.2 0.3 0.4 0.5 Kilometres

Source: Esri, DigitalGlobe, GeoEye, Earthstar Geographics, CNES/Airbus DS, USDA, USGS, AeroGRID, IGN, and the GIS User Community



2118 - 30 year, eroded flood extent



Legend

 2118 - 30 year, eroded flood extent

Source: Esri, DigitalGlobe, GeoEye, Earthstar Geographics, CNES/Airbus DS, USDA, USGS, AeroGRID, IGN, and the GIS User Community



Contains OS data © Crown copyright and database right 2018



2118 - 200 year, eroded flood extent



Legend

 2118 - 200 year, eroded flood extent

Source: Esri, DigitalGlobe, GeoEye, Earthstar Geographics, CNES/Airbus DS, USDA, USGS, AeroGRID, IGN, and the GIS User Community



Contains OS data © Crown copyright and database right 2018

JBA
consulting

Offices at:

Coleshill
Doncaster
Dublin
Edinburgh
Exeter
Glasgow
Haywards Heath
Isle of Man
Limerick
Newcastle upon Tyne
Newport
Peterborough
Saltaire
Skipton
Tadcaster
Thirsk
Wallingford
Warrington

Registered Office
South Barn
Broughton Hall
SKIPTON
North Yorkshire
BD23 3AE
United Kingdom

+44(0)1756 799919
info@JBA - consulting.com
www.JBA - consulting.com
Follow us:  

Jeremy Benn Associates Limited

Registered in England 3246693

JBA - Group Ltd is certified to:
ISO 9001:2015
ISO 14001:2015
OHSAS 18001:2007

